©2013

Alexander I. Son

THE ROLE OF EPHRIN-A5 IN LENS MAINTENANCE AND VITREOUS HUMOR

DEVELOPMENT

by

ALEXANDER I. SON

A Dissertation submitted to the

Graduate School-New Brunswick

Rutgers, The State University of New Jersey

and

the Graduate School of Biomedical Sciences

in partial fulfillment of the requirements

for the degree of

Doctor of Philosophy

Graduate Program in Neuroscience

written under the direction of

Renping Zhou, PhD

and approved by

_____

_____

_____

_____

_____

New Brunswick, New Jersey

January, 2013

ABSTRACT OF THE DISSERTATION

The Role of Ephrin-A5 in Lens Maintenance and Vitreous Humor Development

By ALEXANDER I. SON

Dissertation Director:
Renping Zhou, PhD

The development of the eye requires the orchestration of precise regulatory

signals and events in constructing a complex structure capable of collecting visual inputs.

Recent observations have identified one group of molecules, the Eph family of receptor

tyrosine kinases, to be critical in the formation of and maintenance of ocular tissues. This

present work focuses on the role of the Eph ligand ephrin-A5 in the development and

function of the lens and vitreous humor.

We have found ephrin-A5 to be a major contributor to lens development and

maintenance, as mice lacking ephrin-A5 develop cataracts. Major lens abnormalities in

the ephrin-A5$^{-/-}$ animals are observed at postnatal stages with lens opacity occurring by

P21. Examination of the expression of ephrin-A5 and its putative receptor EphA2 in the

lens supports a fundamental role for this receptor-ligand complex in lens development.

As alterations in lens fiber cell shape were observed in the ephrin-A5$^{-/-}$ lens, we examined

the role of ephrin-A5 and its receptor EphA2 on the control of the adherens junction.   N-

cadherin localization is disrupted in the ephrin-A5$^{-/-}$ lens; however, β-catenin, a regulator

of N-cadherin interaction with the actin cytoskeleton, remains on the membrane in the

ephrin-A5$^{-/-}$ lens and co-localizes with EphA2. Further examinations reveal Ephrin-A5 and EphA2 to regulate β-catenin interaction with N-cadherin, indicate that ephrin-A5 is required for maintaining proper lens fiber cell architecture through the regulation of the adherens junction.

We have also identified critical roles of ephrin-A5 in regression of the primary vitreous. Failure of this event results in the eye disease Persistent Hyperplastic Primary Vitreous (PHPV). Ephrin-A5$^{-/-}$ animals develop phenotypes representative of PHPV, most notably the presence a large hyperplastic mass posterior to the lens that remains throughout the lifetime of the animal. The aberrant tissue consists of vascularized cells surrounded by pigmented cells of neural crest origin. The mass in ephrin-A5$^{-/-}$ animals was also found to be mitotically active in both embryonic and postnatal stages signifying that ephrin-A5 has a role in cell cycle regulation in the developing vitreous. Together, these studies demonstrate the critical and varied roles of ephrin-A5 throughout ocular development.

Acknowledgements

I am tremendously grateful to my advisor, Dr. Renping Zhou, for his expertise, encouragement, guidance, and patience. I would also like to thank my committee members, Dr. Cheryl Dreyfus, Dr. John Pintar, Dr. Michael Matise, and Dr. Suzy Chen for their time, support, and advice. Many people within the Zhou laboratory have provided immeasurable aid to make this work possible, including Dr. Margaret Cooper who had originally identified the catarct phenotype in ephrin-A5$^{-/-}$ mice; Dr. Guanfang Shi for her instruction on biochemistry techniques; and Ms. Yuhai Sun for her general support. Several others have provided their time and expertise on several fronts that I would like to thank, including Dr. Norman Kleiman for his lens expertise and support; Dr. James Zheng and Dr. Daniel Komlos for their confocal imaging aid; Dr. Janet Alder, Dr. Smita Thakker-Varia, and Mr. Clifton Fulmer for their expertise and assitance on the RNA amplification and RT-PCR experiments; and Dr. Suzie Chen and Mr. Brian Wall for their support in providing cell lines and helping in conducting the MTT Assay. I am also indebted to the Rutgers/UMDNJ Neuroscience Graduate Program, the Department of Chemical Biology, and Laboratory Animal Services for their immeasurable help and support. Most importantly, I would like to thank my family and friends, especially my father, mother, and brother, who have given me constant support throughout my graduate career.

Table of Contents

Lists of Tables

List of Illustrations

CHAPTER 1: GENERAL INTRODUCTION - THE EPH FAMILY OF

RECEPTOR TYROSINE KINSASES

Receptor tyrosine kinases (RTKs) are crucial factors in regulating wide arrays of basic cellular processes (Robinson, Wu et al. 2000; Schlessinger 2000). Of this group, the largest subclass is the Eph family, named after the erythropoietin-producing hepatocellular carcinoma cell lines in which the first Eph receptor was isolated (Hirai, Maru et al. 1987). The Ephs had originally been associated with the guidance of neuronal processes to their respective targets through repulsive effects during neuronal development (Pasquale 2005). Since their initial discovery, Ephs have been found to be expressed in an assortment of tissues and are implicated in several key biological functions including axonal guidance, neural plasticity, angiogenesis, tissue patterning, cell proliferation, differentiation, and pathogenic processes such as cancer.

A. Families and Structure

Eph receptors are divided into the EphA and EphB subgroups based on both their extracellular surface sequence homology and their preference for interacting with either the ephrin-A or ephrin-B ligands, respectively (Pasquale 2005; Klein 2009). Interactions between the receptors and ligands are promiscuous within their respective classes; EphA receptors have the capacity to interact with ephrin-A ligands, while EphB receptors have the ability to bind to ephrin-B ligands. Binding between receptor-ligand classes are also possible and may also play important biological roles (Mellitzer, Xu et al. 1999; Yokoyama, Romero et al. 2001; Grunwald, Korte et al. 2004; Himanen, Chumley et al. 2004). To date, 14 Eph receptors (EphA1 – EphA8, EphA10; EphB1 – EphB4, EphB6)

and 8 ephrin ligands (ephrin-A1 – ephrin-A5, ephrin-B1 – ephrin-B3) have been identified in mammals (Klein 2009). The large size of this family and the promiscuous binding between ligand and receptor pairs also allows for a high degree of redundancy and compensation.

Receptor structure is highly conserved between both the EphA and EphB subgroups (Kullander and Klein 2002; Pasquale 2005; Klein 2009). The extracellular portion of the receptors contains an ephrin ligand-binding domain at the N-terminus, followed by a cystein-rich region epidermal growth factor (EGF) repeat motif and two fibronectin type-III repeats. The intercellular portion contains the signaling component which includes a juxtamembrane region, a tyrosine kinase domain, a sterile alpha motif (SAM), and a PDZ binding domain at the end of the C-terminus.

Recent studies on Eph receptor activities in the lens have found the SAM domain to be of particular importance in maintaining lens clarity (Shiels, Bennett et al. 2008; Jun, Guo et al. 2009; Zhang, Hua et al. 2009). The SAM domain is among the most ubiquitous protein interaction domains and is involved with the regulation of several biological processes, amongst which include protein clustering, kinase regulation, and transcriptional and translational control (Qiao and Bowie 2005). However, the role of the SAM domain in regards to Eph receptor function remains poorly understood. Structural studies on the EphA4 and EphB2 SAM domains have yielded the potential for Eph receptor clustering; the EphA4 SAM domain may be capable of forming dimers while the EphB2 SAM domain has the capacity of forming oligomers, though the biological relevance of these interactions remains unclear (Stapleton, Balan et al. 1999; Thanos, Faham et al. 1999; Thanos, Goodwill et al. 1999). Deletion of the EphA4 SAM domain

does not affect the activity of the receptor during the development of thalamocortical axons and does not affect kinase activity or clustering and ligand activation (Kullander, Mather et al. 2001; Dufour, Egea et al. 2006). Interestingly, Phe-for-Tyr mutations at position 928 within the EphA4 SAM domain had a pronounced effect in Xenopus development by enhancing ectopic induction of posterior protrusions, indicating that the EphA4 SAM domain may play some role in inhibiting EphA4 activity *in vivo* (Park, Warner et al. 2004).

Ephrin ligands are physically bound to the cell surface, with the major distinction between the two subclasses being in the mechanism of attachment; ephrin-A ligands interact with the surface through a glycosylphosphatidylinositol (GPI) anchor, while ephrin-B ligands have a transmembrane domain. This surface localization of the ephrin ligands plays a key role in their signaling attributes, particularly in the ability for the ligand to cluster and oligomerize to induce signaling (Himanen, Rajashankar et al. 2001; Toth, Cutforth et al. 2001; Smith, Vearing et al. 2004; Pasquale 2005). The GPI-anchored ephrin-As have the capacity of being cleaved (Hattori, Osterfield et al. 2000). More recent studies have also found that soluble ephrin-As, both in monomeric and oligomeric forms, may have biological roles and can also affect signaling (Wykosky, Palma et al. 2008; Alford, Watson-Hurthig et al. 2010).

B. Activation and Signaling

Eph receptor activation is induced by interactions with their respective ephrin ligands. Because both the receptors and ligands are typically membrane-bound, interactions between Eph-ephrin pairs requires direct intercellular contact. The Eph-ephrin system is particularly unique in that signaling can occur in a bidirectional manner,

in which interactions between the Eph receptor and ephrin ligand can induce activation in the receptor-expressing cell (forward signaling), ligand-expressing cell (reverse signaling), or both cells (bidirectional signaling) (Himanen, Rajashankar et al. 2001; Toth, Cutforth et al. 2001; Smith, Vearing et al. 2004; Pasquale 2005). The surface localization of the ephrin ligands plays a key role in their signaling attributes, particularly in the ability for the ligand to cluster and oligomerize to induce signaling (Himanen, Rajashankar et al. 2001; Toth, Cutforth et al. 2001; Smith, Vearing et al. 2004; Pasquale 2005). Crystallography studies have suggested that Eph-ephrin complexes are capable of interacting and forming tetrameric structures in a ring-like formation to initiate signaling in both interacting cells (Himanen, Rajashankar et al. 2001; Himanen, Saha et al. 2007). These interactions, in turn, result in conformational changes within the Eph receptor in a manner to support kinase domain activation (Huse and Kuriyan 2002; Himanen, Saha et al. 2007). Analysis of the EphB2 intracellular domain have also found that the juxtamembrane domain plays a key role in kinase activation as its unphosphorylated form is capable of interacting with the N-termainal region of the kinase domain and inhibits activity (Wybenga-Groot, Baskin et al. 2001; Himanen, Saha et al. 2007). Upon Eph receptor interaction with its respective ephrin ligand, this site becomes phosphorylated, causing structural changes that alleviate these constraints to allow for kinase domain activation (West and Valmadrid 1995; Wybenga-Groot, Baskin et al. 2001).

Eph receptors and ephrin ligands are associated with various effector proteins that are dependent or independent of kinase activity upon interaction between receptor-ligand pairs (Pasquale 2008). These effectors include the Src kinase family and the Ras and Rho

GTPases, which in turn can cause changes in actin cytoskeletal dynamics (Pasquale 2008; Pasquale 2010).

C. Ephrin-A5

Ephrin-A5 [also identified as AL-1, repulsive axonal guidance signal (RAGS), and ligand for Eph-related kinase-7 (LERK-7)], was isolated by two independent groups through affinity purification using an EphA5-IgG fusion protein column from the human breast carcinoma line BT20 (Winslow, Moran et al. 1995) and by 2D gel electrophoresis of the posterior tectum from embryonic day 9 (E9) chickens (Drescher, Kremoser et al. 1995). As the name suggests, the 25 kD protein is an A-classed ephrin ligand ligand, with expression being reported in several adult tissues including brain, heart, placenta, lung, and kidney (Winslow, Moran et al. 1995; Kozlosky, VandenBos et al. 1997).

Early studies of biological functions associated with ephrin-A5 have identified the ligand as a prominent axonal guidance factor as it inhibits axonal migration and evokes growth cone collapse (Drescher, Kremoser et al. 1995; Winslow, Moran et al. 1995). This activity has major implications *in vivo*, as ephrin-A5 has been shown to play an integral role in the formation of the retinotopic map of the visual system. Both ephrin-A5 and ephrin-A2 are expressed in the murine tectum; ephrin-A5 expression is expressed in a graded fashion with the highest concentrations observed in the posterior pole and the lowest levels in the anterior segment (Drescher, Kremoser et al. 1995; Frisen, Yates et al. 1998; Feldheim, Kim et al. 2000). In wild-type mice, axons projecting from the temporal retina migrating towards the optic tectum are restricted to the rostral portion of the superior colliculus. However, mice lacking ephrin-A5 experience aberrant growth of retinal axons normally targeted for the superior colliculus into the inferior colliculus

(Frisen, Yates et al. 1998). The patterning of projections by ephrin-A5 is, in large part, established through interactions with EphA3, which has high levels of expression in the temporal retina and low levels in the nasal retina (Cheng, Nakamoto et al. 1995). The retinal expression of EphA3 complements the ephrin-A5 tectum expression in relation to retinotectal mapping and further indicates an inhibition of axonal migration.

The involvement of ephrin-A5 in axonal guidance is also apparent in other neural systems, though the effects are context-dependent. Ephrin-A5 plays a role in the development of thalamocortical projections, inhibiting the outgrowth of thalamic and cortical limbic axons and not affecting thalamic sensorimotor axons (Gao, Yue et al. 1998; Ellsworth, Lyckman et al. 2005; Wilks, Rodger et al. 2010). The ligand is a critical factor in hippocampal development, affecting hippocampal neurite outgrowth, neurogenesis, and early synapse formation (Brownlee, Gao et al. 2000; Yue, Dreyfus et al. 2008; Akaneya, Sohya et al. 2010; Hara, Nomura et al. 2010). In addition, ephrin-A5 has the ability to inhibit neurite outgrowth of olfactory and striatal neurons, while promoting the survival and neurite growth of sympathetic and midbrain dopaminergic neurons (Gao, Sun et al. 2000; Cooper, Kobayashi et al. 2009).

Ephrin-A5 activity is not restricted to neural development and has important functions within other systems. The ligand is involved in spinal cord development, with expression in the dorsolateral portion of the spinal cord, and is capable of inhibiting the outgrowth of spinal motor neurites (Wang, Chadaram et al. 2001; Washburn, Cooper et al. 2007). The factor plays an important role in regulating cellular adhesion in neural tube development, as a subpopulation of mice lacking ephrin-A5 develop craniofacial deformations as a result of a failure of proper neural tube closure (Holmberg, Clarke et al.

2000). Ephrin-A5 plays roles in vascular biology, as its expression is observed in rat

cardiomyocytes (Li, Mi et al. 2001); additionally, ephrin-A5 null mutants have been

reported to have impaired vasculature in the hippocampus (Hara, Nomura et al. 2010).

Ephrin-A5 also has implications in cancers, as reports have indicated its ability as a

tumor suppressor in gliomas and colon cancer through regulation of epithelial growth

factor receptor (EGFR) (Hafner, Schmitz et al. 2004; Li, Liu et al. 2009; Wang, Chang et

al. 2012) and lowered expression in chondrosarcomas in comparison to normal articular

cartilage (Kalinski, Ropke et al. 2009). Paradoxically, ephrin-A5 has been found to be

over-expressed in ovarian cancer (Herath, Spanevello et al. 2006). The contradictory

results may be due to the nature of the cancer and particular mechanisms of action that

ephrin-A5 may play under each circumstance. Differences in experimental design, such

as the use of *in vivo* tissues versus *in vitro* cell lines, may also account for the variance.

Recent investigations from our laboratory have identified ephrin-A5 to be a major

factor in eye development. We have shown that ephrin-A5$^{-/-}$ mice develop ocular

abnormalities, namely cataracts and persistent hyperplastic primary vitreous (PHPV),

documenting critical roles in ocular development.

CHAPTER 2: REGULATION OF LENS DEVELOPMENT AND FUNCTION BY EPHRIN-A5

Introduction

Proper vision requires the precise focusing of light from the extraocular environment onto the retina. This task is accomplished through the lens, a transparent biconvex ellipsoid tissue situated posterior to the cornea and anterior to the retina. The key role of this tissue lies in providing proper light refraction to the retina and allowing for clear vision, a function made possible by its high refractive index and transparency.

A. Lens Development and Morphology

The bulk of the lens consists of organelle-less lens fiber cells; the oldest cells, formed during embryonic development (known as primary fiber cells), comprise the core of the tissue while the youngest and most newly formed cells (known as secondary fiber cells) are found more distally away from the center (Fig. 2-1). The anterior face of the tissue comprises of a single layer of epithelium that consistently divides and differentiates into mature fiber cells. The entirety of the structure is encompassed within an elastic capsule.

The distinct anterior-posterior polarity of the lens is established during the initial developmental stages of the tissue and has been extensively reviewed (Lovicu and McAvoy 2005; Danysh and Duncan 2009) (Fig. 2-2). The murine eye begins to form as early as embryonic day 8.5 (E8.5) with the protrusion of the optic vesicle from the developing forebrain near the head ectoderm. The head ectoderm and optic vesicle are closely associated though not touching, and by E9.5 the overlying optic vesicle thickens

to form the lens placode. At E10.5 these two areas invaginate, the lens placode forming the lens pit and the optic vesicle producing the optic cup. The lens pit deepens at E11.5 to form the lens vesicle, and by E12.5 the vesicle has completely closed and pinched off from the surface ectoderm. At E13.5, lens cells at the posterior portion of the lens extend outwards towards the anterior layer of cells and fill the lumen, with the single stratum of cells in the anterior portion becoming the lens epithelium and the elongated cells forming the primary lens fiber cells.

Growth of the lens after initial formation continues through embryonic development and into the postnatal stages (Lovicu and McAvoy 2005). Cells of the lens epithelium anterior to the lens equator, a region known as the germinative zone, continue to divide, replacing cells undergoing differentiation. Meanwhile, the epithelial cells posterior to the equator, an area known as the transitional zone, elongate and differentiate into secondary lens fiber cells, continually adding onto the preexisting lens structure and comprising the majority of the lens.

While the primary fiber cells are irregularly-shaped (Shestopalov and Bassnett 2000), the secondary fiber cells are highly organized elongated structures arranged in meridonal rows (Kuszak, Zoltoski et al. 2004) (Fig. 2-1). In cross-section, the secondary fiber cells are arranged into flattened hexagons with two parallel long edges connected by four shorter edges. Enlargement of the lens involves the overlaying of mature fiber cells with additional layers of newly formed differentiated cells, or growth shells. Each additional shell adds to the diameter of the lens, a combination of the addition of more secondary fiber cells per growth shell as well as the widening of fiber cells with each additional growth shell (Kuszak, Zoltoski et al. 2004).

B. Cataracts

Visual impairments, a disability which include both blindness and low vision, continue to be a major global health problem in the 21st century, affecting over 161 million people worldwide (Resnikoff, Pascolini et al. 2004; Resnikoff, Pascolini et al. 2008). Of this, the single largest contributor of global blindness is cataract, or the development of opacity within the lens. This condition is widespread, accounting for nearly 50% of all cases of visual deficits (Congdon, Friedman et al. 2003; Resnikoff, Pascolini et al. 2004; Resnikoff, Pascolini et al. 2008).

Cataract formation is a disease often associated with aging and environmental factors. Intrinsic changes in the aging lens, including increased light-scattering, decreased tissue elasticity, alterations in lens protein composition, and losses in chaperone function to handle antioxidant and free-radical stressors may contribute to opacification of the tissue. Additional external risk factors, including environmental factors such as ultraviolet-B (UV-B) light exposure (McCarty and Taylor 1996), lifestyle-associated aspects such as smoking (West and Valmadrid 1995), and nutrition and disease-related risk factors such diabetes (Hodge, Whitcher et al. 1995), are also are known to play roles in cataract formation (Hodge, Whitcher et al. 1995; Robman and Taylor 2005).

Heredity also has been found to play an important role in the susceptibility of cataracts. More recent advances in human disease gene mapping have revealed a strong genetic component related to cataract formation (Hammond, Duncan et al. 2001; McCarty and Taylor 2001). To date, mutations in more than 35 loci within the human genome have been linked to cataracts, and the affected genes have been associated with

lens development and maintenance (Zhang, Guo et al. 2004; Hejtmancik 2008; Santana, Waiswol et al. 2009). These include mutations in lens crystallins, transcription factors, growth factors, and proteins regulating interlenticular circulation and lens cell structure (Hejtmancik 2008).

My recent studies and work from known genetic analyses have implicated roles of gene mutations in the Eph family to lead to cataracts (Cooper, Son et al. 2008; Jun, Guo et al. 2009; Zhang, Hua et al. 2009; Kaul, Riazuddin et al. 2010; Cheng and Gong 2011; Tan, Hou et al. 2011; Shi, De Maria et al. 2012). I have shown that mice lacking ephrin-A5 develop cataracts at postnatal stages (Cooper, Son et al. 2008). The Eph family receptor EphA2 has also been implicated in lens development, as mice lacking EphA2 have been found to also develop cataracts (Jun, Guo et al. 2009). Additionally, mutations in EphA2 have been implicated in cataract formation within human populations (Shiels, Bennett et al. 2008; Jun, Guo et al. 2009; Zhang, Hua et al. 2009; Kaul, Riazuddin et al. 2010).

Results

A. Ephrin-A5$^{-/-}$ mice develop cataracts

In our analysis of ephrin-A5 functions, we had noticed that ephrin-A5$^{-/-}$ mice develop cataracts (Fig. 2-3). Both slit lamp and scheimpflug revealed aberrations in light refraction and the formation of cataracts in the ephrin-A5$^{-/-}$ mice (Fig. 2-3A-D). Further histological analysis of adult ephrin-A5$^{-/-}$ eyes indicated varying degrees of severity in the cataract phenotype (Fig. 2-3E-J). These deformations include posterior lens rupture (Fig. 2-3F) and complete tissue degeneration (Fig. 2-3G). Aberrations in the ephrin-A5$^{-/-}$ lens

were consistently evident in the bow region with the presence of abnormally shaped lens fiber cells and the formation of vacuoles (Fig. 2-3I, see arrow and arrowhead).

B. Alterations in gross morphology of the postnatal ephrin-A5$^{-/-}$ lens

With ephrin-A5$^{-/-}$ mice developing severe lens deficits, we next asked how these changes affected the gross morphology of ephrin-A5$^{-/-}$ lenses (Fig. 2-4). In order to determine the refractive properties of wild-type and ephrin-A5$^{-/-}$ lenses, eyes were enucleated and lenses were imaged under warmed media over a mesh grid. Imaging at P7 and P14 showed no distinct alteration overall in lens morphology or light refraction between wild-type and ephrin-A5$^{-/-}$ lenses. However, by P21 a dense opacity in the ephrin-A5$^{-/-}$ lens had become visible while the wild-type controls remained transparent (Fig. 2-4A). When comparing lens diameters of wild-type versus ephrin-A5$^{-/-}$ animals, no significant differences were observed until P21, at which point ephrin-A5$^{-/-}$ lenses were found to be slightly but significantly smaller than wild-type controls (Fig. 2-4B). No significant differences in lens weight were observed between the two groups at any of the early postnatal stages (Fig. 2-4C). Analysis of posterior suture formation prior to cataract formation indicated that a normal Y-shaped structure was present in wild-type and ephrin-A5$^{-/-}$ lenses (Fig. 2-4D). These observations indicate that alterations in lens cell morphology in ephrin-A5$^{-/-}$ animals results in structural deformities by P21.

C. Deformations in lens structure in the ephrin-A5$^{-/-}$ postnatal eyes

We next set out to determine the developmental time in which lens abnormalities occurred in the ephrin-A5$^{-/-}$ mouse by analyzing histological sections of wild-type and ephrin-A5$^{-/-}$ eyes from several embryonic and postnatal stages (Fig. 2-5). Sections of

embryonic and newborn ephrin-A5$^{-/-}$ lenses revealed no clear morphological differences in comparison to wild-type controls, indicating that the overall development of ephrin-A5$^{-/-}$ lenses during embryogenesis was normal (Fig. 2-5A-F). However, analysis of ephrin-A5$^{-/-}$ lenses at postnatal stages revealed the presence of lens deformities (Fig 2-5G-L). Lens deficits were observed in some mice as early as P7 and easily identified by P21 with the formation of large vacuoles near the lens bow region (compare Fig. 2-5H and K, see arrows). These lens abnormalities were exacerbated in later stages, as complete lens degeneration was observed in the ephrin-A5$^{-/-}$ lens by P60 (compare Fig. 2-5I-L). Together, these observations indicate that the integrity of the ephrin-A5$^{-/-}$ lens structure begins to fail at postnatal stages.

D. Disruption of lens fiber cell organization in the ephrin-A5$^{-/-}$ lens

Our initial morphological analysis of ephrin-A5$^{-/-}$ lenses revealed major alterations in the lens at postnatal stages. However, the specific nature of these deficits remained to be elucidated, as changes in the regulation of the lens fiber cells, epithelium, or both could be resulting in vacuole formation in the mutant lenses. As a result, we set out to determine whether alterations of fiber cell organization were responsible for cataract formation in ephrin-A5$^{-/-}$ animals. P21 lenses were cryosectioned coronally and immunostained for various markers, including the adherens junction molecule β-catenin and the tight-junction protein ZO-1, to delineate fiber cell borders and regions (Fig. 2-6). Wild-type lens fiber cells were arranged in organized rows, with ZO-1 expression displaying distinct cortical, subcortical, and central regions (Fig. 2-6A-C). Ephrin-A5$^{-/-}$ lens fiber cells also showed the distinct ZO-1 layers; however, the fiber cells in these lenses were in disarray, with severe alterations being observed in the fiber cell shape (Fig.

2-6D-F). Fiber cell disorganization is observed throughout the entirety of the fiber cell layers, as the cortical, subcortical, and central regions all exhibited a loss of organization (Fig. 2-6G-I). These findings indicate that while the overall differentiation of the ephrin-A5^{-/-} fiber cells is maintained, the organization of ephrin-A5^{-/-} fiber cells is severely disrupted.

While alterations in lens fiber cell organization were observed in the ephrin-A5^{-/-} lenses, these disruptions could be a result of initial defects in the lens epithelium. We therefore asked whether the lens epithelium is altered in these mutant mice which may contribute to cataract formation (Fig. 2-7). To identify if any noticeable structural changes were present in the lens epithelium, lens epithelial explants of P21 wild-type and ephrin-A5^{-/-} lenses were stained for the adherens junction proteins β-catenin (Fig. 2-7A-D) and E-cadherin (Fig. 2-7E-H) to delineate lens epithelial cells. No differences were observed between the wild-type and mutant lens epithelium in regards to morphology or adherens junction expression (Fig. 2-7). In addition, saggital sections through wild-type and ephrin-A5^{-/-} lens epithelia were analyzed for β-catenin or E-cadherin expression. These results indicate that the alterations observed within the ephrin-A5^{-/-} lens are a result of defective lens fiber cell structures.

E. CP49 status does not affect cataract formation in ephrin-A5^{-/-} mice

The wild-type and ephrin-A5^{-/-} mice had been bred under a mixed background of C57BL/6 and S129. Mice under the S129 background have been previously found to have deficiencies in the lens-specific intermediate filament protein CP49 (Alizadeh, Clark et al. 2004; Sandilands, Wang et al. 2004). We therefore analyzed whether the status of CP49 affected the formation of cataracts in ephrin-A5^{-/-} mice (Fig. 2-8). Ephrin-

A5$^{+/+}$ mice with the CP49 mutation at P60 (Ephrin-A5$^{+/+}$;CP49$^{-/-}$) were found to be transparent with no observable light obstruction (Fig. 2-8A), while ephrin-A5$^{-/-}$ mice with wild-type, heterozygous, or homozygous mutant CP49 all developed cataracts at similar frequences [Ephrin-A5$^{-/-}$;CP49$^{+/+}$: 100% (n=4); Ephrin-A5$^{-/-}$;CP49$^{+/-}$: 73% (n=11); Ephrin-A5$^{-/-}$;CP49$^{-/-}$: 83% (n=6), Fig. 2-8B-D). Together, this evidence suggests that the cataracts observed in ephrin-A5$^{-/-}$ mice occur independently of CP49.

F. Ephrin-A5 expression found throughout the developing eye

To determine whether the spatial and temporal features of deficiencies in ephrin-A5 corroborate with the expression of the gene, we examined the localization of ephrin-A5 throughout murine eye development (Fig. 2-9). Wild-type and ephrin-A5$^{-/-}$ animals at several pre- and postnatal stages were sectioned and stained with EphA5-AP, a receptor for ephrin-A ligands. EphA5-AP staining was observed as early as E12 in the wild-type eye, as expression was observed in both the retina and lens, with continued expression in the eye through P7 (Fig. 2-9A-E). In contrast, the ephrin-A5$^{-/-}$ eye showed little staining with EphA5-AP (Fig. 2-9F-J).

EphA5-AP staining in wild-type tissues was particularly prominent in several parts of the eye (Fig. 2-10). At E14, expression of ephrin ligands was observed in the lens bow, lens epithelium, ciliary body, and cornea by E14 (Fig. 2-10A). Continued expression was observed in these areas at P0 and P7 (2-10C and D), though in lower concentrations. The robust staining of EphA5-AP in the wild-type eyes and absence of detection in the ephrin-A5$^{-/-}$ eyes (Fig. 2-10E-H) confirms ephrin-A5 to be the major ephrin-A ligand in the developing murine eye.

G. Expression of the EphA2 receptor in the developing lens

Ephrin activity is mediated through its interactions with Eph receptors. Previous reports have indicated that EphA2 is important in lens development, as mutations in this Eph receptor are known to result in cataractogenesis (Shiels, Bennett et al. 2008; Jun, Guo et al. 2009; Zhang, Hua et al. 2009; Kaul, Riazuddin et al. 2010; Tan, Hou et al. 2011). We therefore analyzed the expression profile of EphA2 at various developmental stages (Fig. 2-12). Similar to ephrin-A ligand localization in the lens, EphA2 localization is observed early in lens development, being detected in the presumptive lens as early as E11 (Fig. 2-11A). This expression continues through lens development and well into adulthood, with expression in the lens being observed as late as P60 (Fig. 2-11B-F). At E14, EphA2 expression is observed in both the lens epithelium and in the lens fiber region near the bow region similar to that observed in the ephrin-A ligand expression (Fig. 2-11G). In addition, levels of EphA2 are also seen at the junctions between the lens fibers and epithelium in the anterior portion of the lens (Fig. 2-11H). At P7, expression of EphA2 is still observed in both the lens fiber subcortical region and in the lens epithelium (Fig. 2-11I and J). Together, these data indicate that strong expression of EphA2 is present throughout lens at embryonic and postnatal periods.

H. Subcortical localization of ephrin-A5 and EphA2 in the mature lens

While strong ephrin-A5 expression is observed in the prenatal lens, cataract formation in ephrin-A5$^{-/-}$ mice occurs during the postnatal stages. To determine the location of this activity in the adult lens, P21 lenses were analyzed in cross-section for both ephrin-A5 and EphA2 expression (Fig. 2-12). EphA2 expression determined using a goat anti-EphA2 antibody labeled with a CY3-conjugated anti-goat secondary antibody.

Ephrin-A5 levels were established using an EphA3-Fc fusion protein to label all ephrin-A ligands, and levels were compared between wild-type and ephrin-A5$^{-/-}$ tissues. Expression of both the EphA2 receptor and ephrin-A ligands were observed predominantly in the subcortical region of the adult lens (Fig. 2-12B and C). The majority of the labeling for ephrin-A ligands is specific for ephrin-A5, as ephrin-A5$^{-/-}$ lenses show reduced labeling under equal time exposure (Fig. 2-12D). Higher magnification imaging revealed both EphA2 and ephrin-A5 expression to be specifically on the short edges of the lens fiber cells, with stronger levels at the intercellular junctions (Fig. 2-12B'-D').

We further verified that both ephrin-A5 and EphA2 were localized in the same regions through double labeling studies (Fig. 2-13). In the wild-type lens, both EphA2 and ephrin-A ligand expression using EphA3-Fc was observed to be co-localized with each other (Fig. 2-13A-C). Ephrin-A5-/- also displayed expression of EphA2 in the lens fiber cell layer (Fig. 2-13D); however, a significant reduction of EphA3-Fc staining was observed in these lenses (Fig. 2-13E), further verifying ephrin-A5 to be the major ephrin-A ligand in the mature lens.

I. Ephrin-A5 activation of EphA2 in the lens

Ephrin-A5 and EphA2 expression in embryonic and adult lenses show similar localization in the subcortical region in the lens. As a result, we asked whether ephrin-A5 is capable of activating EphA2 both *in vitro* and in the lens (Fig. 2-14). We first analyzed whether ephrin-A5 is capable of activating EphA2 *in vitro*. 293T cells were transfected with EphA2 and treated with or without ephrin-A5. EphA2 activation was determined through immunoprecipitation of EphA2 from the cell lysate followed by

Western blot analysis. Cells treated with ephrin-A5 displayed robust tyrosine phosphorylation in comparison to the control group indicating that ephrin-A5 is capable of activating the EphA2 receptor (Fig. 2-14A).

We next asked whether ephrin-A5 is involved with EphA2 phosphorylation in lens tissue. For this experiment, EphA2 was immunoprecipitated from P6 wild-type and ephrin-A5$^{-/-}$ lens lysates and examined for tyrosine phosphorylation through Western blotting. Tyrosine phosphorylation in EphA2 from the ephrin-A5$^{-/-}$ was found to be reduced in comparison with wild-type controls (Fig. 2-14B). Together, these studies indicate that ephrin-A5 is responsible for EphA2 activation in the lens.

Discussion

This section has characterized and detailed the cataract phenotype in ephrin-A5$^{-/-}$ mice. Lens abnormalities in the ephrin-A5$^{-/-}$ animals are observed at postnatal stages, with lens opacity occurring by P21. Structural defects in the lens are first observed in the outer lens fiber cell region where cells in the ephrin-A5$^{-/-}$ lens are severely disorganized. In addition, we have found that ephrin-A5 and EphA2, Eph family molecules known to play significant roles in lens development, are expressed throughout the lens starting during early prenatal development and are expressed at postnatal stages with similar localization. The cataracts in the ephrin-A5$^{-/-}$ mutants occur regardless of the presence of the CP49 mutation.

A. Eph Signaling and Cataracts

Recent genetic studies in congenital and age-related cataracts have identified the Eph family to be a key regulator of lens development. The human chromosome region

1p36 has been previously identified as a locus associated with autosomal dominant posterior polar cataracts (Eiberg, Lund et al. 1995; Ionides, Berry et al. 1997; Burdon, Hattersley et al. 2008; Hattersley, Laurie et al. 2010). Analysis of affected genes within this region has identified mutations in the Eph receptor *EPHA2* to be linked with congenital and age-related cataract patients (Table 2-1).

Thus far, six studies have associated human populations with both congenital and age-related cataracts connected with mutations within *EPHA2* (Shiels, Bennett et al. 2008; Jun, Guo et al. 2009; Zhang, Hua et al. 2009; Kaul, Riazuddin et al. 2010; Tan, Hou et al. 2011; Sundaresan, Ravindran et al. 2012). Of the identified human mutations, five variants were associated with autosomal dominant-inherited cataracts (Shiels, Bennett et al. 2008; Zhang, Hua et al. 2009) while one mutation is linked to recessive congenital cataracts (Kaul, Riazuddin et al. 2010). The human *EPHA2* cataract mutations have been localized to the intracellular compartment of the receptor.

Four of the known mutations identified from independent families thus far have been located within the SAM domain. Two are point mutations that are associated with posterior polar cataracts: Shiels et al. (2008) identified a transversion mutation (c.2842G>T) which changed the translation of glycine into tryptophan at codon 948 (G948W) (Shiels, Bennett et al. 2008), while Zhang et al. (2009) identified a missense mutation (c.2819C>T) which replaced a threonine at codon 940 with an isoleucine residue (T940I) (Zhang, Hua et al. 2009). Additionally, Zhang et al. (2009) identified two more cataract mutations, including a splicing mutation (c.2826-9G>A) (Zhang, Hua et al. 2009) which creates a splice acceptor site at intron 16 resulting in a 7 base pair intron sequence insertion that is associated with posterior polar cataracts, and a frameshift

mutation (c.2915_2916delTG) (Zhang, Hua et al. 2009) that is linked to total cataracts.
These latter two mutations result in novel C-terminal sequences of EPHA2; c.2826-9G>A forms a C-terminal polypeptide of 71 amino acid residues, while
c.2915_2916delTG forms a polypeptide of 39 amino acids (Zhang, Hua et al. 2009).
Interestingly, these latter two described mutations share the same last 39 amino acid residues. To date, all described SAM domain mutations associated with human cataracts have been autosomal dominant (Shiels, Bennett et al. 2008; Zhang, Hua et al. 2009) suggesting inactivating interactions with the wild-type EPHA2 receptor.

The kinase domain of EPHA2 also plays important roles in lens regulation, as mutations within this region have been linked to cataracts in human populations (Jun, Guo et al. 2009; Kaul, Riazuddin et al. 2010). Jun et al. (2009) identified a transversion mutation (c.2162G>T) (Jun, Guo et al. 2009) resulting in a change of codon 721 from an arginine to a glutamine residue (R721N) and being linked to cortical cataract with autosomal dominant inheritance. Kaul et al. (2010) has also described a missense mutation (c.2353 G>A) (Kaul, Riazuddin et al. 2010) within the kinase domain resulting in the substitution of alanine for a threonine at codon 785 (A785T) and being associated with the formation of a nuclear cataract. This is the only EPHA2 cataract mutation identified so far to be of autosomal recessive inheritance.

B. Ephrin-A5 and the organization of lens fiber cells

Our current study indicates that deficits in the ephrin-A5 lens are primarily in the lens fiber cell layers. Unlike the typical lens fiber cell architecture in which cells have uniformly elongated hexagonal shapes arranged in regular rows, lens fiber cells in ephrin-A5^{-/-} animals are disarrayed with fiber cells in various orientations. In addition, large

vacuoles are formed between fiber cells, contributing to the disorganization and eventual cataract formation of the ephrin-A5$^{-/-}$ lens.

The deficits in the lens fiber cells of the ephrin-A5$^{-/-}$ lens may result in additional consequences as a result of the disorganization in lens architecture. The uniform packing of lens fiber cells is particularly important in order to maintain proper lens circulation given the absence of vasculature (Ito and Yoshioka 1999; Zhu, Madigan et al. 2000). Our present study had found that while localization of ZO-1, a protein involved with lens circulation and gap junction regulation, remains along the cell membrane in the ephrin-A5$^{-/-}$ lens, the organization of these structures is highly disrupted. The correct regionalized localization of ZO-1 in the cortical, subcortical, and central lens areas implies that ephrin-A5 may have only an indirect impact on the regulation of gap junction proteins. However, the disorganization of the fiber cell layers may severely impact the circulation of nutrients throughout the lens, further contributing to cataract formation.

C. Discrepancies in Cataract Onset in Ephrin-A5$^{-/-}$ and EphA2$^{LacZ/LacZ}$ mice

EphA2$^{-/-}$ mice suffer from congenital cataracts in a manner similar to ephrin-A5$^{-/-}$ mice, as they have been found to develop subcapsular vacuoles leading to lens opacity and rupture (Jun, Guo et al. 2009). In the current study, EphA2 expression in the lens during development was found in similar locations with ephrin-A5, including the lens fiber regions near the bow and the lens epithelium. Additionally, a significant amount of EphA2 expression was also observed in the anterior regions of the fiber cell layer near the junction with epithelial cells. Based on our expression data and previous studies, the Eph family may have additional roles in lens development in addition to the maintenance of fiber cell organization. EphA2$^{-/-}$ lenses have been previously reported to have sutural

deficits and form epithelial lesions (Shi, De Maria et al. 2012). Together, this may indicate that EphA2 may play a role in the formation of epithelial and fiber cell junctions.

Though both ephrin-A5 and EphA2 share a similar expression profile in the lens, the ephrin-A5 and EphA2 mutant mouse models indicate a distinct difference in the timing of cataract onset. Ephrin-A5$^{-/-}$ animals have noticeable lens deficits as early as P7 and become opaque by P21, while EphA2$^{-/-}$ animals develop lens deficits at 1 month of age and cataracts by 5 months (Jun, Guo et al. 2009). One possibility for this difference is the compensation of other EphA receptors in the mature lens; several Eph receptors are present in the lens (data not shown) and may play compensatory roles in the absence of EphA2. In contrast, EphA5-AP and EphA3-Fc staining detected high levels of ephrin ligand expression in the wild-type lens but very little in the ephrin-A5$^{-/-}$ lens indicating ephrin-A5 to be the major A-class ligand in the mature lens. The lack of compensation by other ephrin-A ligands may therefore result in an earlier cataract phenotype in the ephrin-A5$^{-/-}$ lens, while the presence of other distinct EphA receptors aside from just EphA2 may cause a delay in the lens phenotype. The later onset of the phenotype by the EphA2$^{-/-}$ animal may also be due to the animal background of the ephrin-A5$^{-/-}$ mice and the EphA2$^{-/-}$ animals, as variability of the cataract phenotype has documented in other studies (Jun, Guo et al. 2009; Shi, De Maria et al. 2012).

Mouse strains may play a role in the difference of observed phenotype as differences in gene expression between backgrounds have been previously reported (Cooper, Son et al. 2008; Jun, Guo et al. 2009; Cheng and Gong 2011; Shi, De Maria et al. 2012). The ephrin-A5$^{-/-}$ mice used for this study are under a mixed background of C57BL/6, S129, and CD-1 strains, while the EphA2$^{LacZ/LacZ}$ mice are under a FVB/NJ

background. Other studies on the effects of ephrin-A5 on the lens using mice under a pure C57BL/6 background have found alterations in the lens epithelium with minimal alterations in the lens fiber cells and severe changes in the lens epithelium (Cheng and Gong 2011). In our current study we observed major alterations in lens fiber cell organization but observed no disruptions in the lens epithelium. One known mutation in S129 strains affecting the lens is the deletion of the intermediate filament CP49 (Alizadeh, Clark et al. 2004; Sandilands, Wang et al. 2004). Our own observations have found that regardless of the status of CP49, ephrin-A5$^{-/-}$ mice under this mixed background still develop cataracts indicating the factor may not directly affect the cataracts observed in ephrin-A5$^{-/-}$ mutants. However, his does not discount other differences between mouse strains that may be contributing to the differences in cataract formation.

D. The role of the Eph family in early lens development

While ephrin-A5 and EphA2 are expressed in the lens at early stages, the role of ephrins in prenatal lens development, if any, remains unclear. The embryonic development of the ephrin-A5$^{-/-}$ lens is grossly normal, as abnormalities were not observed in the ephrin-A5$^{-/-}$ lens until early postnatal stages. One possibility for this lack of phenotype in early development is that the need for highly ordered and structured fiber cells may not be required in the embryonic lens. In normal lens development, primary lens fiber cell layers are polygonal and disorganized, whereas the secondary fiber cell layer are highly regular flattened hexagonal cells (Taylor, al-Ghoul et al. 1996; Shestopalov and Bassnett 2000). Another possibility is that the lack of phenotype at early developmental periods may be dependent on other ephrin ligands at the embryonic

stages that are insufficient or absent in postnatal periods. Specifically, other Eph-ephrin interactions that are not detected by EphA5-AP staining, including the B-class ephrins, may be playing concurrent roles in early lens development and preserving the majority of developmental activity that this family of molecules plays during early development. It may also be possible that the major roles of ephrin-A5 regulation of the lens occur in early stages of development and not during the postnatal periods, with its absence during these critical periods making the lens susceptible to alterations during maturation ultimately leading to cataracts. This may explain for ephrin-A5 lens expression being seen prominently at earlier embryonic stages of ocular development and with reduced levels in postnatal stages.
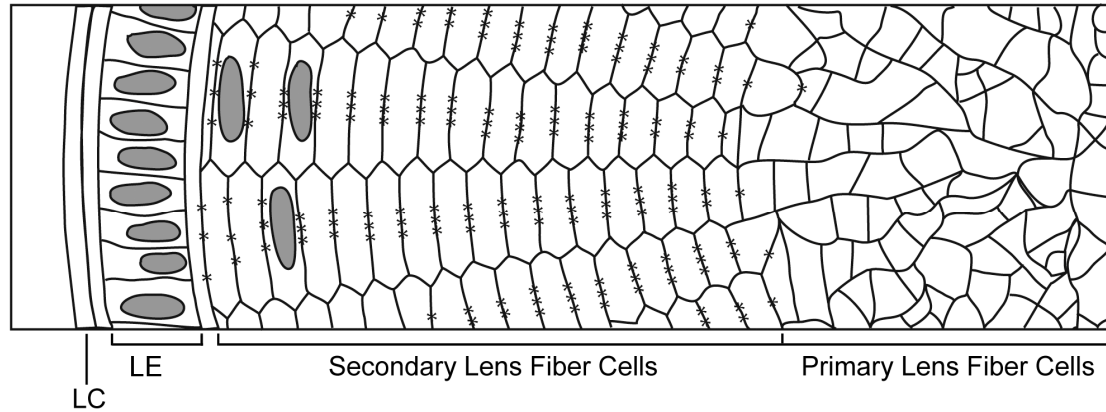
Figure 2-1: Cross-section of the mature lens
The core of the lens consists of irregularly-shaped primary lens fiber cells formed during the early stages of lens development. After the initial development of primary fiber cells, secondary lens fiber cells form continuously from this core and are arranged in regular hexagonal structures. The anterior face of the lens contains a monolayer of lens epithelial cells (LE) that continually divide and differentiate into secondary lens fiber cells. The entire structure is encapsulated by a lens capsule (LC). * denotes gap junction complexes along the long edges of secondary fiber cells.
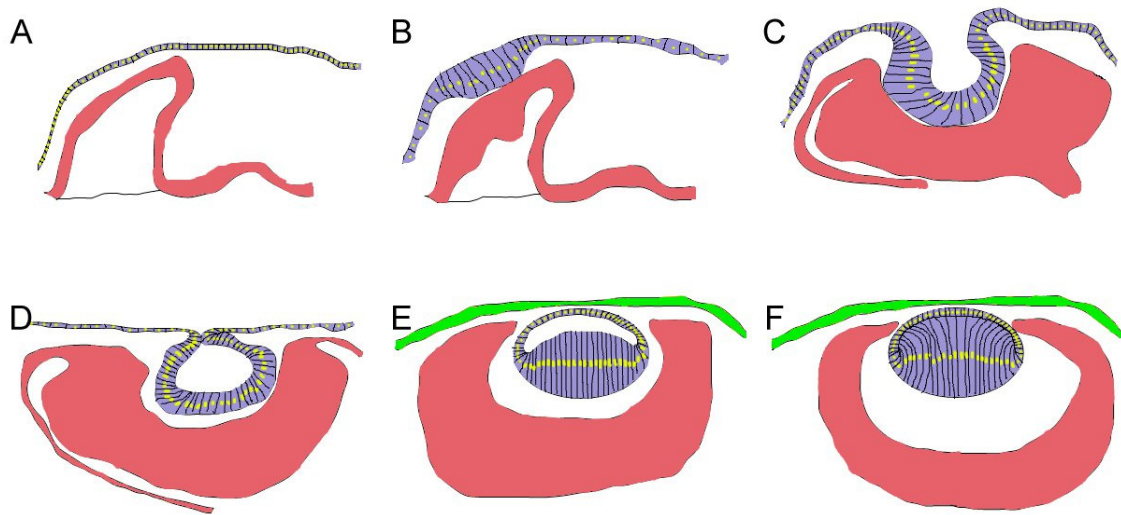
Figure 2-2: Stages of early lens development
(A) E8.5: Optic vesicle protrudes (in pink) from the developing forebrain and closely associates with the head ectroderm (in blue). (B) E9.5: Optic vesicle thickens to form the lens placcode. (C) E10.5: Both the head ectoderm and lens placcode invaginate. The lens placcode forms the lens pit, while the optic vesicle becomes the optic cup. (D) E11.5: The lens pit deepens and forms the lens vesicle. (E) E12.5: The lens vesicle has completely pinched off to from the surface ectoderm. (F) E13.5: Posterior lens cells extend towards the anterior layer to fill the lumen. Figure adapted from Lovicu and McAvoy (2005).
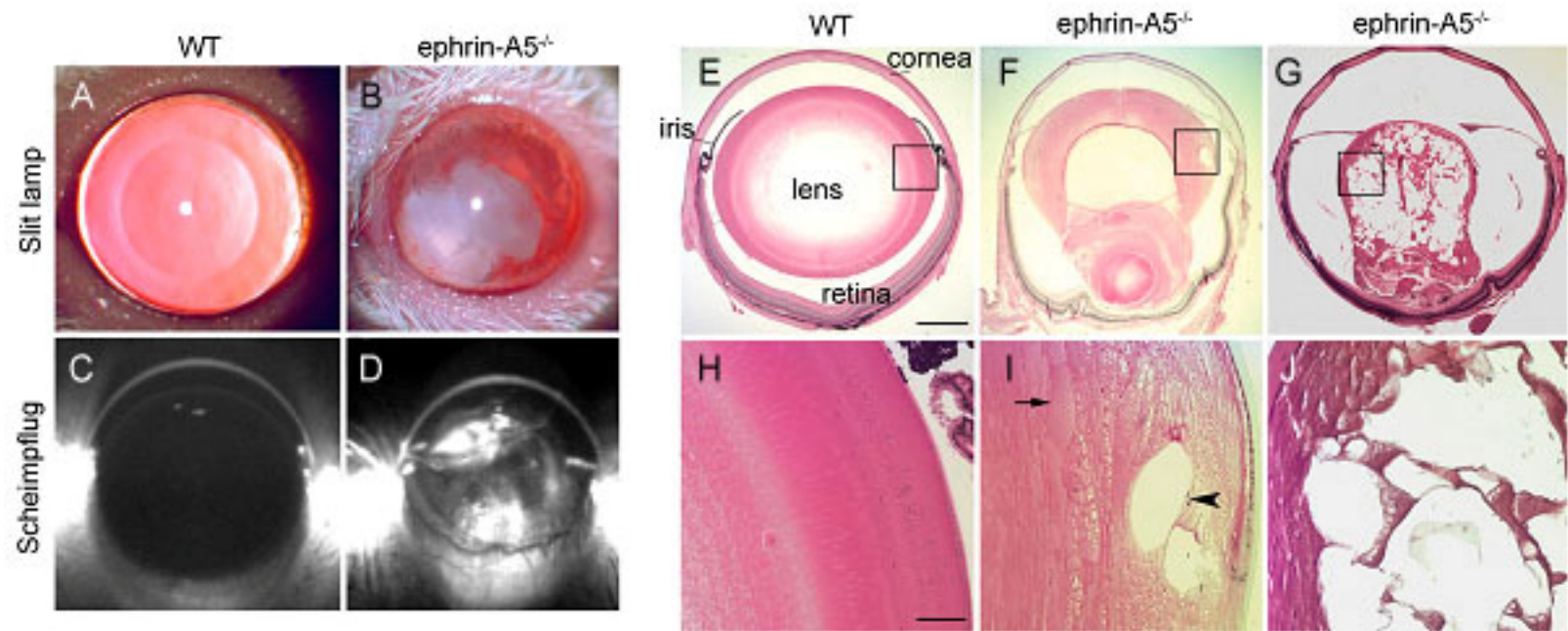
Figure 2-3: Cataract formation in ephrin-A5$^{-/-}$ mice

(A and B) Slit-lamp imaging of wild-type (A) and ephrin-A5$^{-/-}$ (B) mouse lenses. Wild-type lenses show a clear and crystalline lens while ephrin-A5$^{-/-}$ lenses develop cataracts.

(C and D) Scheimpflug imaging of wild-type (C) and ephrin-A5$^{-/-}$ (D) mouse lenses. Wild-type lenses are transparent while ephrin-A5$^{-/-}$ display an obstruction of light within the lens.

(E-J) Histological sections of adults lenses in wild-type (E and H) and ephrin-A5$^{-/-}$ (F and G, I and J) animals. Large aberrant fiber cells (arrow), vacuole formation (arrowhead) is apparent in the ephrin-A5$^{-/-}$ lens, ultimately resulting in complete lens degeneration. H, I, and J are higher magnification images of the lens bow in E, F, and G, respectively. Scale bar in E = 500 μm; in H = 100 μm.
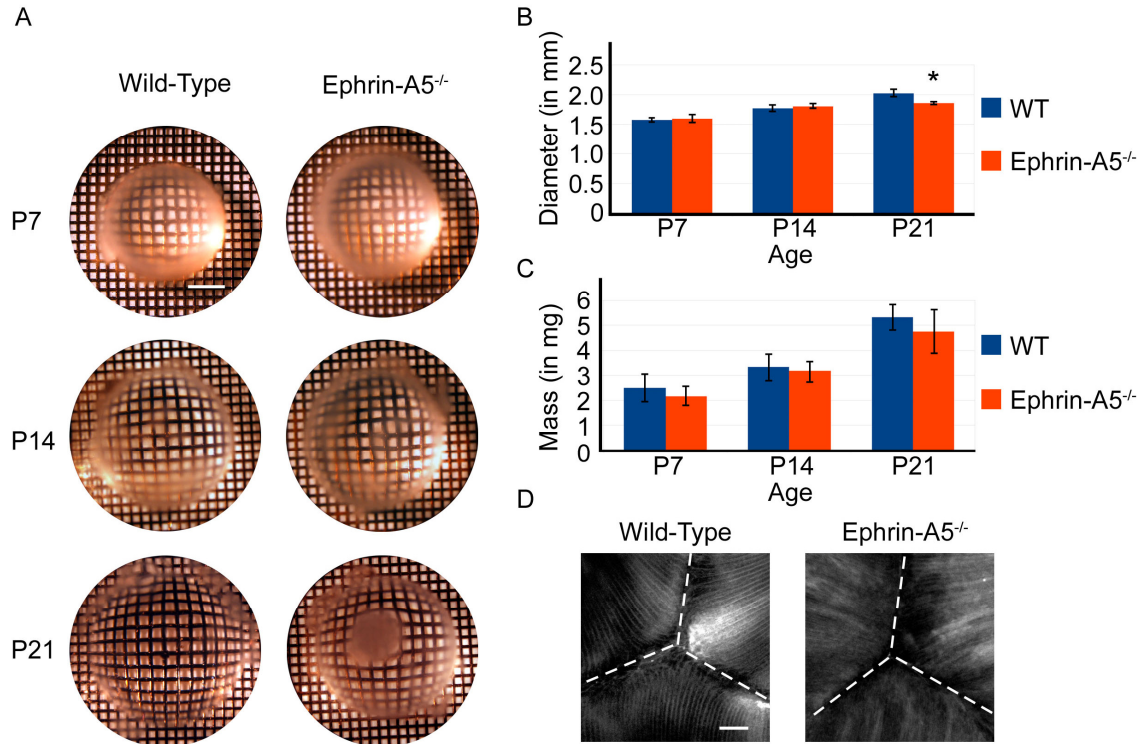
Figure 2-4: Gross morphology of wild-type and ephrin-A5$^{-/-}$ lenses
(A) Postnatal lens morphology of wild-type and ephrin-A5$^{-/-}$ lenses at P7, P14, and P21. P7 and P14 ephrin-A5 mutant lenses appear grossly normal. However, by P21 opacity becomes quite prominent in the ephrin-A5$^{-/-}$ lens while the wild-type lens remains transparent. Scale bar in top left panel = 500 μm.
(B) Comparison of wild-type and ephrin-A5$^{-/-}$ lens diameters at various postnatal stages. While the lens sizes are comparable at P7 and P14 ($p > 0.05$, Student's t-test, n = 12 lenses per group.), the ephrin-A5$^{-/-}$ lens becomes significantly smaller than the wild-type counterpart at P21 ($p < 0.05$, Student's t-test, n = 12 lenses per group).
(C) Weight comparisons of wild-type and ephrin-A5$^{-/-}$ postnatal lenses. Weights of the wild-type and ephrin-A5$^{-/-}$ lenses are comparable at each of the stages ($p > 0.05$, Student's t-test, n = 12 lenses per group).
(D) Suture analysis of wild-type and ephrin-A5$^{-/-}$ lenses. Lens sutures were observed at P14 prior to lens opacification. No differences are observed in posterior suture formation between both groups as both groups show the classical Y-suture formation, though fiber cells appear more disorganized in the ephrin-A5$^{-/-}$ lenses. Scale bar = 50 μm.
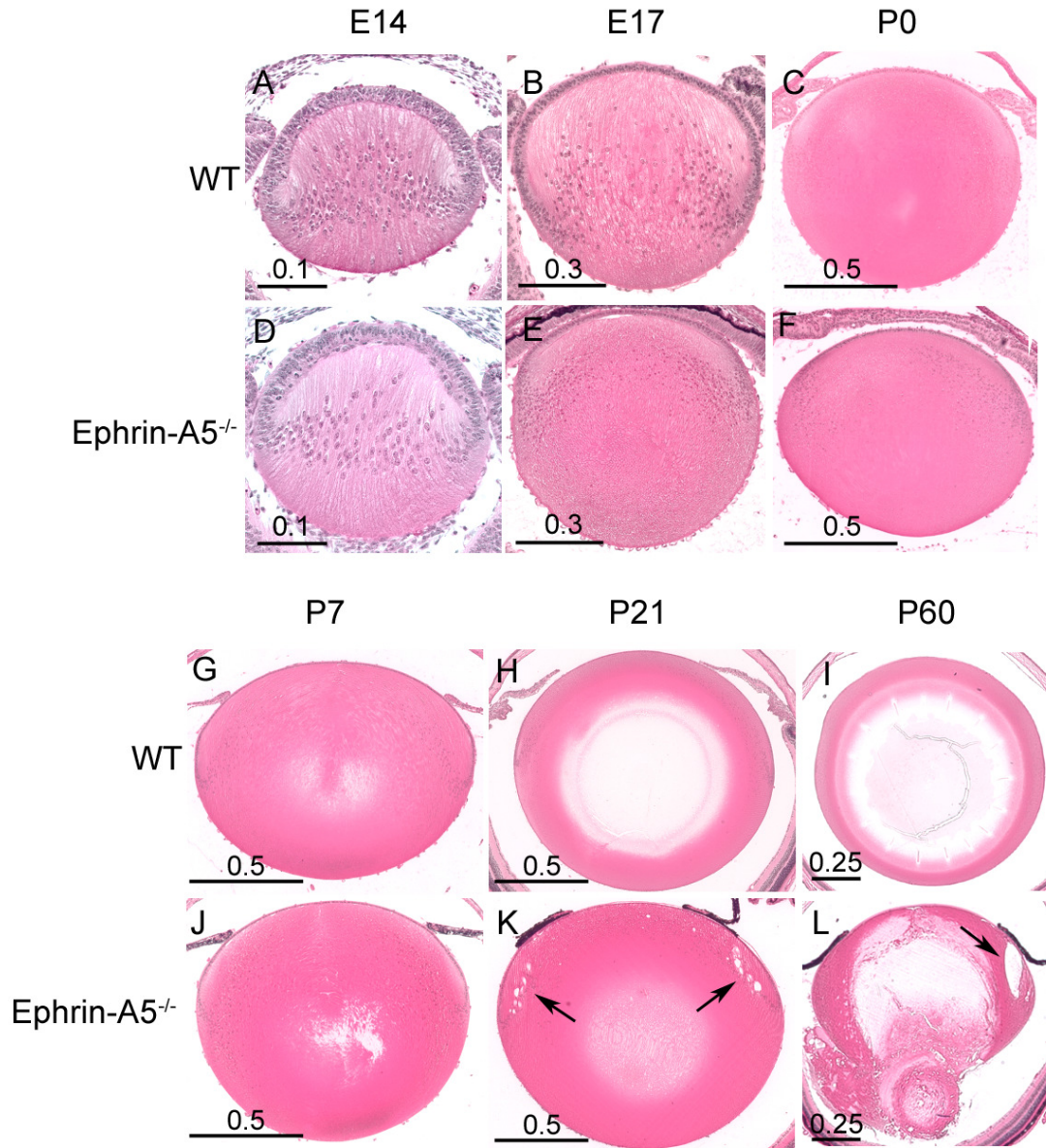
Figure 2-5: Development of ephrin-A5$^{-/-}$ lens

(A-F) Embryonic development of wild-type (A-C) and ephrin-A5$^{-/-}$ (D-F) lenses. Embryonic development of the ephrin-A5$^{-/-}$ lens appears similar to that of wild-type controls with no abnormalities observed. Scale bars in mm.

(G-L) Postnatal lens development of wild-type (G-I) and ephrin-A5$^{-/-}$ (J-L). Lens deficits are noticeable in ephrin-A5$^{-/-}$ lenses by P21 with the presence of vacuoles around the lens bow (compare H and K, see arrows). The deficits become progressively more severe, as larger vacuoles and complete posterior lens rupture is observed by P60 (Compare I and L, see arrow). Scale bars in mm.
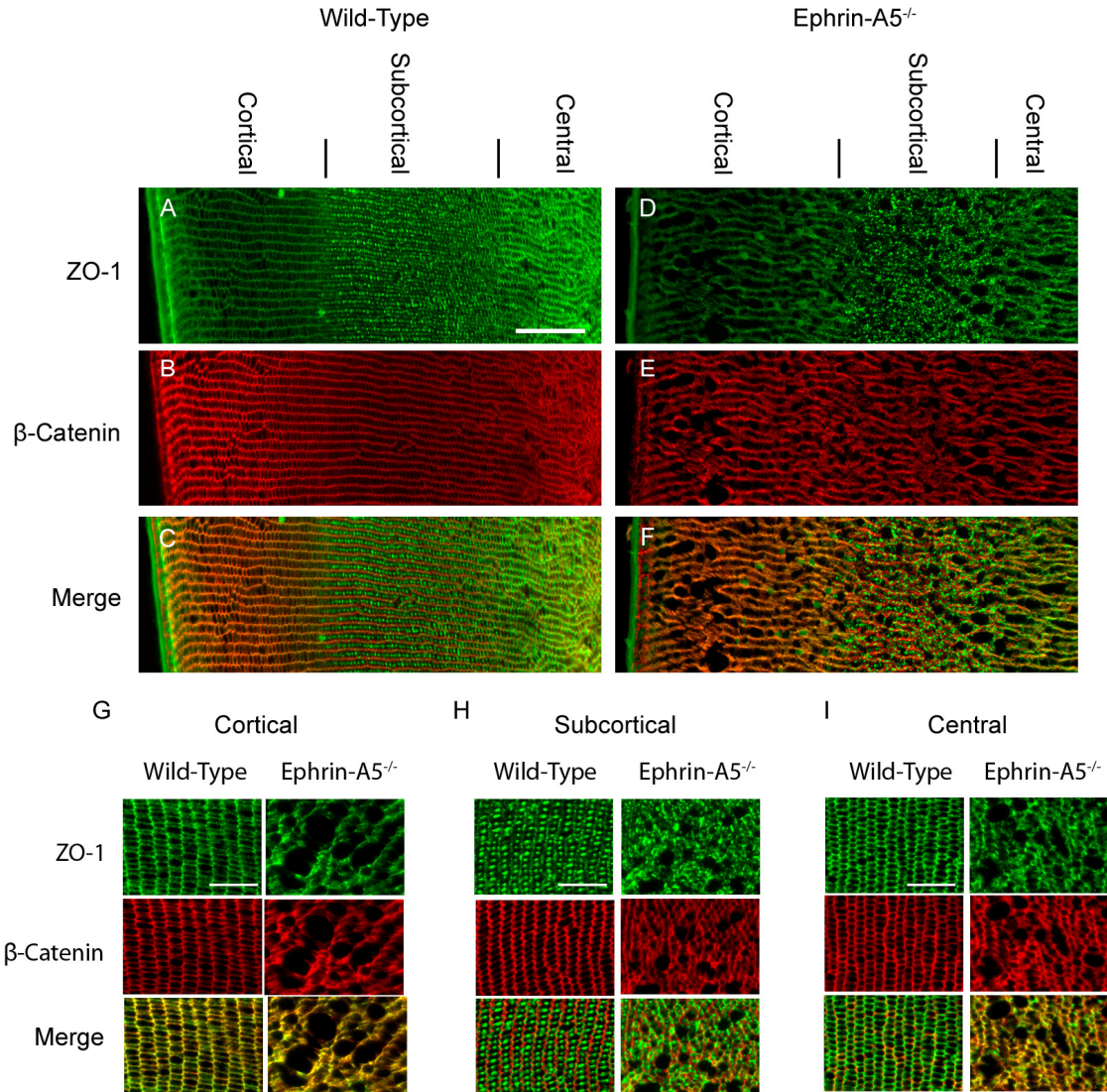
Figure 2-6: Lens fiber cell disorganization in ephrin-A5^{-/-} lens fiber cell layers
(A-F) Cross-section of P21 wild-type and ephrin-A5^{-/-} lenses displaying fiber cell organization. Wild-type (A-C) and ephrin-A5^{-/-} (D-F) P21 lenses are labeled for ZO-1 (A and D) and β-Catenin (B and E) to delineate cell borders or to distinguish distinct lens fiber areas. Scale bar = 200 μm.
(G-I) Higher magnification images of wild-type and ephrin-A5^{-/-} lens fiber regions in the cortical (G), subcortical (H), and central (I) areas. Disorganization of the fiber cells in the ephrin-A5^{-/-} lens can be observed in all fiber cell areas. Scale bar = 50 μm.
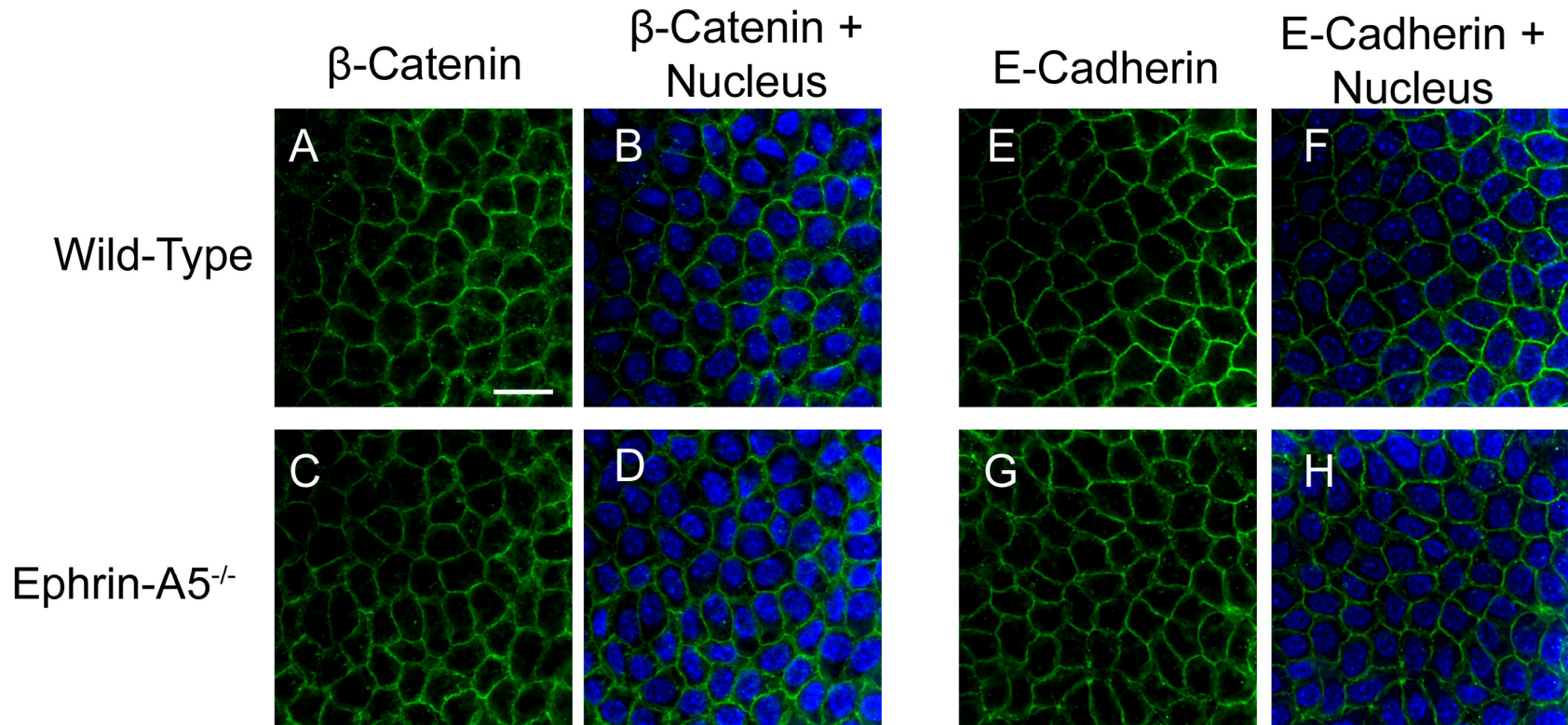
Figure 2-7: Lens epithelial regions appear undisturbed in ephrin-A5^{-/-} animals
(A-H) P21 lens epithelium whole mounts stained for β-catenin (A-D) and E-cadherin (E-H). No distinct differences in cellular morphology or adherens junction protein expression are observed between the wild-type (A and B, E and F) and ephrin-A5^{-/-} (C and D, G and H) lenses in these regions. Scale bar = 20 μm.

A
Ephrin-A5$^{+/+}$;CP49$^{-/-}$

B
Ephrin-A5$^{-/-}$;CP49$^{+/+}$

C
Ephrin-A5$^{-/-}$;CP49$^{+/-}$

D
Ephrin-A5$^{-/-}$;CP49$^{-/-}$
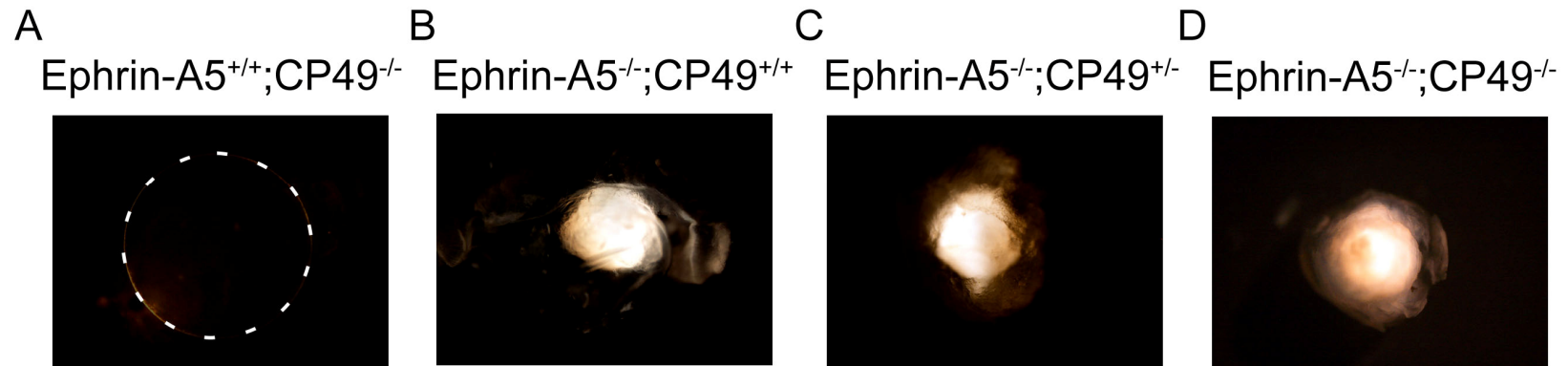
Figure 2-8: Effect of CP49 on ephrin-A5$^{-/-}$ cataract formation
(A-D) Whole mount lenses of 2 month old wild-type and ephrin-A5$^{-/-}$ lenses with and without the CP49 mutation. Ephrin-A5$^{+/+}$ lenses with the CP49 mutation (Ephrin-A5$^{+/+}$;CP49$^{-/-}$) appear transparent (A, lens is denoted by dotted line), while ephrin-A5$^{-/-}$ lenses, regardless of the status of CP49, display cataract formation (B-D). Lens deformations were observed in 100% of the ephrin-A5$^{-/-}$;CP49$^{+/+}$ lenses (n=4), 73% of the ephrin-A5$^{-/-}$;CP49$^{+/-}$ lenses (n=11), and 83% of the ephrin-A5$^{-/-}$;CP49$^{-/-}$ lenses (n=6).
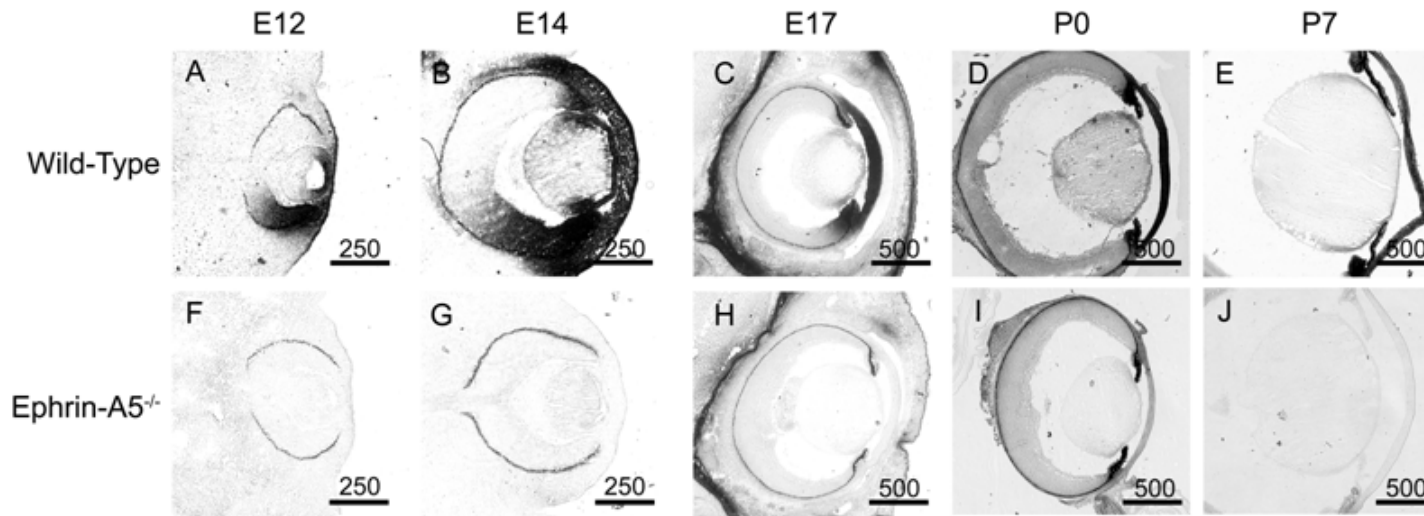
Figure 2-9: Expression of ephrin-A ligands in the developing eye
(A-E) EphA5-AP staining of wild-type lenses at various developmental stages. Significant expression of ephrin-A ligand is observed in the wild-type eye as early as E12 and persists through postnatal ages. Scale bars are in micrometers.
(F-J) EphA5-AP staining of ephrin-A5$^{-/-}$ lenses at several developmental periods. EphA5-AP staining is observed in the ephrin-A5$^{-/-}$ eye indicating that ephrin-A5 is the major ephrin-A ligand expressed in the eye. Scale bars are in micrometers.
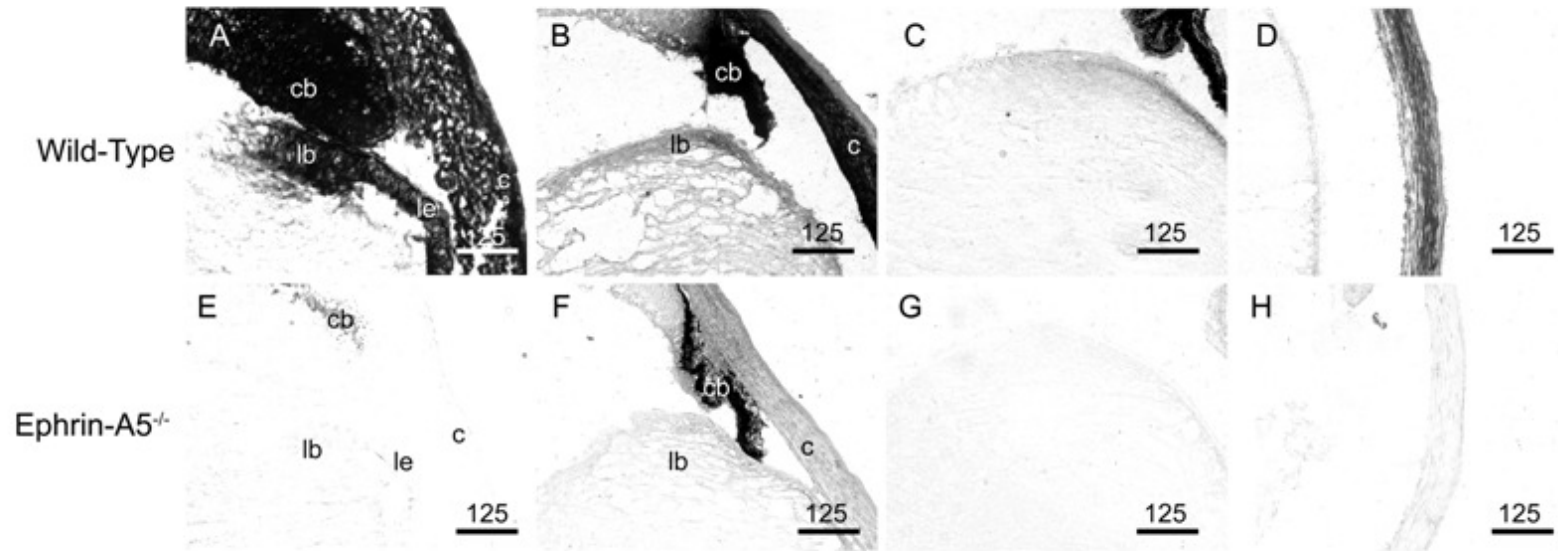
Figure 2-10: Localization of ephrin-A5 in the eye

(A and E) EphA5-AP staining of wild-type and ephrin-A5$^{-/-}$ eyes at E14. Staining is observed in the lens epithelium (le), lens bow (lb), cornea (c), and ciliary body (cb) in the wild-type while absent in the ephrin-A5$^{-/-}$ animal.

(B and F) EphA5-AP staining of wild-type and ephrin-A5$^{-/-}$ eyes at P0. Expression of ephrin-A ligands are maintained in the wild-type, though in lower levels in comparison with earlier embryonic stages, while remaining absent in the ephrin-A5$^{-/-}$ eye.

(C and G) EphA5-AP staining of wild-type and ephrin-A5$^{-/-}$ lenses at P7. Ephrin-A expression is observed in the lens bow region of wild-type mice in early postnatal stages while absent in ephrin-A5$^{-/-}$ mice.

(D and H) EphA5-AP staining of wild-type and ephrin-A5$^{-/-}$ cornea at P7. High levels of ephrin-A ligand is observed in the cornea of wild-type mice and not present in ephrin-A5$^{-/-}$ mice. Scale bars are in micrometers.
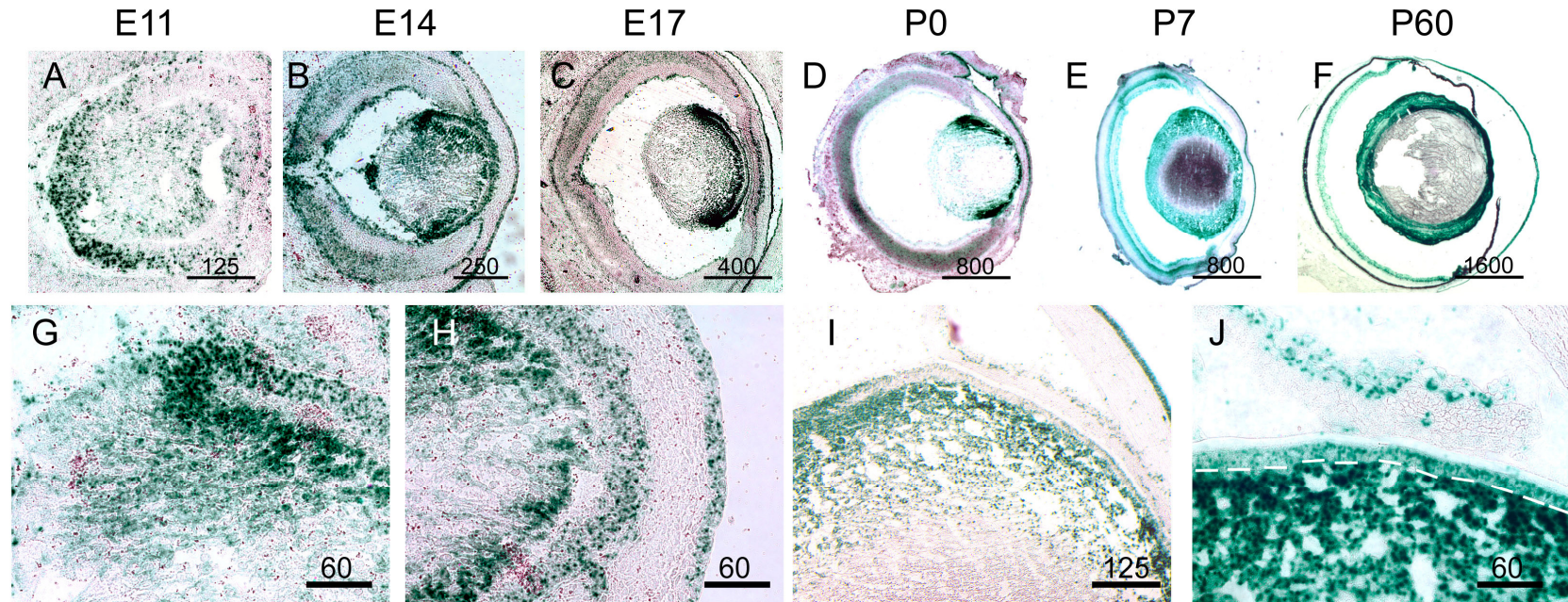
Figure 2-11: Expression of EphA2 throughout the developing lens

(A-F) EphA2 expression during embryonic eye development. EphA2[LacZ/+] tissue was reacted with X-gal to detect EphA2 expression in the developing eye. Staining is observed in the E11 lens and found throughout lens development in subsequent embryonic and postnatal stages. Scale bars are in micrometers.

(G and H) Higher magnification of EphA2 expression in the E14 lens. Expression is observed in the lens fiber cells near the bow and lens epithelium lens epithelium (G). Extensive expression is also observed and near the junction between fiber cells and epithelium (H).

(I and J) Localization of EphA2 in the P7 lens. EphA2 is expressed in the outer lens fiber cell regions (I) as well as in the lens epithelium (G, epithelium is delineated by white dotted line). Scale bars are in mictrometers.
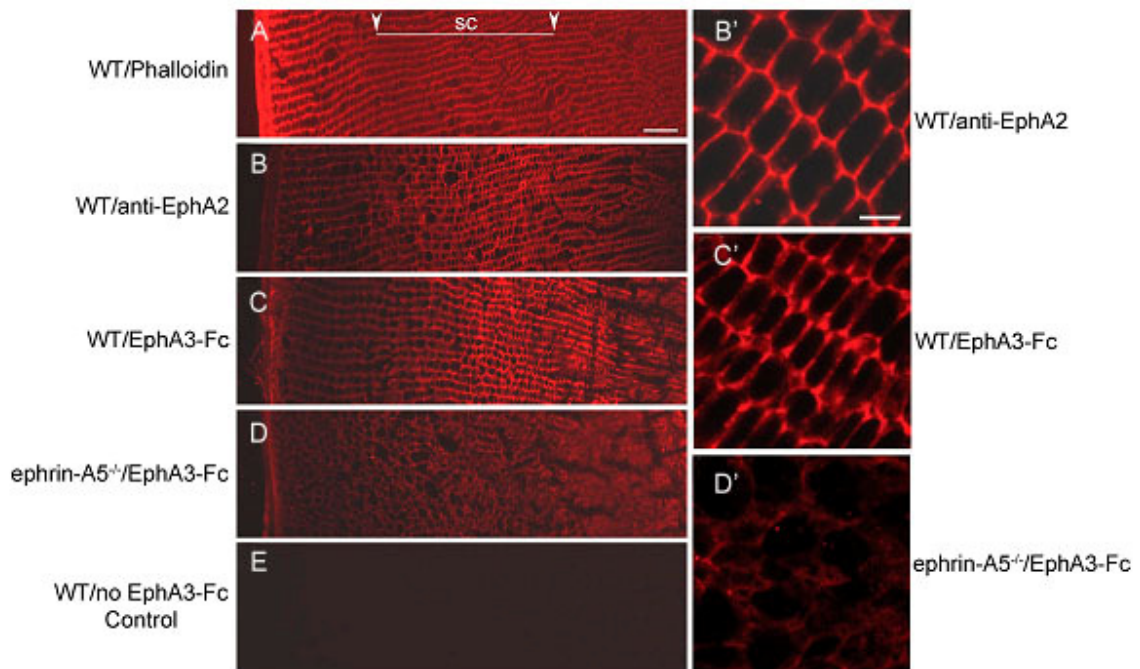
Figure 2-12: Ephrin-A5 and EphA2 expression in the mature lens
(A) Alexa Fluor 546-conjugated phalloidin staining of wild-type lens showing mature lens fiber cell organization. SC = Subcortical Zone. Scale bar = 20 µm.
(B and B') EphA2 expression in the wild-type lens using an anti-EphA2 antibody. Low magnification images (B) show distinct expression of EphA2 in the subcortical lens fiber cell regions. Higher magnification images (B') shows this localization to be highest as the intercellular junctions between fiber cells. Scale bar = 5 µm.
(C and C') EphA3-Fc labeling for ephrin-A ligand expression in the wild-type lens. Ephrin-A expression is observed in the subcortical region of the lens fiber cell layer (C), specifically in the cell-cell junctions (C') similar to EphA2 labeling.
(D and D') EphA3-Fc labeling in the ephrin-A5$^{-/-}$ lens. Little positive labeling is observed in the ephrin-A5$^{-/-}$ lens tissue, indicating ephrin-A5 to be the major ephrin-A ligand in the lens.
(E) Wild-type control without primary antibody. Lack of positive expression indicates high specificity in the labeling.
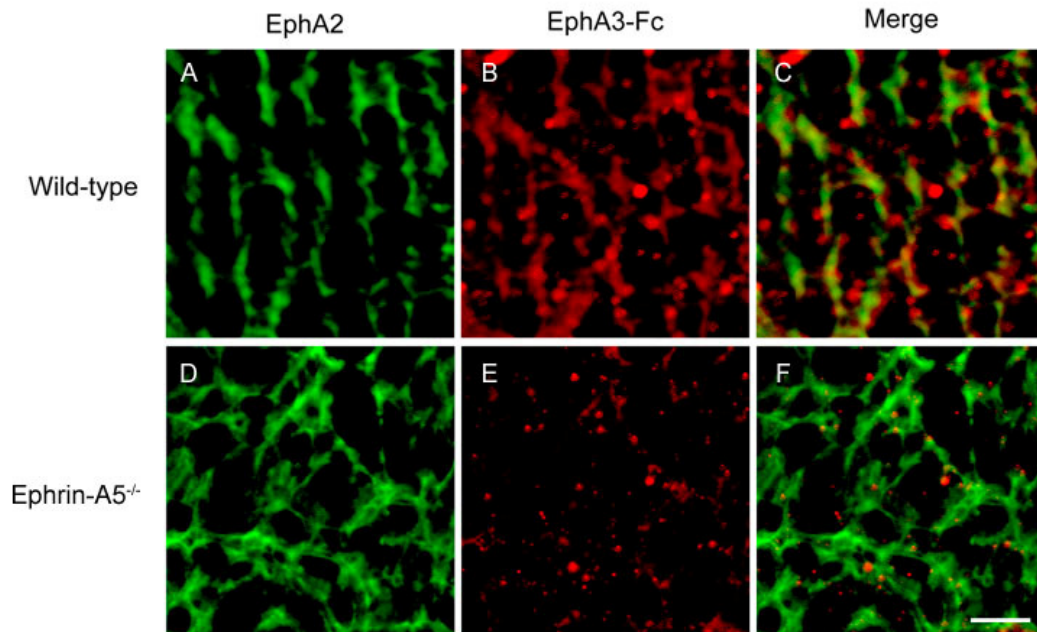
Figure 2-13: EphA2 and Ephrin-A5 co-localize in mature lens fiber cells
(A-C) EphA2 and ephrin-A localization in wild-type lens fiber cells. Both EphA2 expression (A) and EphA3-Fc labeling (B) is observed in the short edges of lens fiber cells and co-localize (C).
(D-F) EphA2 and ephrin-A localization in ephrin-A5$^{-/-}$ lens fiber cells. EphA2 expression is observed on the lens fiber cell membranes (D), little positive EphA3-Fc staining is observed in the ephrin-A5$^{-/-}$ lens.
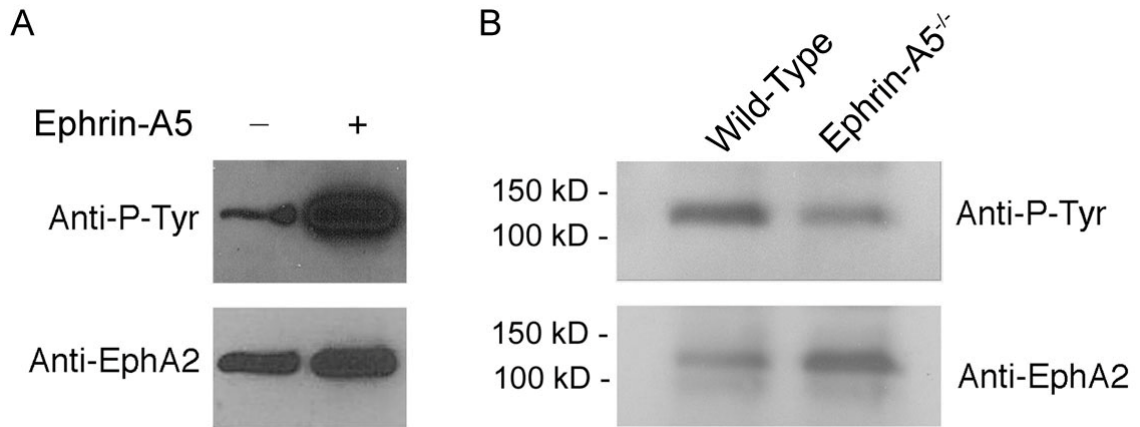
Figure 2-14: Ephrin-A5 activates EphA2 in the lens
(A) Ephrin-A5 activates EphA2. EphA2 was transfected into 293T cells and treated with or without ephrin-A5. Cells were lysed, immunoprecipitated for EphA2, and analyzed via Western blotting. Treatment of EphA2 transfected cells with ephrin-A5 shows robust tyrosine phosphorylation. Blots were reprobed for EphA2 to ensure equal loading.
(B) Reduced activation of EphA2 in the ephrin-A5^{-/-} lens. Wild-type and ephrin-A5^{-/-} P6 lenses were lysed and immunoprecipitated for EphA2. The resulting immunoprecipitates were then subject to Western blot analysis. Ephrin-A5^{-/-} lenses show a distinct down-regulation of tyrosine phosphorylation in comparison to wild-type controls, indicating ephrin-A5 to be a major ligand of EphA2 activation in the lens.
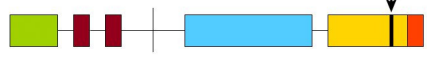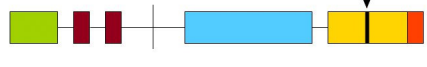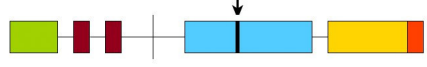
		Mutation	Effect	Cataract Phenotype	Reference
A	EphA2 Wild-Type	None	None	None	Jun et al., 2009
B	SAM Domain Mutants				
	c.2842G>T	Transversion	G948W	Autosomal Dominant Posterior Polar Cataract	Shiels et al., 2008
	c.2819C>T	Missense	T940I	Autosomal Dominant Posterior Polar Cataract	Zhang et al., 2009
	c.2826-9G>A	Splicing Mutation	Novel 71 AA, C-Terminus	Autosomal Dominant Total Cataract	Zhang et al., 2009
	c.2915_2916delTG	Frame Shift	Novel 39 AA, C-Terminus	Autosomal Dominant Posterior Polar Cataract	Zhang et al., 2009
C	Kinase Domain Mutants				
	c.2162G>T	Transversion	R721N	Autosomal Dominant Cortical Cataract	Jun et al., 2009
	c.2353G>A	Missense	A785T	Autosomal Recessive Nuclear Cataract	Kaul et al., 2010

Table 2-1: Human EphA2 Cataract Mutations
(A) Structure of wild-type EphA2. BD = Ephrin Ligand Binding Domain; FN = Fibronectin Repeats; Kin = Kinase Domain; SAM = Sterile Alpha Motif; PDZ = PDZ Domain.
(B) EphA2 SAM Domain cataract mutants.
(C) EphA2 Kinase Domain cataract mutants. Arrows denote relative location of point mutations in indicated mutations. Black sections denote novel amino acid changes

CHAPTER 3: REGULATION OF THE ADHERENS JUNCTION IN THE LENS BY EPHRIN-A5 AND EPHA2

Introduction

The early embryonic lens is supplied with nutrients through a blood vessel network known as the hyaloid vasculature. However, this complex regresses in later stages of ocular development, leaving the mature lens in an avascular environment (Ito and Yoshioka 1999; Zhu, Madigan et al. 2000). To preserve homeostasis, the lens depends on both a unique cytoarchitecture and an internal circulation system to maintain proper water and nutrient content. Proper regulation in maintaining this very specific cellular structure is required for preserving the integrity of the lens.

A. Lens Cell Interactions

The unique hexagonal shape of lens fiber cells requires the precise regulation of intercellular interactions. This role is mediated in part by the cadherins, a major family of intercellular adhesion molecules involved with the dynamic regulation of tissue morphogenesis (Gumbiner 2005). The most extensively studied of these molecules are the classical cadherins, transmembrane homophilic adhesion molecules whose interactions are regulated by calcium (Takeichi 1995; Gumbiner 2005) (Fig. 3-1).

The classical cadherins affect cellular connections and shape through interactions with the actin cytoskeleton (Weis and Nelson 2006).   This interaction is regulated in the C-terminus of the cadherin molecule through a complex collectively known as the adherens junction. The proteins of this complex include several molecules of the catenin family, including β-catenin, p120-catenin, and α-catenin. β- and p120-catenin are

armadillo repeat proteins that interact directly with the cadherin molecules; p120-catenin

binds to cadherin molecules at the juxtamembrane domain, while β-catenin interacts with

the cytoplasmic domain in competition with another catenin molecule, γ-catenin

(alternatively known as plakoglobin), which is often associated with desmosomes

(Nagafuchi and Takeichi 1988; Nagafuchi and Takeichi 1989; Yap, Niessen et al. 1998;

Thoreson, Anastasiadis et al. 2000). The binding between the catenin and cadherin

molecules are mediated by the phosphorylation of tyrosine residues (Hoschuetzky,

Aberle et al. 1994; Kinch, Clark et al. 1995; Roura, Miravet et al. 1999; Piedra, Martinez

et al. 2001). Phosphorylation of β-catenin has been found to disrupt interactions with

cadherins, while phosphorylation of γ-catenin can either enhance or reduce affinity to

cadherin complex depending on the affected residue (Roura, Miravet et al. 1999; Piedra,

Martinez et al. 2001; Miravet, Piedra et al. 2003). The adherens junction complex

interacts with the actin cytoskeleton and is dependent on α-catenin (Weis and Nelson

2006).

The lens contains two of the classical cadherins: E-cadherin is expressed

exclusively in the lens epithelial layer, while N-cadherin is present in both the epithelial

and fiber cell layers (Leonard, Chan et al. 2008; Pontoriero, Smith et al. 2009; Leonard,

Zhang et al. 2011). These molecules are essential in lens development and maintenance,

as conditional deletions of either cadherin result in severe lens deficits (Pontoriero, Smith

et al. 2009). Both E- and N-cadherin have been previously found to be necessary for lens

vesicle separation (Pontoriero, Smith et al. 2009). In addition, N-cadherin has been

reported to play important roles in lens fiber cell elongation and morphogenesis (Ferreira-

Cornwell, Veneziale et al. 2000; Pontoriero, Smith et al. 2009; Leonard, Zhang et al. 2011).

B. Interlenticular Circulation

In addition to a distinct cytoarchitecture, the lens depends on specific membrane factors to regulate internal water and nutrient distribution. This is made possible predominantly through the use of two major protein families: gap junctions and aquaporin channels.

Gap junctions are specialized intercellular channels formed by two adjacent cells that allow for the passage of small molecules. The structures consist of connexin molecules, with six molecules of either the same (homomeric) or different (heteromeric) connexins forming a hemichannel known as a connexon, which in turn interacts with another hemichannel from an adjacent cell (Mathias, White et al. 2010). The lens consists of three main connexin molecules: connexin-43 (Cx-43) is expressed in low levels exclusively in the lens epithelium (Beyer, Kistler et al. 1989), connexin-46 (Cx-46) is observed solely in the differentiated lens fiber cells (Paul, Ebihara et al. 1991; Gong, Li et al. 1997; Nielsen, Baruch et al. 2003), and connexin-50 (Cx-50) is observed in both the lens epithelium and fiber cell layers. Both Cx-46 and Cx-50 are capable of interacting to form heteromeric hemichannels, but Cx-43 has not been found to interact with either Cx-46 or Cx-50 (Mathias, White et al. 2010). Connexins in the lens also interact with the scaffolding protein zona occludens-1 (ZO-1), and this interaction has been found to play a role in gap junction assembly (Nielsen, Baruch et al. 2001; Nielsen, Baruch et al. 2003; Chai, Goodenough et al. 2011; Rhett, Jourdan et al. 2011).

Gap junction complexes are the major driver of communication, circulation, and exchange of resources within the lens. Studies using knock-out mouse models of Cx-46 (Cx-46$^{-/-}$) and Cx-50 (Cx-50$^{-/-}$) have found reductions in fiber cell conductivity (Gong, Baldo et al. 1998; Baldo, Gong et al. 2001). In addition, Cx-50 plays a critical role in lens growth and development, as Cx-50$^{-/-}$ lenses experience growth deficits in lens fiber maturation (White, Goodenough et al. 1998; Rong, Wang et al. 2002).

Lens circulation is also mediated through the passive diffusion of water in the lens. This process is regulated by the Aquaporin family of molecules, transmembrane molecules that form tetramers and are permeable to water (Mathias, White et al. 2010). The lens consists of two main Aquaporins: the lens epithelium consists of predominantly Aquaporin 1 (AQP1) (Patil, Saito et al. 1997; Hamann, Zeuthen et al. 1998) while the lens fiber cells express Aquaporin 0 (AQP0), formerly known as Major Intrinsic Protein (MIP) (Fitzgerald, Bok et al. 1983; Zampighi, Hall et al. 1989).

Our analyses of the lens fiber cell structure in ephrin-A5$^{-/-}$ animals have found disorganization and rounding of the mutant lens fiber cells. Additional examinations have identified that ephrin-A5 regulates the localization of the adherens junction molecule N-cadherin in the lens, as ephrin-A5$^{-/-}$ lenses experience severe alterations in N-cadherin localization. Furthermore, both ephrin-A5 and EphA2 were found to enhance the interaction between N-cadherin and β-catenin.

Results

A. Alterations in Lens Fiber Cell Shape and Organization in the Ephrin-A5$^{-/-}$ Lens

The severe degeneration seen in ephrin-A5$^{-/-}$ lenses led us to examine morphological changes during lens maturation. We therefore looked at the cell

morphology in mouse lenses at P6 and P21, times at which the lenses of ephrin-A5^{-/-} mice were still mostly intact (Fig. 3-2). When sectioning the lens in a coronal plane, the wild-type secondary lens fiber cells were observed to be in the form of flattened hexagons organized in a highly ordered and regular configuration (Fig. 3-2A and B). In contrast, ephrin-A5 mutant fiber cells were more round and far less organized (Fig 3-2A and B; compare wild-type and ephrin-A5^{-/-}). The length/width ratio was significantly smaller for the ephrin-A5^{-/-} lens fiber cells than for the wild-type cells (Fig. 3-2C). These morphological differences are indicative of changes in cell adhesion in the mutant lens (Hayashi and Carthew 2004).

B. Disruption of the N-cadherin complex in the ephrin-A5 mutant lens

Ephrin-A5^{-/-} lenses experience extensive morphological changes in differentiated lens fiber cells prior to developing cataracts. One possible cause of these alterations is the improper regulation to intercellular adhesion. In lens fiber layers, cell-cell interactions are governed in part by N-cadherin (Leonard, Chan et al. 2008; Pontoriero, Smith et al. 2009; Leonard, Zhang et al. 2011). We therefore examined whether alterations in N-cadherin expression occurred in the ephrin-A5^{-/-} lens through immunofluorescence microscopy of early postnatal lenses (Fig. 3-3). N-cadherin expression in P21 wild-type lenses was observed along the short edges of the hexagonal fiber cells with particularly strong expression along the vertices (Fig. 3-3A-C). In contrast, ephrin-A5^{-/-} lenses displayed disruptions in N-cadherin localization with significant amounts of cytoplasmic expression observed within the lens fiber layers (Fig. 3-3D-F). Since disruptions in lens fiber cell morphology in ephrin-A5 null lenses occur at early postnatal stages, we also examined N-cadherin localization in wild-type and

ephrin-A5$^{-/-}$ lenses at P7 (Fig. 3-3G-L). Similar to the P21 lenses, wild-type fiber cells

showed N-cadherin expression along the short edges of mature fiber cells (Fig. 3-3G-I)

while ephrin-A5$^{-/-}$ lenses displayed cytoplasmic localization (Fig. 3-3J-L).   Together,

these results indicate that ephrin-A5 affects the localization of N-cadherin in the lens.

C. Gap junction disorganized in the ephrin-A5$^{-/-}$ lens

We next examined whether other molecules responsible for intercellular adhesion

and communication within the lens showed similar levels of disruption in the ephrin-A5-

/- lens. The tight junction protein ZO-1 plays essential roles in regulating gap junction

proteins within the lens (Nielsen, Baruch et al. 2001; Nielsen, Baruch et al. 2003; Chai,

Goodenough et al. 2011; Rhett, Jourdan et al. 2011). We therefore observed ZO-1

expression in comparison to N-cadherin localization in the lens (Fig. 3-4). N-cadherin

staining in the wild-type lens was observed on the short edges of mature fiber cells with

strong expression at the vertices. This expression was distinct from that of the tight

junction protein ZO-1, which showed complexes expressed in the short edges of fiber

cells in the outer and deep cortical regions and on the long edges of fiber cells in distinct

complexes within the mid-cortical sections (Fig. 3-4A-C). In contrast, significant

expression of N-cadherin in ephrin-A5$^{-/-}$ lenses was observed in the cytoplasm, while ZO-

1 showed disorganization but continued expression along the cell membranes (Fig. 3-4D-

F). Higher magnification imaging of the middle cortical regions further show the distinct

membrane localization of N-cadherin wild-type lenses and the cytoplasmic staining in the

ephrin-A5$^{-/-}$ lenses while ZO-1 expression is observed along cell membranes and with the

large complexes still intact (Fig. 3-4G-L).

We also examined the localization of gap junction protein Cx-46 in relation to ZO-1 in wild-type and ephrin-A5$^{-/-}$ lenses (Fig. 3-5). Cx-46 in the subcortical region of the lens at P21 is found on the long edges of mature fiber cells in large complexes and co-localizes with ZO-1 (Fig. 3-5A-C). In ephrin-A5 mutant lenses, Cx-46 organization is disrupted; however, the large complexes are still observed and continue to be co-localized with ZO-1 (Fig. 3-5D-F). Together, these data indicate that gap junction complexes in the ephrin-A5$^{-/-}$ lens are disorganized by alterations in cellular structure.

D. EphA2 partially co-localizes with adherens junction molecules in the lens fiber cell

Alterations in N-cadherin localization in the ephrin-A5$^{-/-}$ provides evidence that the adherens junction in the lens is regulated, at least in part, by ephrin-A5. We therefore determined the localization of adherens junction molecules in relation to EphA2, a receptor for the ephrin-A5 ligand in the lens as established previously (Fig. 3-6). In postnatal wild-type lenses, both N-cadherin and EphA2 are observed on the short edges of lens fiber cells and are co-localized in the subcortical region (Fig. 3-6A-C). The localization of N-cadherin is disrupted in the ephrin-A5$^{-/-}$ lens, though EphA2 is still observed along the cell borders (Fig. 3-6D-F).

We next examined the expression of other adherens junction molecules known to regulate N-cadherin, most specifically β-catenin, a key regulator of cadherin interaction with the actin cytoskeleton. To determine whether β-catenin localization experienced similar alterations in the ephrin-A5$^{-/-}$ lens like that observed with N-cadherin, P21 wild-type and ephrin-A5$^{-/-}$ lenses were sectioned and immunostained for β-catenin and EphA2 (Fig. 3-6G-L). β-catenin localization in wild-type tissues is similar to that of N-cadherin

and EphA2, with expression being observed on the short edges of fiber cells (Fig. 3-6G-I). In the ephrin-A5 mutant lens, β-catenin localization continues to be observed in the fiber cell membrane and continues to be co-localized with EphA2 (Fig. 3-6J-L), distinct from the N-cadherin staining showing mislocalization in the cytoplasm, indicating that β-catenin localization is unaffected by the absence of ephrin-A5.

E. EphA2 and β-catenin exist in the same protein complex

The co-localization between EphA2 and β-catenin in both wild-type and ephrin-A5$^{-/-}$ lenses implies that the both molecules are capable of interaction. To test whether the Eph receptor and adherens junction molecule were located in the same protein complex, we implemented co-immunoprecipitation assays between both molecules (Fig. 3-7). 293T cells were transfected with or without EphA2 and treated with or without ephrin-A5 were lysed. EphA2 was subsequently immunoprecipitated from the resulting lysate, and the sample was examined through Western blot. β-catenin was observed in cell lysates immunoprecipitated from EphA2 transfected cells, and this effect was seen independent of treatment of ephrin-A5 (Fig. 3-7A). We further confirmed this doing the reciprocal experiment, in which 293T cells transfected with or without EphA2 was lysed and immunoprecipitated for β-catenin. In concurrence with the previous results, we found that EphA2 was pulled down along with β-catenin (Fig. 3-7B). Together, these results indicate that EphA2 and β-catenin are capable of close interaction.

F. Ephrin-A5 and EphA2 regulate the interaction between N-cadherin and β-catenin

The cytoplasmic localization of N-cadherin and continued membrane localization β-catenin in the ephrin-A5 mutant lens and the direct interaction between EphA2 and β-

catenin suggests ephrin-A5 to be an important regulator of the adherens junction complex. We therefore set to determine whether ephrin-A5 is capable of enhancing the interaction between N-cadherin and β-catenin (Fig. 3-8). 293T cells were treated with IgG or ephrin-A5, after which the cells were washed, lysed, and immunoprecipitated for N-cadherin. Treatment of 293T cells with ephrin-A5 showed increased pulldown of β-catenin compared to the controls, indicating that ephrin-A5 enhances the interaction between these two adherens junction molecules (Fig. 3-8A). As ephrin-A5 phosphorylates EphA2 within the lens (Fig. 2-14), we also determined whether EphA2 also affected the interaction between N-cadherin and β-catenin. N-cadherin immunoprecipitated from 293T cells transfected with EphA2 displayed enhanced levels of β-catenin compared to untransfected controls (Fig. 3-8B). Together, these data indicate that both ephrin-A5 and EphA2 are capable of enhancing the binding between N-cadherin and β-catenin.

G. Ephrin-A5 inhibits EGF-mediated β-catenin phosphorylation

β-catenin interaction with cadherin molecules is governed by its phosphorylation status (Kinch, Clark et al. 1995; Roura, Miravet et al. 1999; Piedra, Martinez et al. 2001). EGF stimulation has previously been found to enhance β-catenin phosphorylation in tyrosine residue 654 and inhibit its interaction with cadherin molecules (Kinch, Clark et al. 1995; Roura, Miravet et al. 1999; Daugherty and Gottardi 2007). As ephrin-A5 and EphA2 have been both found to enhance β-catenin-N-cadherin interaction, we asked whether ephrin-A5 activation of EphA2 was capable of inhibiting β-catenin phosphorylation (Fig. 3-9). For these experiments, the A431 breast cancer cell line was used because of their endogenous expression of EGFR and EphA2. Ephrin-A5 treatment

of A431 cells induced EphA2 tyrosine phosphorylation, while EGF treatment had no effect on EphA2 activation (Fig. 3-9A). EGF stimulation also induced Erk phosphorylation, while ephrin-A5 inhibited this activity (Fig. 3-9B).

To determine whether ephrin-A5 treatment affected β-catenin, A431 cells were treated with EGF, ephrin-A5, or both. Cell lysates from these samples were immunoprecipitated for β-catenin. EGF induced high levels of tyrosine phosphorylation in β-catenin, while ephrin-A5 alone displayed no phosphorylation. However, combined treatment of EGF and ephrin-A5 induced drastically inhibited β-catenin phosphorylation (Fig. 3-9C). Together, these experiments further support the ability of ephrin-A5 to enhance β-catenin interaction with cadherins.

H. β-catenin dephosphorylation by EphA2 is kinase-dependent and SAM domain-independent

As EphA2 enhances the interaction between and N-cadherin and β-catenin, we next asked whether EphA2 transfection was capable of inhibiting β-catenin dephosphorylation and how this activity was regulated (Fig. 3-10). 293T cells were transfected with EGFR alone or co-transfected with EphA2. Cells were then treated with EGF and lysed, with the lysate immunoprecipitated for β-catenin and the resulting samples analyzed by Western blotting. EGFR transfection alone showed robust phosphorylation of β-catenin, while EGFR-EphA2 wild-type co-transfected cells displayed a significant reduction of β-catenin phosphorylation (Fig. 3-10A).

We also examined whether EphA2 dephosphorylation of β-catenin was regulated by either the kinase or SAM domains. Mutations in both of these EphA2 domains have been previously identified to play major roles in human cataracts (Shiels, Bennett et al.

2008; Jun, Guo et al. 2009; Zhang, Hua et al. 2009; Kaul, Riazuddin et al. 2010), and as such their activities may play integral roles in adherens junction maintenance in the lens. To address this possibility, various EphA2 mutants co-transfected with EGFR were also analyzed, including an EphA2 construct with the kinase domain deleted (dKin), an EphA2 mutant lacking the SAM domain (dSAM), and several of the EphA2 SAM domain human cataract mutations that have been previously identified (Shiels, Bennett et al. 2008; Zhang, Hua et al. 2009). Cells co-transfected with EGFR and the EphA2 SAM domain mutations showed reduced β-catenin phosphorylation, indicating that the SAM domain mutations retain this activity (Fig. 3-10A). In contrast, EphA2-dKin showed higher levels of β-catenin phosphorylation comparable to the EGFR-alone transfected group, indicating that the kinase domain plays an important role in β-catenin dephosphorylation (Fig. 3-10A). Together, these results indicate β-catenin dephosphorylation by EphA2 to be a kinase-dependent activity.

Discussion

The maintenance of lens fiber cell architecture is dependent in large part on the interactions between adhesion molecules and the organization of cytoskeletal elements. The alterations in the organization of the fiber cell cytoarchitecture in the ephrin-A5^{-/-} mouse lens presented the possibility that the Eph family plays a role in the regulation of intercellular interactions, leading us to analyze the role of ephrin-A5 in adherens junction regulation.   N-cadherin is internalized in the lens fiber cells as early as P6, at which point lens fiber cell architecture is already disordered in the ephrin-A5^{-/-} lens, although β-catenin, a regulator of cadherin binding with the actin cytoskeleton, was observed on the membranes of the lens fiber cells. *In vitro* experiments have found that ephrin-A5 and

EphA2 are capable of enhancing the interaction between N-cadherin and β-catenin in a kinase-dependent manner, and EphA2 interacts directly with β-catenin.

A. Regulation of the Adherens Junction by the Eph family in the Postnatal Lens

N-cadherin is the predominant cadherin molecule in the lens fiber cells regulating intercellular interactions, and has been found to be an important factor in the organization and packing of the differentiated cells (Xu, Overbeek et al. 2002; Straub, Boda et al. 2003; Leonard, Chan et al. 2008; Leonard, Zhang et al. 2011). In this current work, we have found severe disruption of N-cadherin localization in the ephrin-A5$^{-/-}$, which we believe results in the disruption of lens fiber cells ultimately resulting in cataract formation.

The relationship between the Eph family and the cadherins has been previously documented in a wide array of contexts (Zantek, Azimi et al. 1999; Orsulic and Kemler 2000; Kasemeier-Kulesa, Bradley et al. 2006; Fang, Ireton et al. 2008; Miura, Nam et al. 2009; Solanas, Cortina et al. 2011). In addition, along with our own findings of disruptions of N-cadherin localization in the ephrin-A5$^{-/-}$ lens, EphA2$^{-/-}$ lenses were observed to have disruptions of N-cadherin expression in the lens fiber cell layers (Cheng and Gong 2011), further confirming the role of the Ephs in regulating the adherens junction in mature lens fiber cells. Interestingly, Cheng and Gong (2011) also reported disruptions in E-cadherin and β-catenin localization in the lens epithelium of ephrin-A5$^{-/-}$ mice, though we did not observe this phenotype (see Fig. 2-7). This discrepancy may be a result of differences in mouse backgrounds between both studies.

Our results indicate that the Eph family plays key roles in cadherin regulation through the regulatory molecule β-catenin. Several lines of evidence indicate this

importance, including the enhanced interaction between N-cadherin and β-catenin after treatment with ephrin-A5 and transfection of EphA2, direct interaction between EphA2 and β-catenin and the inhibition of EGF-induced β-catenin phosphorylation after EphA2 activation and ephrin-A5 treatment. β-catenin phosphorylation of Tyr-654, in part mediated by EGF, plays a particularly important role in the interaction between cadherin molecules, as phosphorylation of this residue inhibits this interaction (Hoschuetzky, Aberle et al. 1994; Kinch, Clark et al. 1995; Roura, Miravet et al. 1999; Piedra, Martinez et al. 2001). The inhibition of β-catenin phosphorylation by both ephrin-A5 and EphA2 implies that the Eph family regulates adherens junction stability through β-catenin phosphorylation. Future studies exploring how this regulation occurs in the lens will further elucidate the role of the Eph family in lens development.

B. Roles of EPHA2 Kinase Activity

Studies on the function of EPHA2 in human cataracts have revealed the kinase domain to play a critical role in regulating lens activity. Jun et al. (2009) had identified an R732N mutation within the kinase domain as a risk allele for cataracts in human populations. Analysis of the EPHA2 kinase domain crystal structure (Nowakowski, Cronin et al. 2002) identified Arg721 to be important in forming a salt bridge with Asp872. Biochemical experiments found the R721N mutation (R721N-EPHA2) to result in higher basal activation of the EPHA2 receptor compared to wild-type EPHA2, which leads to enhanced basal activity of ERK1/2. Furthermore, HEK293 cells expressing R721N-EPHA2 in the presence of the ephrin-A1 ligand showed an inhibition to growth, while mouse embryonic fibroblasts (MEFs) expressing R721N-EPHA2 showed intracellular retention of the protein (Jun, Guo et al. 2009). The relevance of these results

to lens biology *in vivo* is still unclear. Additionally, the kinase domain missense mutation c.2353G>A has also been identified as a risk allele for cataracts in resulting in an autosomal recessive congenital cataracts (Kaul, Riazuddin et al. 2010). However, effects of this mutation on EPHA2 kinase activity remain to be elucidated.

In this study, we have also found that the kinase domain of EphA2 plays a critical role in regulating β-catenin, as EphA2 constructs lacking the kinase domain fail to inhibit β-catenin dephosphorylation. The EphA2 kinase activity may therefore be required in maintaining N-cadherin on the membrane of lens fiber cells. How the EphA2 kinase domain affects lens biology specifically and whether it affects the adherens junction still requires further study. One possibility is that the c.2353G>A mutation, which results in autosomal recessive congenital cataracts, may have an inhibition of EphA2 kinase activity resulting in disruptions in adherens junction activity. As such, it will be interesting to analyze the kinase activity of this mutated EphA2 receptor and see whether N-cadherin-β-catenin interactions within the lens are altered.

C. Contributions of the EPHA2 SAM Domain

The human EPHA2 cataract studies have yielded a surprising finding in that the SAM domain plays a valuable role in maintaining EphA2 function in the lens. Four mutations out of a total of six known cataract mutations in EPHA2 are within the SAM domain. Significantly, all of the identified SAM domain mutations have been found to be autosomal dominant (Shiels, Bennett et al. 2008; Zhang, Hua et al. 2009). However, we have found here that the EphA2 SAM domain mutations most likely do not affect adherens junction regulation as EphA2 activity was still retained in dephosphorylating β-catenin.

The role of the EPHA2 SAM domain in lens regulation remains to be elucidated. The frameshift mutation c.2915_2916delTG and splicing mutation c.2826-9G>A both show enhanced protein-protein interactions with low molecular weight protein-tyrosine phosphatase (LMW-PTP), which normally associates with the C-terminus of EPHA2 and inhibits its phosphorylation (Kikawa, Vidale et al. 2002; Parri, Buricchi et al. 2005; Fang, Ireton et al. 2008; Zhang, Hua et al. 2009). The amplified interaction is more pronounced in the c.2826-9G>A mutant (Zhang, Hua et al. 2009). This enhancement may be attributed to the novel polypeptide formation in the C-terminus as a result of the mutations, but must be further elucidated as to the direct cause. Further analysis of the EPHA2 SAM domain mutations by our group has found that these mutations affect the stability of EPHA2 through ubiquitin-mediated proteasomal degradation and influence protein solubility. Additionally, these cataract mutations inhibit normal EPHA2 function in promoting cell migration activity (Park, Son et al. 2012).

While the human EPHA2 SAM domain mutations result in an autosomal dominant phenotype, the EphA2 mutant mouse models develop cataracts in an autosomal recessive manner, as EphA2$^{-/-}$ mice develop cataracts while EphA2$^{+/-}$ display normal lenses (Jun, Guo et al. 2009). One possibility for this difference may be that the EphA2 SAM domain mutations have a dominant-negative effect on the normal EphA2; mutations within the EphA2 SAM domain could potentially interrupt proper oligomerization, impeding proper signaling. Another explanation is that interactions between wild-type EphA2 and mutated EphA2 SAM domain proteins result in inhibition of downstream signaling targets. Work by our group has found that the EPHA2 SAM domain mutations impair Akt signaling upon binding with ephrin-A5 (Park, Son et al.

2012). The replacement of wild-type EphA2 with these EphA2 SAM domain mutants in mouse studies will prove insightful to further elucidate this mechanism.
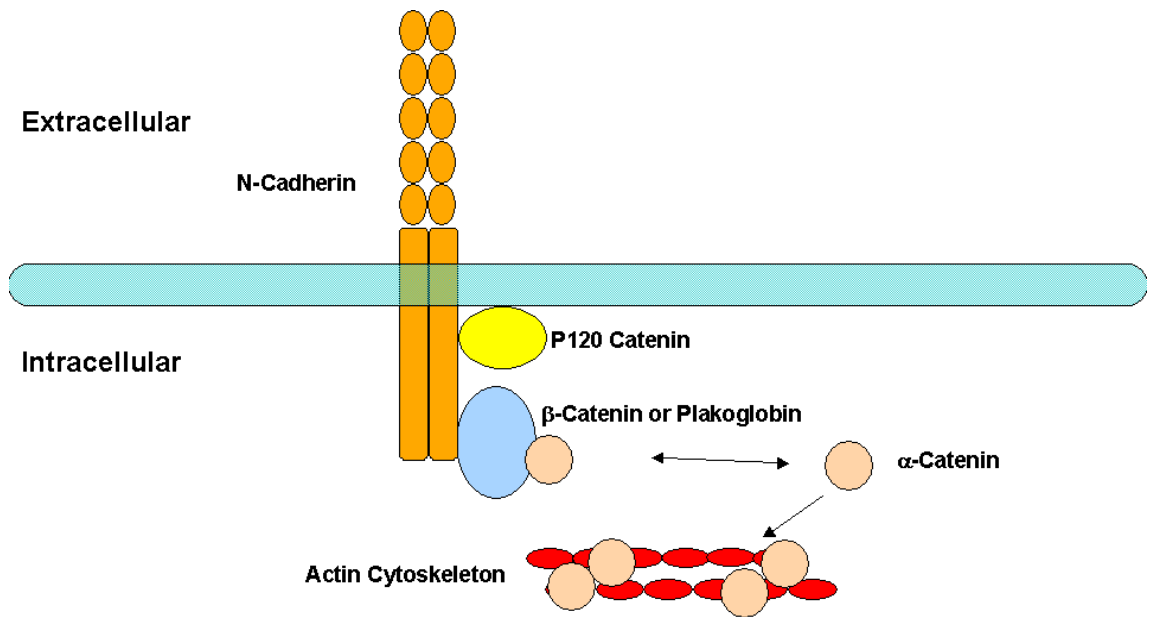
Figure 3-1: Schematic diagram of the cadherin complex
Adhesion by the cadherin complex is regulated by the catenins, namely β-catenin,
plakoglobin, and p120-catenin. p120 interacts with the juxtamembrane domain of
cadherins, while both β-catenin and plakoglobin compete for binding at the C-terminal
domain of the adherens junction. α-catenin is believed to either interact with β-catenin or
dimerize to bundle actin filaments (Weis and Nelson 2006).
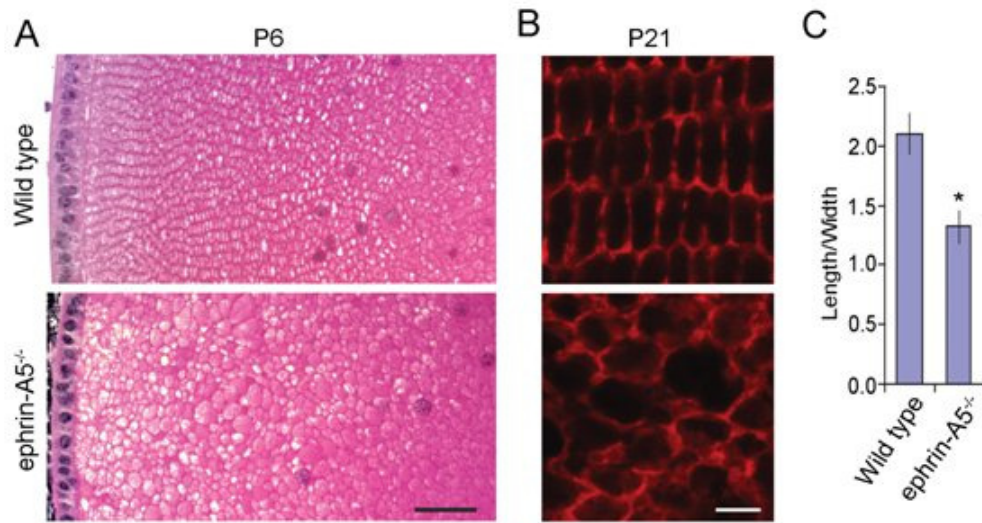
Figure 3-2: Irregular lens fiber cell shape in the ephrin-A5^{-/-} lens

(A) Lens fiber cell morphology of P6 wild-type and ephrin-A5$^{-/-}$ lenses. In cross-section, wild-type lens fiber cells are organized into meridonal rows of consistent shape and size. In contrast, ephrin-A5$^{-/-}$ fiber cells are not uniform and in disarray. Scale bar = 40 μm.

(B) Lens fiber cell shape in P21 wild-type and ephrin-A5$^{-/-}$ lenses. Wild-type lens fiber cells are of a uniform hexagonal shape with two long parallel edges and four shorter sides. Ephrin-A5$^{-/-}$ lenses are inconsistent and more rounded in their morphology. Scale bar = 5 μm.

(C) Length-to-width ratio of wild-type and ephrin-A5$^{-/-}$ lens fiber cells. While wild-type lens fiber cells are in a more elongated ratio of 2.1:1, ephrin-A5$^{-/-}$ fiber cells appear in a more cuboidal 1.3:1 ratio. * = $p < 0.05$, Student's *t*-test, n = 5 animals per group).

N-cadherin   WGA   Merge

Wild-Type

Ephrin-A5$^{-/-}$

N-Cadherin   Phalloidin   Merge
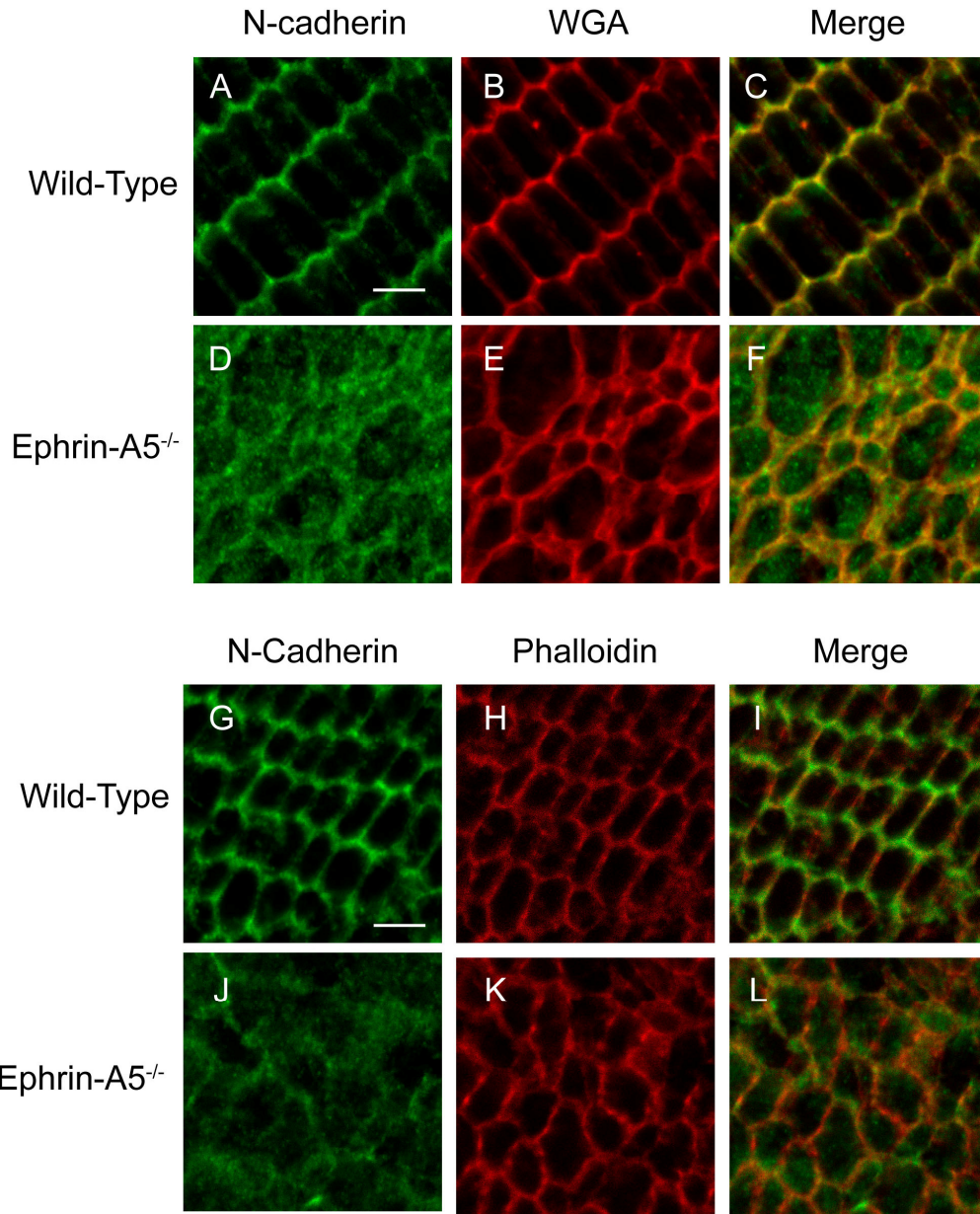
Wild-Type

Ephrin-A5$^{-/-}$

Figure 3-3: N-cadherin mislocalization in the ephrin-A5$^{-/-}$ occurs in the early postnatal lens

(A-F) High magnification images of N-cadherin in the middle cortical region of P21 wild-type (A-C) and ephrin-A5$^{-/-}$ (D-F) lens fiber cells. N-cadherin mislocalization in the lens fiber cell cytoplasm was observed in the ephrin-A5$^{-/-}$ lens. Cell membranes are delineated by Alexa Fluor 543-conjugated wheat germ agglutinin (WGA). Scale bar = 5 µm.

(G-L) High magnification images of N-cadherin in the middle cortical region of P7 wild-type (A-C) and ephrin-A5$^{-/-}$ (D-F) lens fiber cells. N-cadherin mislocalization in the ephrin-A5$^{-/-}$ lens begins as early as P7, when lens fiber cell aberrations are first apparent. Cell membranes are delineated by Alexa Fluor 543-conjugated phalloidin. Scale bar = 5 µm.
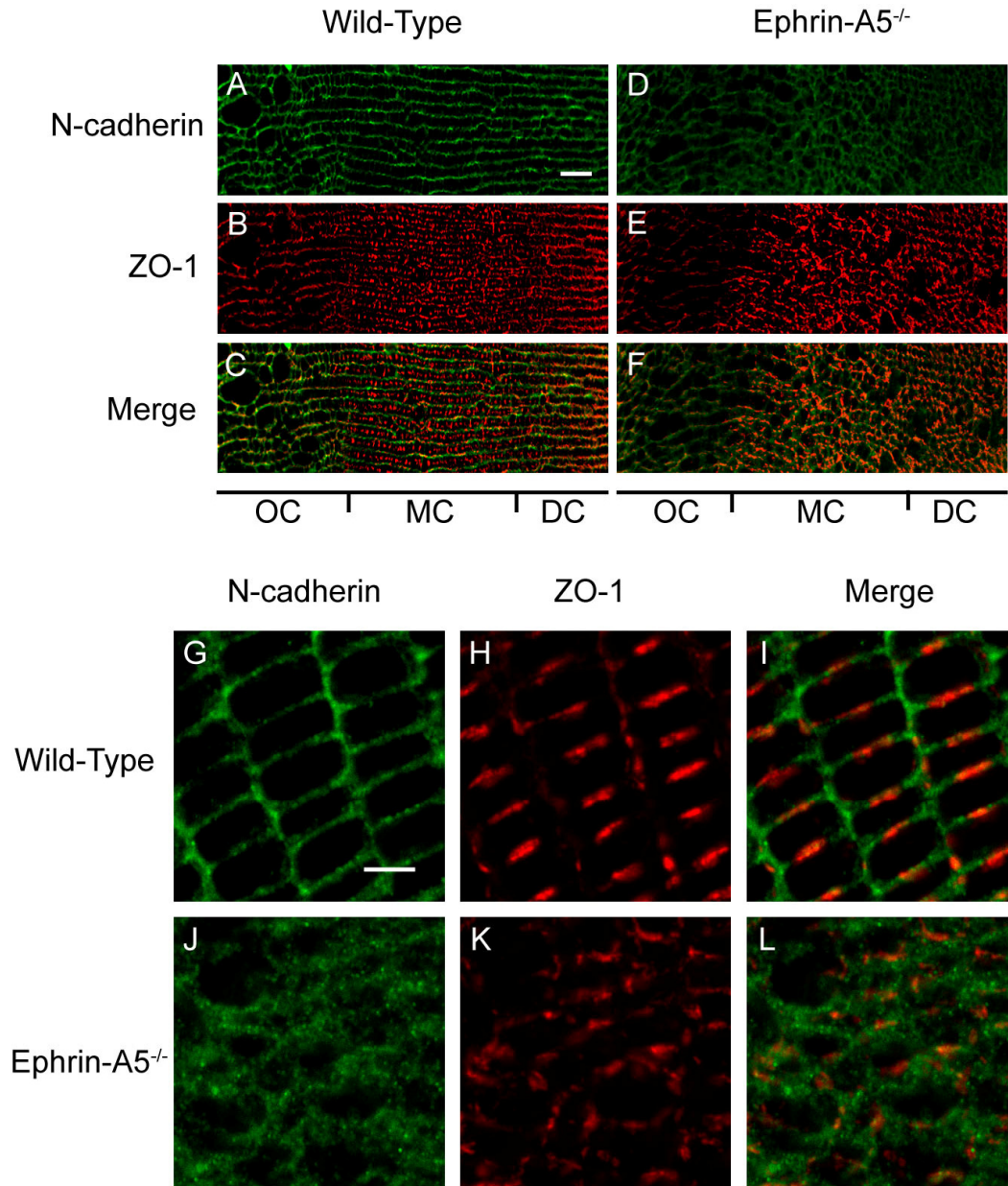
Figure 3-4: Disruption of N-cadherin localization throughout the ephrin-A5^{-/-} lens
(A-F) Low magnification images of P21 lenses in cross-section stained for N-cadherin
and ZO-1. Wild-type (A-C) showed N-cadherin expression in the short hexagonal sides
of lens fiber (A) while ZO-1 is localized in the long sides of the cells (B). In contrast,
ephrin-A5^{-/-} lenses (D-F) has N-cadherin localization both on the cell surface as well as
the cytoplasm (D), while the concentrated ZO-1 regions are still intact (E). OC = Outer
Cortex; MC = Middle Cortex; DC = Deep Cortex. Scale bar = 10 μm.
(G-L) High magnification images of N-cadherin and ZO-1 in the middle cortical region
of wild-type (G-I) and ephrin-A5^{-/-} (J-L) lens fiber cells. N-cadherin mislocalization in
lens fiber cell cytoplasm was observed in the ephrin-A5^{-/-} lens. ZO-1 complexes in this
region, while not organized, still appear intact. Scale bar = 5 μm.
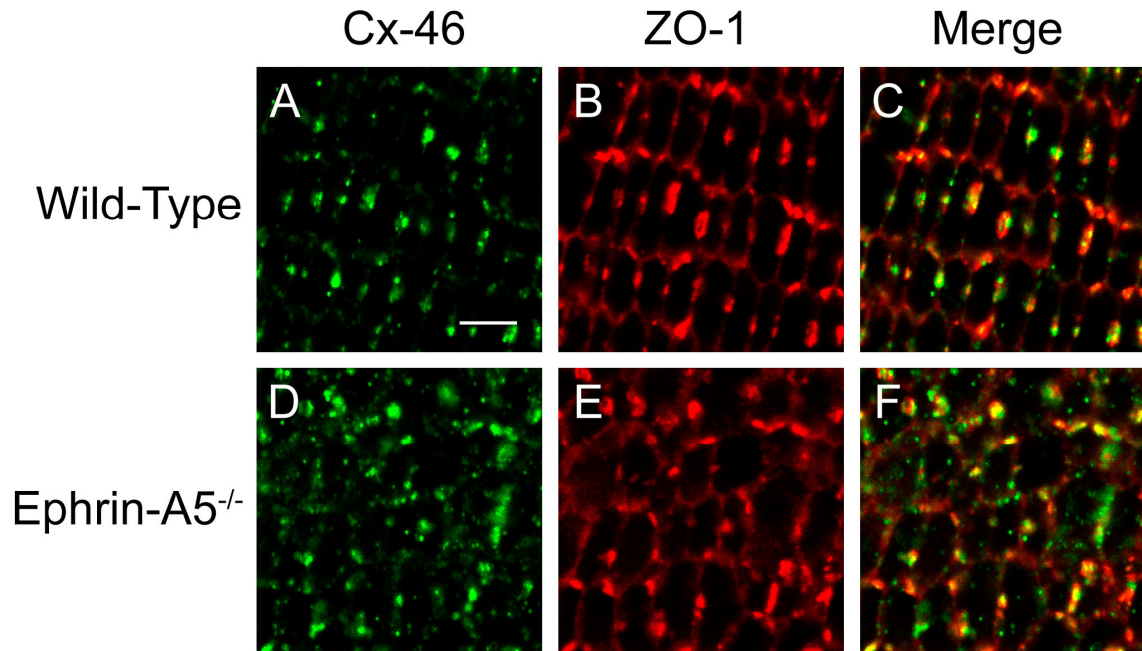
Figure 3-5: Co-localization of Cx-46 and ZO-1 in both wild-type and ephrin-A5^{-/-} lenses
(A-F) Images of Cx-46 (A, D), ZO-1 (B, E), and both (C, F) in the middle cortical layer of wild-type (A-C) and ephrin-A5 null (D-F) lenses. A strong co-localization between Cx-46 and ZO-1 is observed in both sets. In the ephrin-A5 mutant lens, the expression of these structures were disorganized, they were still found along the membranes of lens fiber cells.
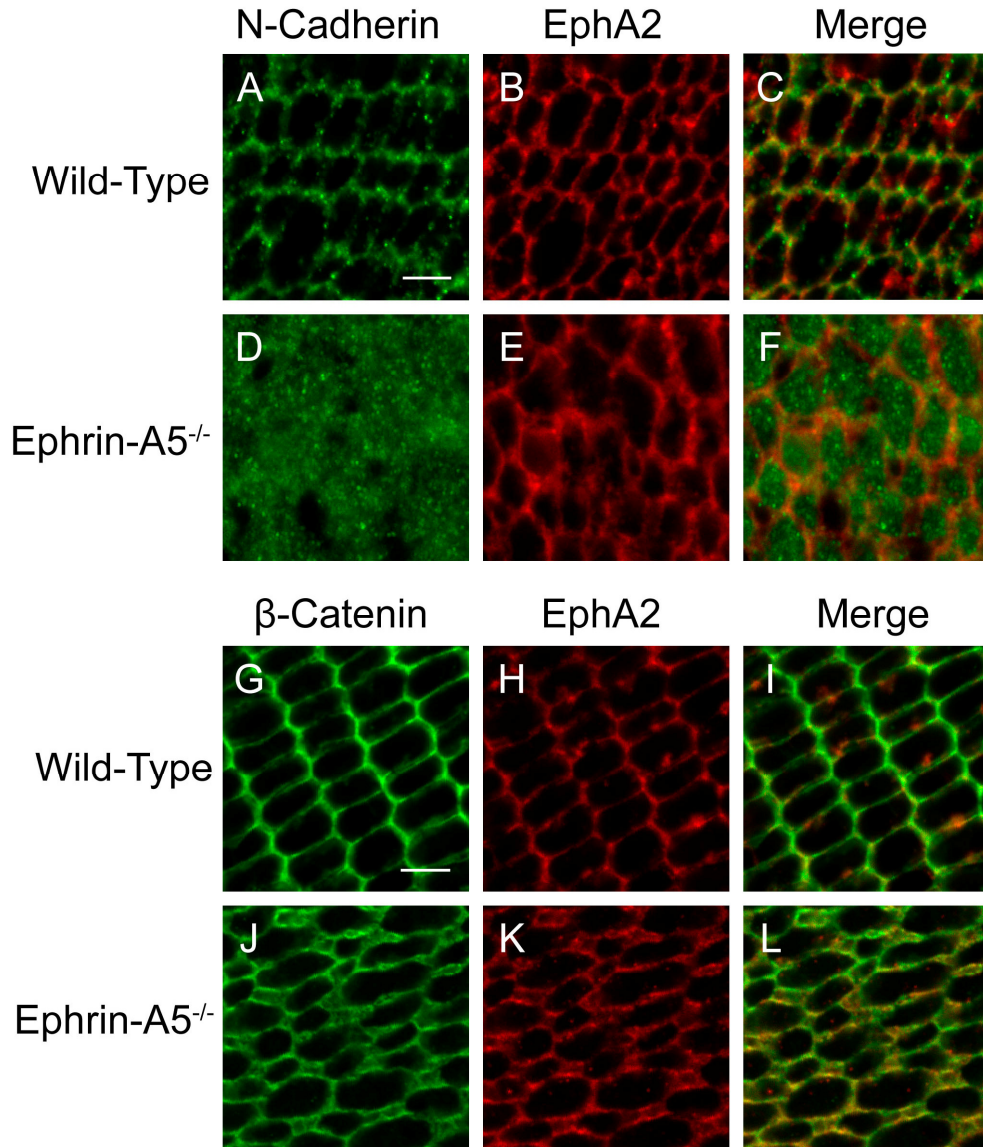
Figure 3-6: Co-localization of Adherens Junction molecules and EphA2
(A-F) N-cadherin and EphA2 in P7 wild-type and ephrin-A5$^{-/-}$ lenses. In the wild-type, both EphA2 and N-cadherin are observed strictly along the membrane of lens fibers cells, with a strong co-localization at the vertices of adjacent cells. In contrast, in ephrin-A5$^{-/-}$ lenses, EphA2 is still localized on the membrane while N-cadherin is now observed in both the membrane and cytoplasm. Scale bar = 5 μm.
(G-L) β-catenin and EphA2 in P21 wild-type and ephrin-A5$^{-/-}$ lenses. In the wild-type, β-catenin co-localizes with EphA2 along the short edges of the lens fiber cells on the membrane, with particular emphasis at the vertices between cells. Membrane co-localization between β-catenin and EphA2 is also observed in the ephrin-A5$^{-/-}$ lens; however note the presence of gaps at the edges between adjacent fiber cells (arrows in J and K). Also note the continued membrane localization of β-catenin in ephrin-A5 null lenses (J-L) as opposed to the cytoplasmic expression of N-cadherin (D-F). Scale bar = 5 μm.

A

IP: EphA2

| ephrin-A5 Treatment | - | + | - | + |
| EphA2 Transfection | - | - | + | + |

Blot: β-catenin

Blot: EphA2

B
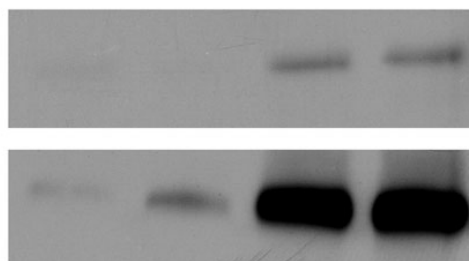
IP: β-catenin

| EphA2 Transfection | - | + |

Blot: EphA2

Blot: β-catenin
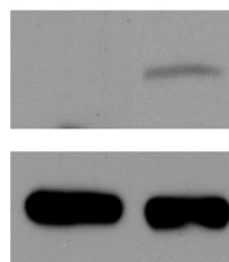
Figure 3-7: EphA2 interacts directly with β-catenin
(A) β-catenin co-immunoprecipitates with EphA2. 293T cells were transfected with EphA2 and/or treated with ephrin-A5. Cell lysates were immunoprecipitated for EphA2, with the resulting products analyzed by Western blot. The immunoprecipitate was probed for β-catenin to determine the interaction between the adherens junction molecule and EphA2. Cells transfected with EphA2 showed pulldown of β-catenin indicating interaction between both molecules.   The blot was reprobed with EphA2 to confirm loading.
(B) EphA2 co-immunoprecipitates with β-catenin. In the reciprocal experiment, β-catenin was pulled down from 293T cells transfected with EphA2, and the resulting product was analyzed through Western blot. EphA2 was found in β-catenin immunoprecipitate from the transfected 293T cells. Blots were reprobed to show equal levels of β-catenin.
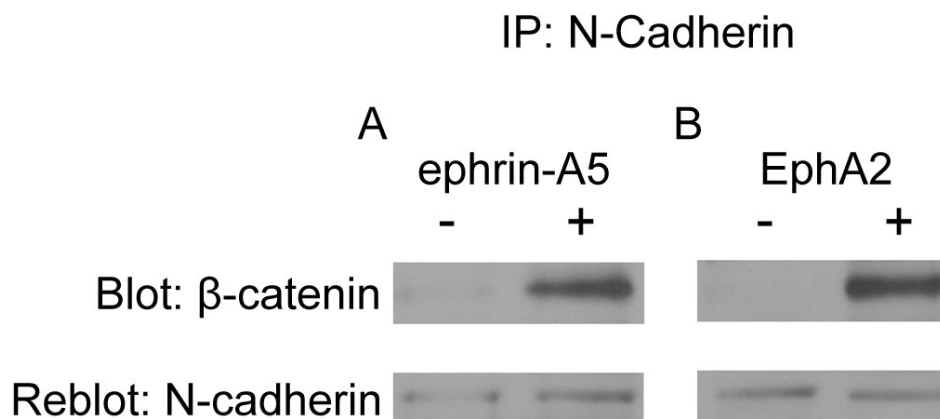
IP: N-Cadherin

Figure 3-8: Ephrin-A5 and EphA2 regulate the interaction between N-cadherin and β-catenin
(A) Ephrin-A5 enhances the interaction between N-cadherin and β-catenin. 293T cells were treated with IgG control or with ephrin-A5. Cells were then lysed and N-cadherin was immunoprecipitated. Resulting product was then analyzed via Western blotting for β-catenin levels. Treatment of cells with ephrin-A5 showed enhanced pulldown of β-catenin by N-cadherin. Blots were reprobed with N-cadherin to show equal loading.
(B) EphA2 increases the binding of N-cadherin to β-catenin. 293T cells were either untransfected or transfected with EphA2. Cells were lysed, with N-cadherin being immunoprecipitated from the lysate. Western blot analysis of the resulting product was done to determine pull-down of β-catenin by N-cadherin. EphA2 transfection of the cells displayed enhanced levels of β-catenin versus untransfected controls, indicating greater interaction between N-cadherin and β-catenin. Blots were reprobed for N-cadherin to determine equal loading.
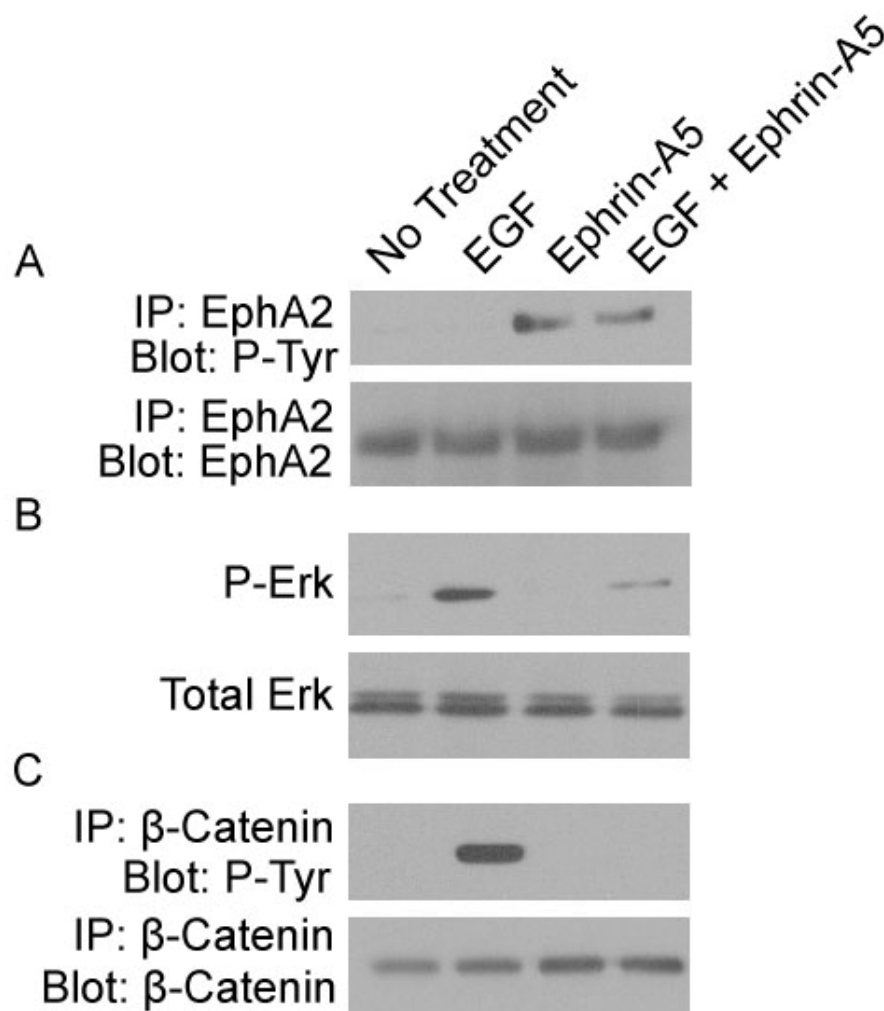
Figure 3-9: Ephrin-A5 inhibts β-catenin phosphorylation
(A) EphA2 activation in A431 cells. A431 cells were treated with EGF, ephrin-A5, or a combination of both. Cells were subsequently lysed and immunoprecipitated for EphA2. Tyrosine phosphorylation of EphA2 was analyzed through Western blot. EphA2 stimulation was only observed upon treatment of ephrin-A5. Samples were reblotted for EphA2 to ensure equal loading of samples.
(B) Erk phosphorylation after EGF and ephrin-A5 treatment in A431 cells. Samples treated with EGF, ephrin-A5, or both were examined for Erk phosphorylation. EGF stimulation enhanced Erk phosphorylation while ephrin-A5 inhibited this activity. Blots were reprobed for total Erk to verify equal loading.
(C) Ephrin-A5 inhibits EGF-induced phosphorylation of β-catenin. A431 cells were treated with EGF, ephrin-A5, or a combination of both. Cells were subsequently lysed and immunoprecipitated for β-catenin, and phosphorylation was determined using an anti-phosphotyrosine antibody. EGF stimulation of A431 cells induced β-catenin phosphorylation while ephrin-A5 alone had no effect. Co-treatment of both EGF and ephrin-A5 inhibited β-catenin activation. Blot was reprobed for β-catenin to ensure equal loading.
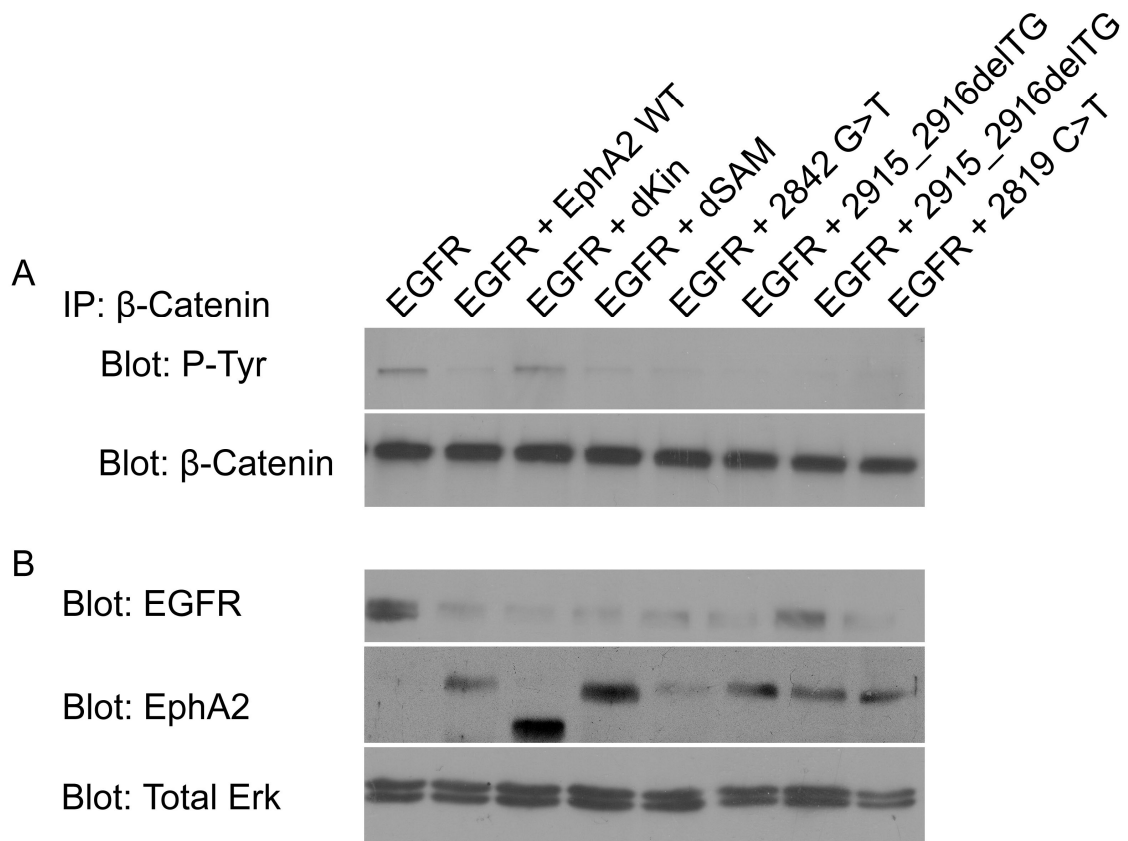
Figure 3-10: EphA2 regulates β-catenin dephosphorylation
(A) EphA2-mediated dephosphorylation of β-catenin is kinase-dependent and not affected by the SAM domain. 293T cells transfected with EGFR alone or with EphA2 were treated with EGF. Cells were subsequently lysed and immunoprecipitated for β-catenin, with the resulting samples analyzed by Western blot. EGFR transfection alone resulted in β-catenin phosphorylation, while co-transfection of EGFR and wild-type EphA2 resulted in a significant decrease in phosphorylation. In contrast, co-transfection of EGFR and the kinase deleted EphA2 resulted in robust phosphorylation of β-catenin similar to the EGFR-alone transfected group. EphA2 SAM domain deletion and SAM domain human cataracts mutants also retained β-catenin dephosphorylation. Blots were stripped and analyzed using an anti-β-catenin antibody to ensure equal loading.
(B) Blot of total lysates indicating levels of EGFR, EphA2, and total Erk.

CHAPTER 4: FORMATION OF PERSISTENT HYPERPLASTIC PRIMARY VITREOUS IN EPHRIN-A5$^{-/-}$ MICE

Introduction

The vitreous humor is a gel-like body situated between the retina and lens composed predominantly of water and extracellular matrix material. This structure plays an invaluable role in maintaining an environment suitable for the lens through its ability to control levels of intraocular oxygen and provide the lens with essential growth and differentiation factors (Lovicu and McAvoy 2005; Beebe 2008; Wang, Stump et al. 2009; Wang, McAvoy et al. 2010; Lovicu, McAvoy et al. 2011). Additionally, its transparent nature plays an important role in vision, particularly in allowing for light to travel without obstruction from the lens to the retina.

A. Development and Formation of the Vitreous

Progression of the vitreous body takes place under a series of stages. The primary vitreous (also referred to as the vascular vitreous) arises during early stages of ocular development, appearing by the 10-mm stage (fourth week) in humans and embryonic day 11 (E11) in mice. The primary vitreous consists of cells derived from mesodermal and ectodermal origins, including mesenchymal and neural crest components, and eventually forms the network of intraocular vessels known as the hyaloid vasculature (Pollard 1997; Gage, Rhoades et al. 2005; Iwao, Inatani et al. 2008). This structure is gradually replaced by the secondary vitreous (or avascular vitreous) forming in the cortical regions of the vitreous and restricting the cells of the primary vitreous (Ito, Nakashima et al. 2007). The

formation of the avascular vitreous occurs at the end of the sixth week of gestation in humans and postnatal day 4 (P4) in mice.

B. Hyaloid Vasculature – Development and Regression

The hyaloid vascular network that arises from the primary vitreous plays an important role in nourishing early ocular tissues with essential nutrients and factors (Saint-Geniez and D'Amore 2004) (Fig. 4-1). These vessels consist of the hyaloid artery (HA) entering into the early eye through the fetal fissure in the optic cup, the vasa hyaloidea propia (VHP) branching from the main artery, and the tunica vasculosa lentis (TVL) forming the dense capillary network that surrounds the posterior portion of the early lens (Goldberg 1997; Ito and Yoshioka 1999). The TVL branches into the annular vessels at the anterior edge of the optic cup which then connects to the choroidal vasculature; the hyaloid network consists of only arteries, with metabolic waste being drained by the choroidal veins (Saint-Geniez and D'Amore 2004). This network of vessels is only temporary; regression of the hyaloid vascular system is a key event in mammalian eye development in producing a transparent vitreous body. The timing of this event is species-dependent, as hyaloid regression in humans occurs late in fetal development while occurring within the first few weeks after birth in mice (Ito and Yoshioka 1999; Zhu, Madigan et al. 2000). The regression of the hyaloid is concurrent with the development and formation of the retinal vasculature (Saint-Geniez and D'Amore 2004).

While the events leading to hyaloid vessel formation have been studied, the factors and mechanisms regulating this vascular network remain unclear. Vascular endothelial growth factor (VEGF), a key molecule responsible for endothelial cell

production, is thought to play key roles in hyaloid vessel formation and organization.
The factor is expressed in the early developing lens (Shui, Wang et al. 2003) and is
responsible for the formation of the TVL surrounding the lens (Garcia, Shui et al. 2009).
Conditional mutant mice deficient in VEGF have inappropriate formation of hyaloid
structures, particularly in the wrapping of the TVL around the developing lens, indicating
the requirement of the growth factor in this transient system (Garcia, Shui et al. 2009).
Additionally, these conditional mutants develop postnatal lens deficiencies, further
supporting the notion that this transient network plays a critical role during early ocular
development (Garcia, Shui et al. 2009).

The mechanisms guiding primary vitreous and hyaloid vessel regression are also
not very well understood. Macrophages are known to play a key role in the deterioration
of the hyaloid vasculature, as their absence results in the persistence of this vasculature in
the postnatal eye (Lang and Bishop 1993; Lobov, Rao et al. 2005). This activity is
mediated through the canonical Wnt signaling pathway through WNT7b to induce
apoptotis (Lobov, Rao et al. 2005).

C. Persistent Hyperplastic Primary Vitreous (PHPV)

Failure of regression by the cells of the primary vitreous has severe physiological
consequences. The most revealing deficit is the development of the pathology persistent
hyperplastic primary vitreous (PHPV), more recently classified as persistent fetal
vasculature (PFV), a disorder in which tissue originating from the primary vitreous
remain in the postnatal eye (Goldberg 1997; Pollard 1997; Shastry 2009).   PHPV has
classically been characterized by the presence of a fibroblastic and vascularized tissue in
the posterior portion of the lens. The disease is classified into an anterior or posterior

form dependent on the formation of the mass in relation to the location of the lens. The anterior form involves the anterior segment and involves the presence of a retrolental mass and cataract. The posterior form affects the posterior segment and is distinguished by a dense opaque membrane and retinal folds (Goldberg 1997; Shastry 2009).

In humans, PHPV is a rare condition that is usually observed unilaterally, although bilateral cases have also been reported (Haddad, Font et al. 1978; Shastry 2009). The disease is often associated with other ophthalmological deformities including microphthalmia, retinal folding, intraocular hemorrhage, and cataracts (Pollard 1997; Shastry 2009). In addition, PHPV is often connected with other known eye disorders including glaucoma, myopia, morning glory syndrome, and retinopathy of prematurity (ROP), amongst several others, indicating a possible complexity in the mechanism of primary vitreous regression (Shastry 2009). Treatment for those with this disorder remains limited, with the main option being surgerical removal of the hyperplastic mass. However, outcomes of these procedures are often poor, with most patients either experiencing blindness or heavily impaired vision (20/200 eyesight) in the affected eye after surgery (Pollard 1997; Shastry 2009). Along with humans, PHPV is also prevalent amongst several breeds of dogs, and a genetic component to the disease has been implicated (Khaliq, Hameed et al. 2001; Shastry 2009).

Several transgenic mouse models develop PHPV-like phenotypes and have elucidated some aspects of primary vitreous regression. The Arf tumor suppressor gene has been extensively studied, as mice lacking the factor have been found to develop a pigmented retrolental mass (McKeller, Fowler et al. 2002; Martin, Thornton et al. 2004; Silva, Thornton et al. 2005; Thornton, Swanson et al. 2007; Freeman-Anderson, Zheng et

al. 2009).   Arf in this system has been found to be regulated by TGFβ2 and affects PDGFRβ-expressing perivascular cells present within the primary vitreous in a p53- and Mdm2-independent manner (Silva, Thornton et al. 2005; Freeman-Anderson, Zheng et al. 2009). Other molecules involved with the cell cycle, including p53, also have been suggested to play roles in primary vitreous regression as mutants of this factor also develop PHPV pathology (Reichel, Ali et al. 1998). Primary vitreous regression also has been found to involve the Wnt signaling pathway, as Frizzled-5 (Fzd5) mutants develop symptoms similar to PHPV (Zhang, Fuhrmann et al. 2008). This activity appears to occur in a non-autonomous manner, as the primary vitreous does not express Fzd5. The over-expression of pro-angiogenic factors involved with hyaloid vessel formation, such as VEGF-A118, also has marked effects in preserving the primary vitreous (Mitchell, Rutland et al. 2006; Rutland, Mitchell et al. 2007). However, knowledge of the nature of PHPV and the mechanisms inducing regression of the cells within the primary vitreous remains limited.

Our investigations on the development of the ephrin-A5$^{-/-}$ eye have uncovered an integral role for ephrin-A5 in the regression of the primary vitreous. Ephrin-A5$^{-/-}$ animals develop a hyperplastic mass posterior to the lens similar to symptoms of PHPV. The mass consisted of pigmented cells of neural crest origin, along with embedded vascular structures. Several Eph receptors were found to be expressed throughout the mass at various levels. However, ephrin-A5 was not detected with the primary vitreous indicating a possible non-cell autonomous activity by the ligand. Ephrin-A5 was also found to play a significant role in affecting the cell cycle within the retrolental structure.

Results

A. Ephrin-A5$^{-/-}$ mice develop symptoms indicative of PHPV

Previous studies by our group and others have shown that ephrin-A5$^{-/-}$ animals develop cataracts (Cooper, Son et al. 2008; Cheng and Gong 2011; Son, Park et al. 2012). As a result, we asked whether other ocular anomalies were present in the ephrin-A5 mutant eye (Fig. 4-2). While wild-type eyes exhibited no abnormalities (Fig. 4-2A), histological investigation of the adult ephrin-A5$^{-/-}$ eye revealed the presence of a large pigmented mass encapsulating vasculature posterior to the lens and extending towards the retina in a funnel-like shape, indicative of the pathology of PHPV (Fig. 4-2B and C). In addition to the attachment of the hyperplastic mass to the neuroretina and the posterior of the lens (Fig. 4-2D, G), ephrin-A5$^{-/-}$ eyes exhibited several additional hallmark characteristics of PHPV including retinal folding, neuroretinal detachment from the retinal pigmented epithelium (RPE) layer, and lens capsule rupture in later ages (Fig. 4-2E and F, H and I).

We further examined the retrolental mass to determine the progression during pre- and postnatal eye development (Fig. 4-3). Wild-type and ephrin-A5$^{-/-}$ eyes were analyzed at embryonic stages (E14 and E17) and at postnatal ages (P0, P6, P21, and P60). In wild-type eyes, the presence of the primary vitreous was observed at E14 (Fig. 4-3A). This mass is noticeably regressed as early as E17 (Fig. 4-3B and C) and is absent in postnatal animals, with no animals past P21 showing signs of the hyperplastic mass (Fig. 4-3G-I, Table 4-1). The primary vitreous is also present in ephrin-A5$^{-/-}$ eyes at E14 (Fig. 4-3B); however, the mass in these animals fails to regress at prenatal stages (Fig. 4-3D-F) and continues to persist at postnatal stages (Fig. 4-3H-L). When analyzing the prevalence of

PHPV, adult wild-type mice (>P60) displayed no presence of a retrolental mass, while all ephrin-A5$^{-/-}$ animals and about half of the ephrin-A5$^{+/-}$ subjects were observed to have the presence of an abnormal retrolental mass with vasculature and pigmented cells (wild-type = 0%, ephrin-A5$^{-/-}$ = 100%, ephrin-A5$^{+/-}$ = 49.2%; Table 4-1).

B. Hyaloid vascular structures are present within the hyperplastic mass in the ephrin-A5$^{-/-}$ eye

PHPV is associated with the failed regression of the hyaloid vascular system (Goldberg 1997; Pollard 1997; Shastry 2009). Histological sections of ephrin-A5$^{-/-}$ eyes displayed the presence of blood vessels within the mass of pigmented cells indicative of the pathological human hyperplastic primary vitreous (Fig. 4-2C). We therefore analyzed the aberrant structures for vascular markers in the postnatal ephrin-A5$^{-/-}$ eyes. The presence of blood vessels were confirmed through immunofluorescence using several known markers including CD-31 and collagen-IV for endothelial cells, α-smooth muscle actin (αSMA) for mature pericytes, platelet derived growth factor receptor (PDGFR)-β for immature pericytes, and tyrosinase-related protein (TRP-1) for melanocytes (Fig. 4-4). At P7, vascular structures within the hyperplastic mass were found to be positive for the indicated blood vessel markers (Fig. 4-4A). However, with the exception of TRP-1, the localization of these markers was restricted to only vessels within the mass, suggesting that the majority of the mass is not of vascular origins. Interestingly, PDGFR-β, a marker known to primarily label pericytes, was also observed on the outer layer of the retrolental structure at P7 as well as on the blood vessels. In contrast, TRP-1 staining was observed throughout much of the hyperplastic tissue, indicating that a major population of cells in this mass is composed of pigmented cells.

To understand the development of the hyaloid vessels within the hyperplastic mass, we determined the expression of these vascular markers at various developmental timepoints in the ephrin-A5$^{-/-}$ vitreous. The primary vitreous showed positive expression for CD-31, αSMA, and collagen-IV at E14 (Fig. 4-4B and C). By E16, the expressions of these markers are more restricted to defined vessels within the mass, with expression only restricted in the hyaloid vessels by P0 (Fig. 4-4B and C). PDGFR-β was found to be throughout the mass at E14; however, in contrast to the CD-31 and αSMA labeling, this expression was still found to be throughout much of the primary vitreous even by P0 (Fig. 4-4D). The presence of endothelium and pericyte precursors in ephrin-A5 eyes confirms that the retrolental mass contains hyaloid vasculature.

C. Hyaloid vasculature regression in areas outside of the hyperplastic mass occurs normally in ephrin-A5$^{-/-}$ mice

While remnants of the hyaloid vasculature within the retrolental tissue were observed, the role these vessels play in the persistence of this pigmented tissue remain unknown. We therefore examined whether the persistent mass in ephrin-A5$^{-/-}$ mice was a direct result of a failure of hyaloid regression (Fig. 4-5). Whole-mount postnatal wild-type and ephrin-A5$^{-/-}$ lenses were enucleated with the hyaloid vasculture attached to the posterior of the lens. Vessels were labeled using FITC-conjugated isolectin B4, and Z-stack images of the posterior lens were taken using confocal microscopy. Vessels of the tunica vasculosa lentis (TVL) were analyzed as previously described (Ito and Yoshioka 1999). At P2, ephrin-A5$^{-/-}$ eyes had consistently more vessels compared to the wild-type controls, though the increase in vessel number was not significant (Fig. 4-5A and D, $p > 0.05$, Student's t-test, $n = 4$ per group). Similar to wild-type tissues, the number of

vessels observed in ephrin-A5$^{-/-}$ eyes consistently decreased over age, with no significant difference observed at P8 and P14 between the wild-type and ephrin-A5$^{-/-}$ eyes (Fig. 4-5B-C, E-F, $p > 0.05$, Student's t-test, n = 4 per group). However, ephrin-A5$^{-/-}$ whole mounts at all stages displayed the presence of the retrolental mass encapsulating the remaining hyaloid vasculature (Fig. 4-5D-F, outlined by white dotted line). Therefore, while the vessels surrounded by the hyperplastic mass persist and do not undergo proper vascular regression, other hyaloid vasculature is able to regress properly in the ephrin-A5$^{-/-}$ eye. Together, these observations suggest that the accumulation of the primary vitreous mass, and not hyaloid vessel regression, may be the predominant cause of the pathological accumulation of the retrolental cellular mass.

Regression of the hyaloid vasculature is regulated in large part by the activity of macrophages (Lobov, Rao et al. 2005). To determine macrophage localization in the context of the retrolental tissue, we labeled cells using the marker F4/80 (Fig. 4-6). F4/80 positive cells are observed throughout the mass in postnatal stages (Fig. 4-6A-C) and are also found within the primary vitreous at embryonic stages in both wild-type and ephrin-A5$^{-/-}$ eyes (Fig. 4-6D and E). Altogether, these data verify the proper regression of the hyaloid vasculature outside of the retrolental mass.

D. Hyperplastic mass exhibits pigmentation at postnatal stages

A characteristic of PHPV is the pigmentation of the retrolental mass (Haddad, Font et al. 1978). Pigmented cells within mammals originate from either the retinal pigmented epithelium (RPE) or the neural crest (Goding 2007). We observed that the retrolental mass in ephrin-A5$^{-/-}$ animals were only pigmented in postnatal mice (Fig. 4-4A) and were lacking pigmentation in prenatal stages (see Fig. 4-10). To determine the

onset of pigmentation within the primary vitreous, we examined the expression profile of the melanin precursor marker TRP-1 in ephrin-A5$^{-/-}$ eyes at various embryonic and postnatal stages (Fig. 4-7). Expression for TRP-1 was noticeably absent in the primary vitreous during embryogenesis (Fig. 4-7A-B) even though it was present in the RPE layer at these time points (Fig. 4-7D-E). Interestingly, positive TRP-1 labeling was observed in many of the cells within the mass by P0 (Fig. 4-7C). This rise in expression of TRP-1 in the hyperplastic mass is concurrent with the expression of the marker in the choroid in the postnatal period (Fig. 4-7F), a tissue of neural crest origin (Hu, Simon et al. 2008), indicating that the pigmented cells of the primary vitreous forming the retrolental mass in ephrin-A5$^{-/-}$ mice are not from the RPE, but rather from the neural crest.

To confirm that the persistent primary vitreous cell mass is of neural crest origin, we labeled cells for the transcription factor AP2β, a marker for cells from the neural crest (Mitchell, Timmons et al. 1991) (Fig. 4-8). Cells expressing AP2β are observed in the retrolental tissue of both wild-type and ephrin-A5$^{-/-}$ mice at early developmental stages including E14 and E16 (Fig. 4-8A and B, D and E). Cells of this lineage are also distinct from hyaloid vessels, as co-labeling of tissue for both AP2β and αSMA shows distinct populations at E16 (Fig. 4-8C and F), revealing that a significant population of cells within the retrolental mass are of neural crest origin. We further established that the persistent retrolental mass in the postnatal ephrin-A5 mutants were of neural crest origin by co-staining P0 ephrin-A5$^{-/-}$ eyes for both AP2β and TRP-1 (Fig. 4-8G-N). Both markers were found throughout the entirety of the hyperplastic mass at this early postnatal stage (Fig. 4-8G-J). Closer inspection showed that both AP2β and TRP-1

labeled the same cells (Fig. 4-8K-N). Together, these data indicates that the pigmented

retrolental mass in the ephrin-A5$^{-/-}$ eye are of neural crest origin.

E. Eph receptors are expressed within the hyperplastic mass

As ephrin activity is initiated by interactions with their respective Eph receptors,

we next set out to identify Eph receptors associated with the hyperplastic mass (Fig. 4-9).

To determine the localization of Eph receptors in the primary vitreous mass capable of

binding to ephrin-A5, we employed a soluble ephrin-A5 protein fused with human-Fc to

label Eph receptors in P7 ephrin-A5$^{-/-}$ sections (Marcus, Matthews et al. 2000). By using

a fluorescent secondary, we observed Eph receptor expression throughout the mass both

within pigmented cells and the blood vessels (Fig. 4-9A-C).

We next set out to identify which specific Eph receptors were present within the

hyperplastic mass using real time RT-PCR. The hyperplastic mass was dissected and

extracted for RNA, and this was followed by a determination of the relative expression of

individual Eph receptors through RT-PCR. As the volume of tissue was limited, an RNA

amplification technique was employed. The expression of several Eph receptors was

observed, most notably EphA6 and EphB4. Other Eph receptors were observed to a

lesser extent, including EphA2, EphA5, EphA8, and EphB6 (Fig. 4-9D). To verify these

results, immunofluorescence staining was employed for EphA2 and EphB4, both of

which were observed in the retrolental tissues of the ephrin-A5 mutants. EphA2 was

observed only on the outer edge (Fig. 4-9E) while EphB4 was observed throughout the

entirety of the mass (Fig. 4-9F), confirming the presence of Eph receptors in the

abnormal tissue. The protein expression of EphA6 was not examined due to a lack of

specific antibody (data not shown).

F. Ephrin-A5 expression is absent in the developing primary vitreous

Because the absence of ephrin-A5 results in the failed regression of the primary vitreous, we set to define the expression of the ligand in the developing eye. In order to detect ephrin ligand localization, we employed the use of a soluble EphA5 conjugated to alkaline phosphatase (EphA5-AP) to label available ephrins and compared the expression between wild-type and ephrin-A5$^{-/-}$ specimens (Fig. 4-10). Wild-type and ephrin-A5$^{-/-}$ embryos at E12, E14, and E17 were analyzed, as the retrolental tissue was still present at these developmental stages. Positive EphA5-AP staining was observed at E12 in the wild-type eyes, with continued expression being present at both E14 and E17 (Fig. 4-10A-C). In wild-type tissues, staining was particularly prominent in the cornea, the lens epithelium and bow regions, the nasal retina, and the ciliary body. Little or no positive staining was observed in the ephrin-A5$^{-/-}$ eye (Fig. 4-10D-F), indicating that ephrin-A5 is the major A-class ephrin ligand within the developing eye.

However, when looking specifically at the primary vitreous, positive AP labeling was notably absent at all stages in wild-type tissues (Fig. 4-10A-C). No EphA5-AP staining was detected in either E17 wild-type or ephrin-A5$^{-/-}$ eyes (Fig. 4-10G and H), indicating little or no ephrin-A ligand expression in this specific region. The absence of positive AP-labeling suggests that ephrin-A5 may be acting upon the primary vitreous in a cell non-autonomous manner.

G. Ephrin-A5 affects cell cycle control in the primary vitreous

The persistent presence of the retrolental mass in ephrin-A5$^{-/-}$ mice implies that there are alterations in cell cycle dynamics in the primary vitreous. To determine whether the tissue continues to grow at postnatal stages, we compared the volumes of the

hyperplastic mass at P7 and P21 (Fig. 4-11). Eyes were sectioned sagittally and cut in 10

micrometer serial sections, after which the total volume of the mass was then calculated

stereologically. Using this analysis, a significant increase in size of the mass of P21

ephrin-A5$^{-/-}$ eyes was found in comparison to P7 eyes (Fig. 4-11A-C, p < 0.05, Student's

t-test, n = 4).

The growth of the retrolental mass in postnatal ephrin-A5$^{-/-}$ eyes led us to

investigate cell division of the primary vitreous during development (Fig. 4-12).

Embryos at E14 and E16 were labeled using BrdU and staining was compared between

wild-type and ephrin-A5$^{-/-}$ animals. Mice at their respective stages were injected with

BrdU two hours prior to sacrifice, after which embryos were dissected and fixed for

cryosectioning. At E14, cells of the primary vitreous in both wild-type (Fig. 4-12A and

B) and ephrin-A5$^{-/-}$ (Fig. 4-12C and D) embryos displayed a large percentage of BrdU

positive cells with no statistical difference observed between the groups (Fig. 4-12G,

wild-type = 19.99% ± 3.99%, ephrin-A5$^{-/-}$ = 24.92% ± 3.32%, p > 0.05, Student's t-test, n

= 4). By E16, the proliferation rate was decreased in both wild-type and ephrin-A5$^{-/-}$

animals; however, the percentage of BrdU positive cells in wild-type animals was

reduced to half that observed in the primary vitreous of ephrin-A5$^{-/-}$ embryos (Fig. 4-12G,

wild-type = 8.6% ± 2.58%, ephrin-A5$^{-/-}$ = 15.4% ± 1.84%, p < 0.05, Student's t-test, n =

4). The mitotic activity of the retrolental mass in ephrin-A5$^{-/-}$ eyes continues into

postnatal stages as BrdU incorporation was observed in P7 ephrin-A5$^{-/-}$ ocular tissues

(Fig. 4-12E). PCNA expression, another marker for cell division, was also observed in

hyperplastic the mass at postnatal stages, further verifying the proliferation of this

aberrant tissue in the ephrin-A5$^{-/-}$ eye (Fig. 4-12F). Together, these data indicate that

mitotic activity within the primary vitreous is significantly reduced by E16 in the wild-type, but is retained in the ephrin-A5$^{-/-}$ eye.

Because we have established that the retrolental mass consists of predominantly neural crest-derived melanocytes, and since ephrin-A5 appears to be affecting the rate of cell proliferation in the primary vitreous, we next analyzed the ability for ephrin-A5 to inhibit the proliferation of pigmented cells of neural crest origin. Melan-A cells, a spontaneously immortalized normal murine melanocyte cell line of neural crest origin (Shin, Wall et al. 2010), were treated with cross-linked ephrin-A5-Fc or an IgG-Fc control and analyzed for differences in cell proliferation using an MTT colorimetric assay. A significant reduction in cells was observed 2 days after plating in groups treated with ephrin-A5-Fc compared to controls (Fig. 4-12H, $p < 0.05$, Student's t-test, n = 4 sets per group), indicating that ephrin-A5-Fc treatment inhibits proliferation of Melan-A cells. This result confirms that ephrin-A5 is capable of inhibiting cell division of neural crest-derived melanocytes.

Wild-type and ephrin-A5$^{-/-}$ primary vitreous tissues were also analyzed for apoptosis using an antibody against cleaved caspase-3 (Fig. 4-13). Both wild-type and ephrin-A5$^{-/-}$ primary vitreous tissues at E14 and E16 showed signs of cells undergoing apoptosis cleaved caspase-3 (Fig. 4-13A and B), but the percentage of cleave caspase-3-positive cells were not significantly different between the two groups (Fig. 4-13C). Altogether, these data indicate that mitotic activity within the primary vitreous is significantly reduced by E16 in the wild-type, but is retained in the ephrin-A5$^{-/-}$ eye.

Discussion

We have observed that mice lacking the Eph receptor ligand ephrin-A5 develop the ocular pathology PHPV, more recently known as PFV. Postnatal ephrin-A5^{-/-} mice develop a large pigmented retrolental mass that persists throughout the lifetime of the animal. The presence of this tissue results in several secondary deficits including retinal displacement and lens capsule rupture. The mass is derived from primary vitreous cells that have failed to regress and consists of neural crest-derived cells encompassing hyaloid vasculature. Eph receptor expression is observed throughout the entirety of the mass, while ephrin-A5 expression was notably absent within the primary vitreous in wild-type tissues. Additionally, the cells within the persistent retrolental structure are mitotically active at postnatal stages in ephrin-A5^{-/-} animals.

A. The complex relationship between PHPV and primary vitreous regression

PHPV and PFV have been classically defined as diseases resulting from the failed regression of intraocular vasculature (Goldberg 1997). However, the mechanisms underlying primary vitreous and hyaloid vasculature degeneration remains limited. In mice, hyaloid vessel formation arises at embryonic stages while regression occurs in the first few weeks of postnatal development, during which time retinal vasculature begins to form (Saint-Geniez and D'Amore 2004). Hyaloid development is dependent on several factors including vascular endothelial growth factor (VEGF) (Mitchell, Rutland et al. 2006; Rutland, Mitchell et al. 2007), which is expressed in the lens during early ocular development and is required for the maintenance of the early vascular network (Mitchell, Risau et al. 1998; Shui, Wang et al. 2003; Gogat, Le Gat et al. 2004; Saint-Geniez and D'Amore 2004). The degradation of this structure is mediated by both apoptotic (Lang

and Bishop 1993; Kato, Patel et al. 2002; Lobov, Rao et al. 2005) and authophagic

mechanisms (Kim, Yu et al. 2010), and responds to levels of oxygen (Patz, Eastham et al.

1953; Gyllensten and Hellstrom 1954; Bischoff, Wajer et al. 1983).

While much of the focus in past research has been on vascular regression, the

etiology of PHPV is likely to be complex. The primary vitreous is a transient tissue

containing cells of neural crest and mesodermal origins, the latter eventually giving way

to the formation of the hyaloid vasculature (Gage, Rhoades et al. 2005; Iwao, Inatani et

al. 2008). As development progresses, the primary vitreous is compressed around the

hyaloid artery by the secondary (or avascular) vitreous (Ito, Nakashima et al. 2007),

eventually regressing to form the crystalline vitreous humor.

The persistent mass observed in ephrin-A5$^{-/-}$ mice verifies the complexity of the

primary vitreous degeneration process containing several aspects that include, but is not

limited to, hyaloid vessel regression (Kato, Patel et al. 2002; Lobov, Rao et al. 2005).

The presence of both pigmented and vascular structures in the retrolental mass along with

the continued degeneration of the TVL in ephrin-A5$^{-/-}$ mice indicates that ephrin-A5 is

important in the overall regression of the primary vitreous and not just the hyaloid

vasculature. Additionally, hyaloid vessels in areas not encapsulated by the pigmented

cell mass, in particular the TVL, regress over time at similar rates between both the wild-

type and ephrin-A5$^{-/-}$ eyes. While the retrolental mass observed in ephrin-A5$^{-/-}$ eyes also

contains extensive vascular structures, the most prominent feature has been the presence

of pigmented cells of neural crest origin surrounding the vasculature. In this sense, the

name Persistent Hyperplastic Primary Vitreous may be more accurate than Persistent

Fetal Vasculature, at least in the context of ephrin-A5$^{-/-}$ mice, since the aberrant structure consists of both vascular and pigmented cells.

B. Pigmented structures in primary vitreous are of neural crest origin

Accumulation of pigmented cells have been previously documented in human PHPV (Haddad, Font et al. 1978) and have been observed in mouse models of the disease (McKeller, Fowler et al. 2002; Martin, Thornton et al. 2004). One of the underlying questions in determining the mechanisms underlying primary vitreous regression has been in understanding the origin of these pigmented cells. Melanocytes arise from two distinct cellular populations: the neural crest or the retinal pigmented epithelium (Goding 2007). It has been previously proposed that PHPV is a result of the accumulation of RPE cells accumulating around hyaloid vasculature (Haddad, Font et al. 1978; Martin, Thornton et al. 2004).

Similarly, we have found the pigmented cells surrounding the hyaloid vasculature in the ephrin-A5$^{-/-}$ mice. However, several lines of evidence, including the difference in onset of pigmentation in the primary vitreous versus the RPE layer and the neural crest marker labeling of the primary vitreous cells, indicate the origin of these pigmented cells in our model to be of neural crest origin and not from the RPE. We believe primary vitreous cells of neural crest origin that have failed to regress in the ephrin-A5$^{-/-}$ eye produce melanin in postnatal periods and continue to proliferate throughout the lifetime of the animal. Whether human PHPV also contains pigmented cells from the neural crest is yet to be determined.

C. Mechanisms of primary vitreous regression

While ephrin-A5 plays a key role in primary vitreous regression, the mechanisms underlying the persistence of the mass remain to be resolved. The importance of the Eph family of molecules in vascular and neural crest biology has been previously identified. EphB4 and its associated ligand, ephrin-B2, are required for the artery and vein specification during development (Wang, Chen et al. 1998; Gerety, Wang et al. 1999). Ephrin-B2 is an important factor in the adhesion and migration of pericytes onto vascular walls (Foo, Turner et al. 2006; Semela, Das et al. 2008). Ephrin-A1 and EphA2 have both also been found to play roles in affecting angiogenic activity (Chen, Hicks et al. 2006; Ojima, Takagi et al. 2006). Our current data indicates that ephrin-A5 also may play a role in the inhibition of vasculature, given that the hyaloid vasculature fails to completely regress in ephrin-A5$^{-/-}$ animals. Additionally, the Ephs have extensive roles in neural crest development and differentiation, particularly in segmental migration (Krull, Lansford et al. 1997; Wang and Anderson 1997; Kasemeier-Kulesa, Bradley et al. 2006). Expression of several EphB receptors have been identified in melanoblasts and identified to be important in the migration of these cells into the dorsalateral migration pathway (Santiago and Erickson 2002). Future studies may offer insight into the role of ephrin-A5 in both of these cellular populations.

D. Ephrin-A5 regulates the regression of the primary vitreous in a cell non-autonomous manner

While the retrolental mass was found express several Eph receptors, we were unable to detect any expression of ephrin-A ligands in the primary vitreous during its development. At present, this finding implies that ephrin-A5 is acting upon the primary

vitreous in a cell non-autonomous manner to influence its regression. Several previous studies have identified A-classed ephrins to be capable of being cleaved while retaining some functional activity (Hattori, Osterfield et al. 2000; Wykosky, Palma et al. 2008; Alford, Watson-Hurthig et al. 2010). Additionally, our current study identified high levels of ephrin-A ligands throughout other developing ocular tissues, including the ciliary body and lens, both of which have been documented to secrete factors into the vitreous humor (Bertazolli Filho, Laicine et al. 1996; Bishop, Takanosu et al. 2002; Beebe 2008; Garcia, Shui et al. 2009). One possibility is that ephrin-A5 from regions of high expression may be cleaved and diffused through the vitreous. These molecules would then be able to directly interact with EphA receptors within the primary vitreous and direct the regression process.

Ephrin-A5 may also be acting away from this region and regulating the release of other factors that would normally affect primary vitreous regression. Diffusible factors within the lens such as VEGF have been previously found to regulate hyaloid vessel formation and regression (Beebe 2008; Garcia, Shui et al. 2009), and platelet-derived growth factor (PDGF) signaling has been implicated in primary vitreous regression (Silva, Thornton et al. 2005). The high levels of ephrin-A5 in surrounding ocular tissues may therefore be negatively regulating the release of mitotic factors such as VEGF or PDGF resulting in the regression of the primary vitreous tissue.

A final possibility is that ephrin-A5 within the primary vitreous is expressed at low levels during the regression process. We detected ephrin-A ligand expression using an EphA5-AP binding method that showed high levels of specificity. However, this staining method may lack the sensitivity to detect low concentrations of ephrin-A5

expression within the primary vitreous tissue that are undergoing degradation. Further studies are required to elucidate the role of ephrin-A5 during this degeneration process.

E. Ephrin-A5 and its role in cell cycle inhibition

The development of PHPV as a result of a loss of cell cycle control has been previously implicated in other transgenic mouse studies, most notably in the development of Arf tumor suppressor knockouts. Arf mutant mice develop PHPV pathology very similar to those found in the ephrin-A5^{-/-} mice, namely the formation of a hyperplastic pigmented mass in the posterior lens segment (McKeller, Fowler et al. 2002; Martin, Thornton et al. 2004; Silva, Thornton et al. 2005; Freeman-Anderson, Zheng et al. 2009). The expression of the Arf tumor suppressor within the persistent mass is regulated in part by PDGF signaling (Silva, Thornton et al. 2005) and driven by TGFβ2 (Freeman-Anderson, Zheng et al. 2009). The similarities between ocular phenotypes between the ephrin-A5 and Arf mutants, along with ephrin-A5 negatively regulating cell cycle dynamics, indicates similar mechanisms in the regression of the primary vitreous. Additionally, ephrin-A5 may be regulating primary vitreous regression through other pathways, such as through Wnt signaling as Frizzled-5 mutants and through the control of VEGF, mutations that also develop PHPV phenotypes. Determining whether ephrin-A5 and these molecules are in the same or parallel pathways may further elucidate the mechanisms underlying primary vitreous regression.
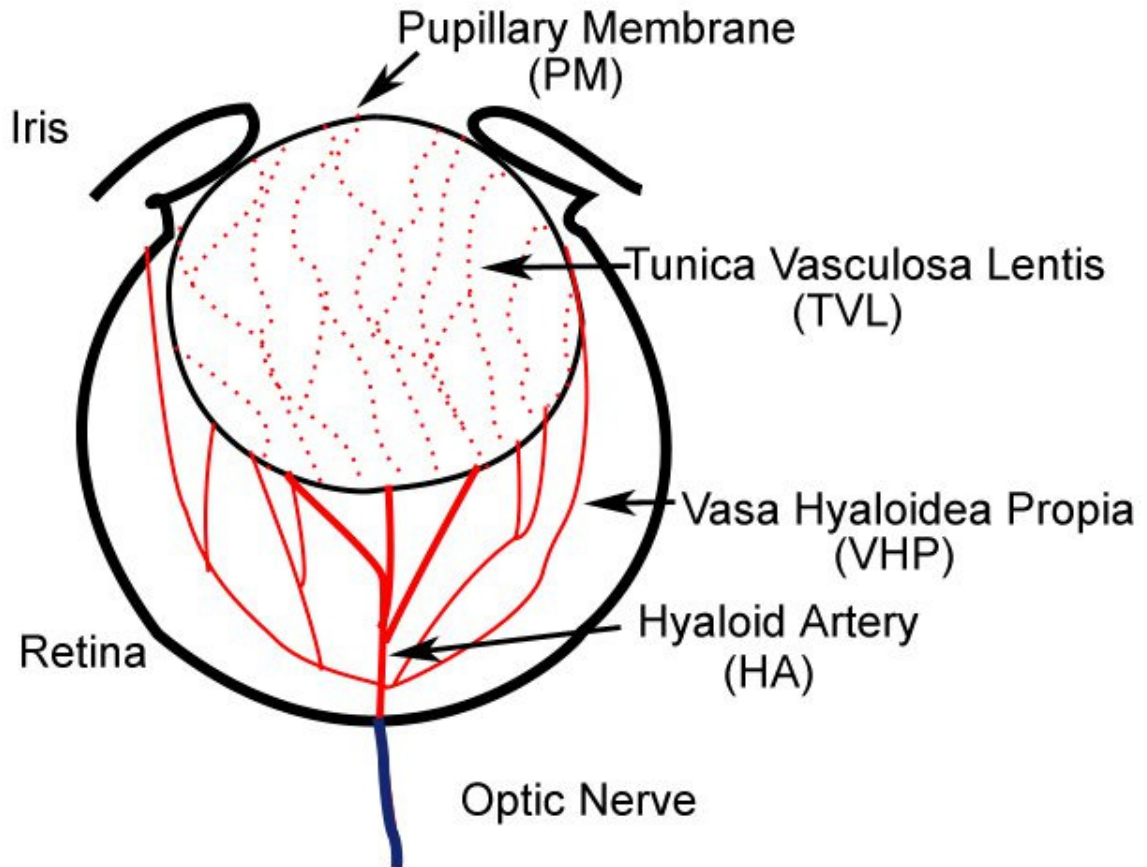
Figure 4-1: Schematic of the hyaloid vasculature
Intraocular vasculature within the mammalian eye provides nutrients to the avascular tissues in early ocular development. This network of vessels include the hyaloid artery (HA), the vasa hyaloidea propia (VHP), the tunica vasculosa lentis (TVL), and the pupillary membrane (PM). Vascular regression is species dependent; hyaloid vessel regression occurs during embryogenesis in humans and during the first few weeks after birth in mice. Vasculature is outlined in red. Figure adapted from Ito and Yoshioka (1999).
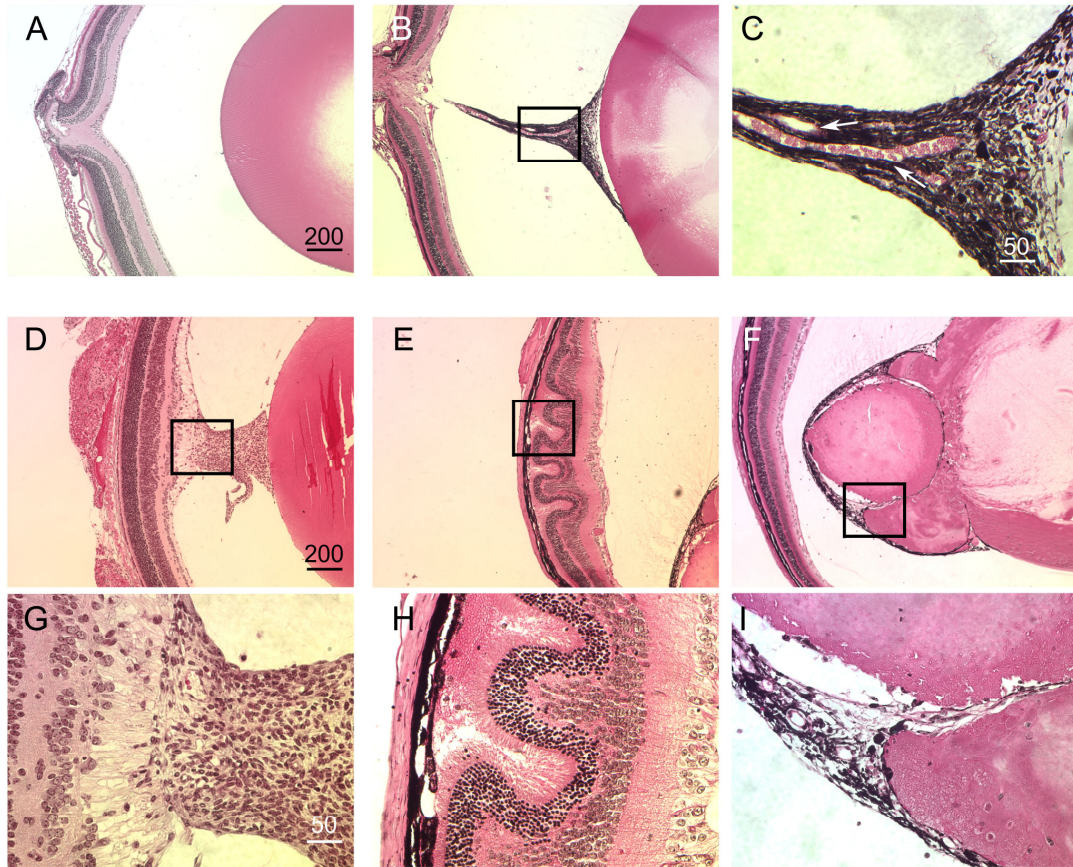
Figure 4-2: Ephrin-A5$^{-/-}$ mice develop hallmark symptoms of PHPV
(A-C) Histological sections of wild-type and ephrin-A5$^{-/-}$ eyes at P21. Whereas no ocular abnormalities are observed in the wild-type mouse (A), ephrin-A5$^{-/-}$ eyes (B) display a large pigmented mass posterior to the lens and attached to the retina. Higher magnification on the mass (C) shows the presence of vasculature embedded in the pigmented cells (see arrows). Scale bars in μm.
(D-I) Ephrin-A5 mutant eyes display other symptomatic characteristics of PHPV. These include tissue attachment to both the retina and lens (D and G), retinal folding and detachment of the RPE layer from the neuroretina (E and H), and lens capsule rupture (F and I). (G, H, I) are magnified images of (D, E, F), respectively. Scale bars in μm.
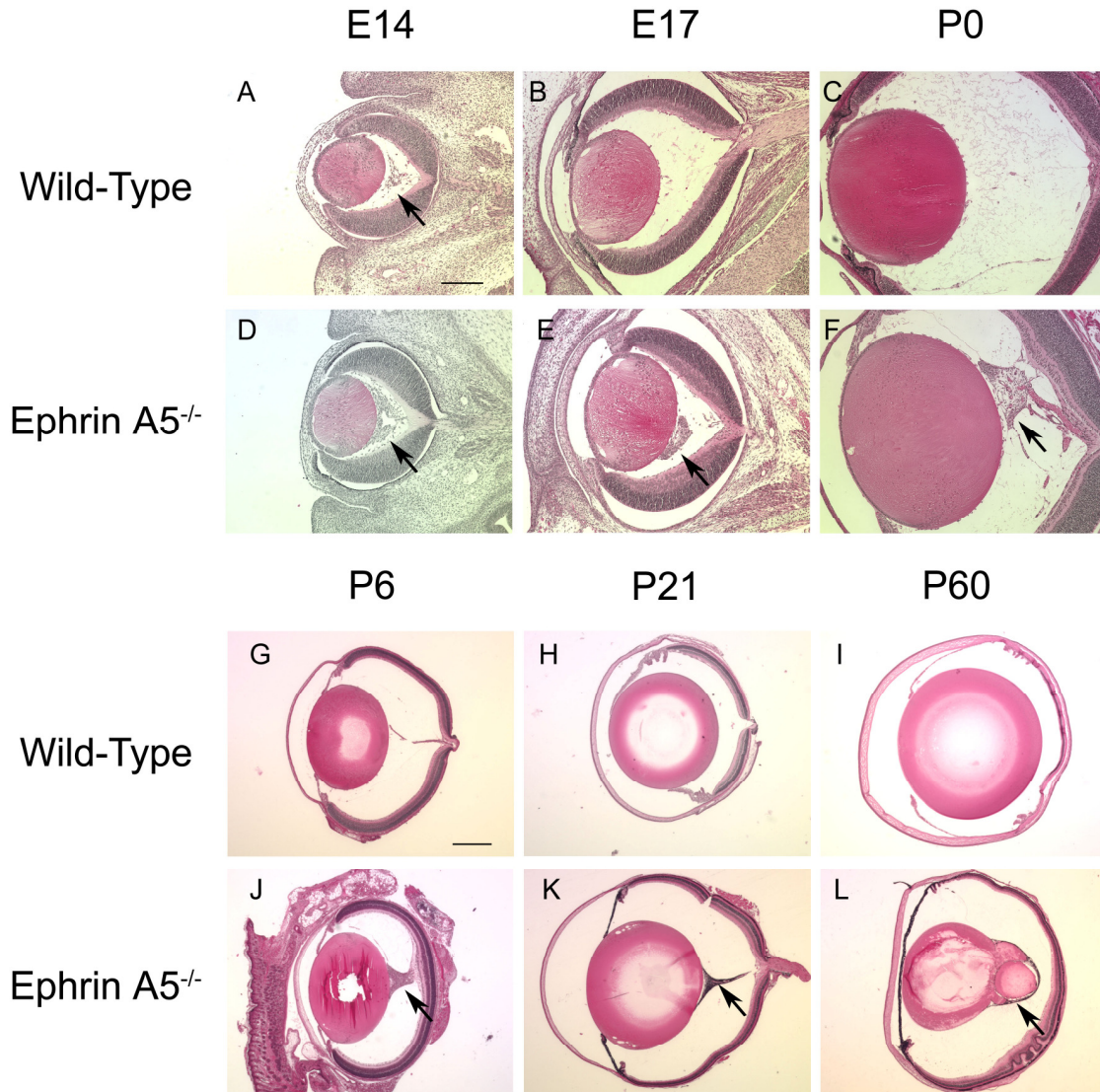
Figure 4-3: Primary vitreous cells in the ephrin-A5$^{-/-}$ eye persists at postnatal stages
(A-F) Sections of wild-type (A-C) and ephrin-A5$^{-/-}$ (D-F) eyes during embryonic
development. The cells of the primary vitreous are present in the wild-type eye at E14
(A, as indicated by the arrows), but soon regress and are absent at later developmental
stages (B and C). In contrast, primary vitreous cells in the ephrin-A5$^{-/-}$ eye that appear in
early embryogenesis (D) fail to regress (E and F). Scale bar = 200 μm.
(G-L) Eye development at postnatal stages of wild-type (G-I) and ephrin-A5$^{-/-}$ (J-L)
animals. Wild-type eyes at early postnatal stages show remnants of hyaloid vessels at
early stages (G) but are largely devoid of cells in the vitreous humor (H and I). Ephrin-
A5$^{-/-}$ eyes show the presence of a pigmented retrolental mass throughout the adult stages
(J-L). Scale bar = 500 μm.

Age	Wild-Type			Ephrin-A5$^{-/-}$			Ephrin-A5$^{+/-}$		
	# with Mass	# Animals	Prevalence	# with Mass	# Animals	Prevalence	# with Mass	# Animals	Prevalence
P0-P5	3	17	17.6%	17	17	100%	8	19	42.1%
P6-P10	3	18	16.7%	20	22	90.9%	8	20	40%
P21	0	29	0%	35	36	97.2%	18	30	60%
>P60	0	53	0%	51	51	100%	29	59	49.2%

Table 4-1: Prevalence of PHPV

Few wild-type animals show the presence of a retrolental mass at early postnatal ages while none are observed in adulthood. In contrast, almost all ephrin-A5$^{-/-}$ animals were found to have an aberrant retrolental mass well into adulthood. Half of the ephrin-A5$^{+/-}$ observed also were found to have an abnormal mass posterior to the lens.
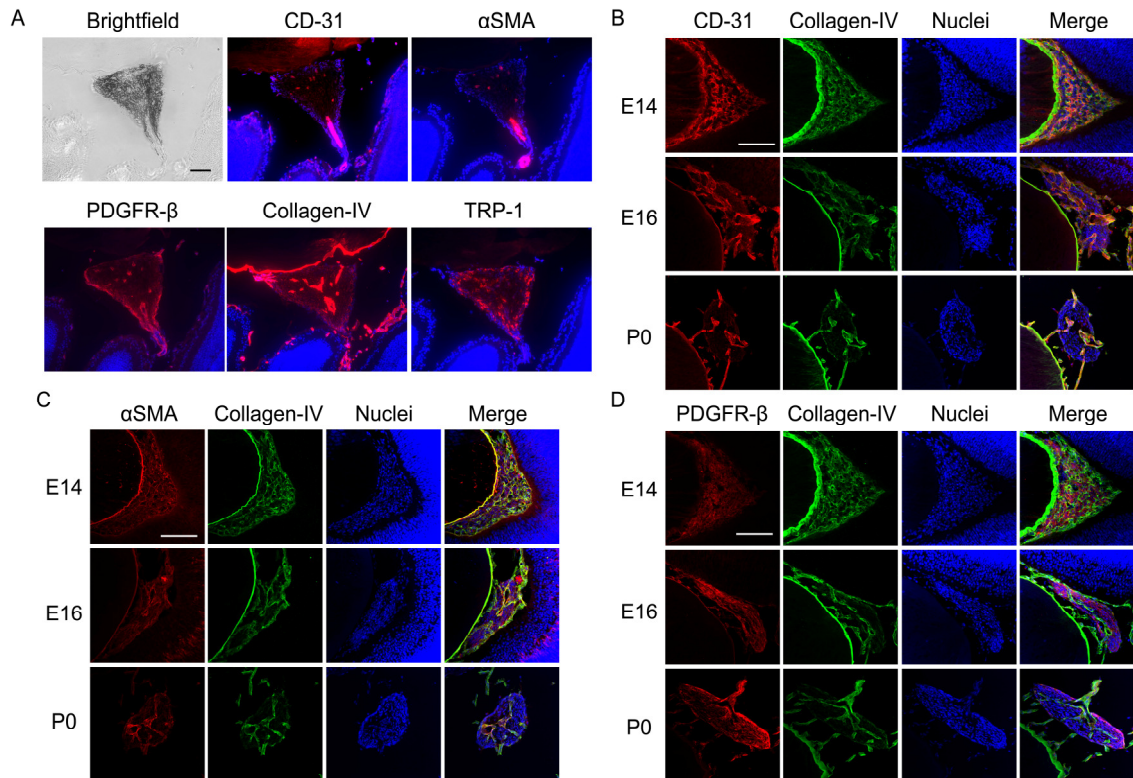
Figure 4-4: Cells of the persistent primary vitreous mass consist of vascular and pigmented cells

(A) Serial sections of a P7 ephrin-A5$^{-/-}$ eye is immunostained for markers indicative of endothelial cells (CD-31 and collagen-IV), smooth muscle cells (αSMA), pericytes (PDGFR-β), and melanocytes (TRP-1). Scale bars = 100 μm.

(B) Expression of CD-31 through the development of the primary vitreous in the ephrin-A5$^{-/-}$ eye. CD-31 positive cells are observed within the primary vitreous at E14, and are restricted in the vessels by P0. Scale bars = 100 μm.

(C) Expression of αSMA of the primary vitreous during embryonic eye development in the ephrin-A5$^{-/-}$ eye. Similar to CD-31 expression, αSMA positive cells are seen in the primary vitreous at E14, with expression only being observed in vessels by P0. Scale bars = 100 μm.

(D) Expression of PDGFR-β of the developing ephrin-A5$^{-/-}$ eye. PDGFR-β is observed in the primary vitreous in the ephrin-A5 null eye at E14. This expression is continued in much of the retrolental mass through P0. Scale bars = 100 μm
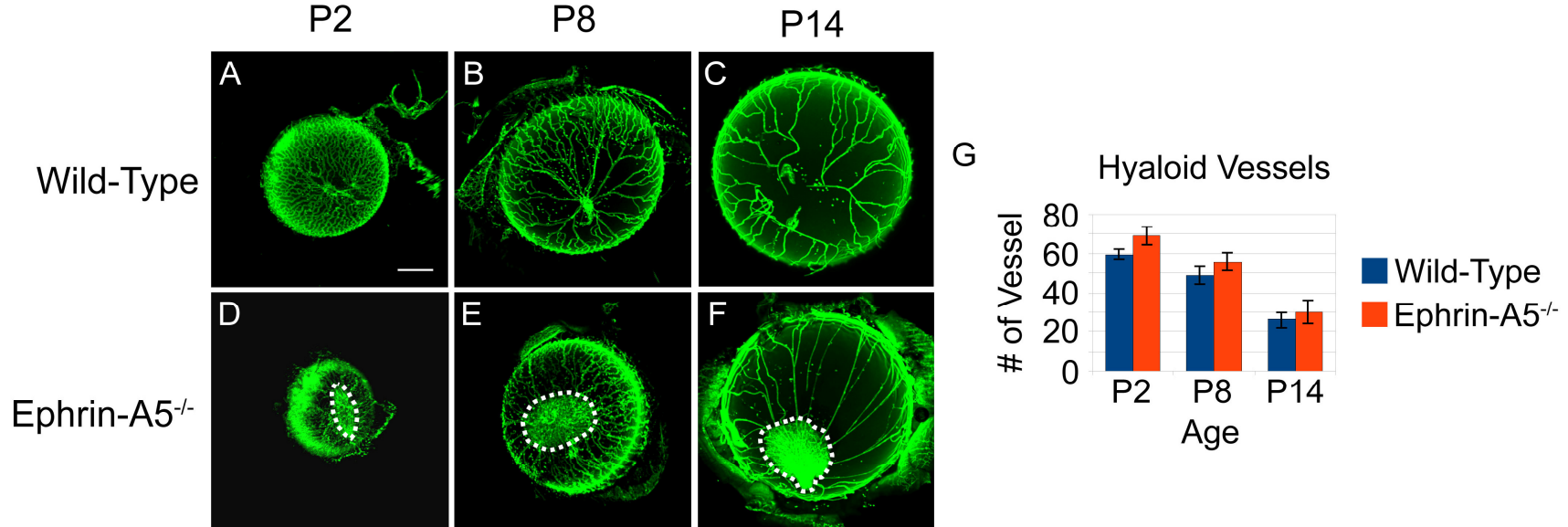
Figure 4-5: TVL regression still occurs in the ephrin-A5$^{-/-}$ eye
(A-F) Whole-mount preparations of lenses viewed from the posterior of wild-type (A-C) and ephrin-A5$^{-/-}$ (D-F) eyes at several early postnatal stages. Lenses are dissected with hyaloid vessels intact and are stained with FITC-conjugated isolectin-B4. Note the presence of the retrolental mass in the ephrin-A5$^{-/-}$ lenses (outlined by a white dotted line). Scale bar = 0.5 mm.
(G) Quantification of vessel numbers of the TVL vessels present at P2, P8, and P14 in WT and ephrin-A5$^{-/-}$ mice. Consistent hyaloid regression is observed in both the wild-type and ephrin-A5$^{-/-}$ eyes. While the number of vessels is consistently higher in the ephrin-A5$^{-/-}$ mice at similar ages, these differences within each age were not found to be statistically significant. $p > 0.05$ for each age, Student's t-test, n = 4 animals for each group.

F4/80 TRP-1 Merge

P7 Ephrin-A5$^{-/-}$

Wild-Type - E16 Ephrin-A5$^{-/-}$ - E16
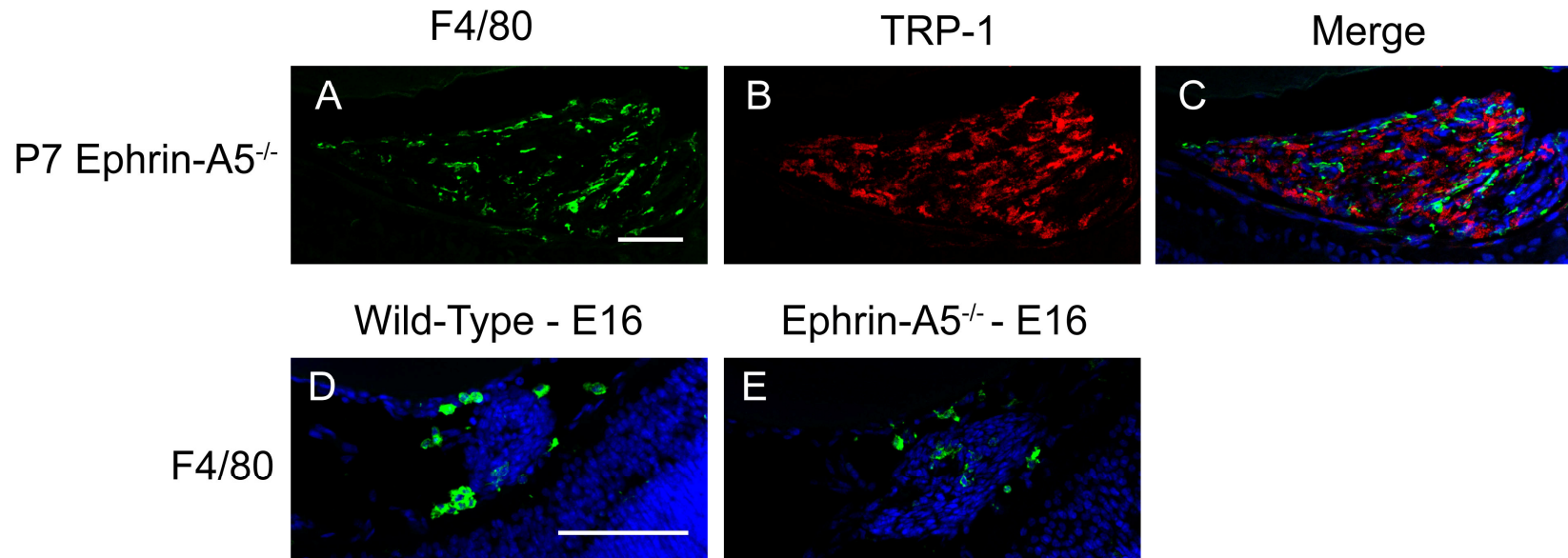
F4/80

Figure 4-6: Macrophage expression observed in the retrolental mass in ephrin-A5$^{-/-}$ animals
(A-C) Retrolental tissue of the P7 ephrin-A5$^{-/-}$ eyes stained for the macrophage marker F4/80. Positive staining is observed throughout the mass (A). TRP-1+ cells delineate the retrolental mass tissue in the mutant eye (B). F4/80+ and TRP-1+ cells do not co-localize (C). Scale bars = 100 μm.
(D and E) The primary vitreous shows expression of F4/80 in both wild-type (D) and ephrin-A5$^{-/-}$ (E) tissues at embryonic stages. Scale bars = 100 μm.
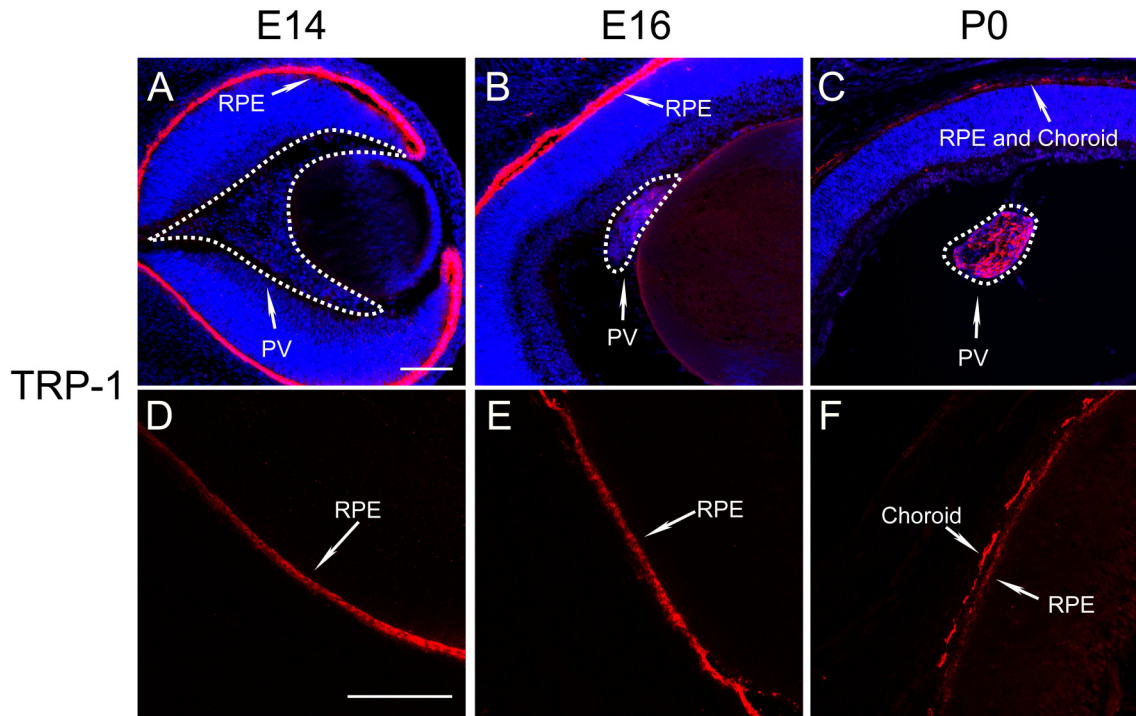
Figure 4-7: The persistent primary vitreous in the ephrin-A5$^{-/-}$ eye are not pigmented until postnatal stages

(A-C) Ephrin-A5$^{-/-}$ eyes stained for TRP-1 at various developmental stages. Cells of the primary vitreous are mostly negative for TRP-1 during prenatal time points E14 and E16 (A and B). At P0, TRP-1 positive cells are observed in the retrolental mass (C). Primary vitreous is outlined by a white dotted line. TRP-1 is stained in red; nuclear staining is shown in blue. RPE = Retinal Pigmented Epithelium, PV = Primary Vitreous. Scale bar = 100 μm.

(D-F) The RPE layer is positive for TRP-1 at embryonic stages. In contrast to the absence of TRP-1 expression in the primary vitreous, the RPE shows positive expression at E14 and E16 (D and E). Positive expression in the choroid is evident by P0 (F). Scale bar = 100 μm.
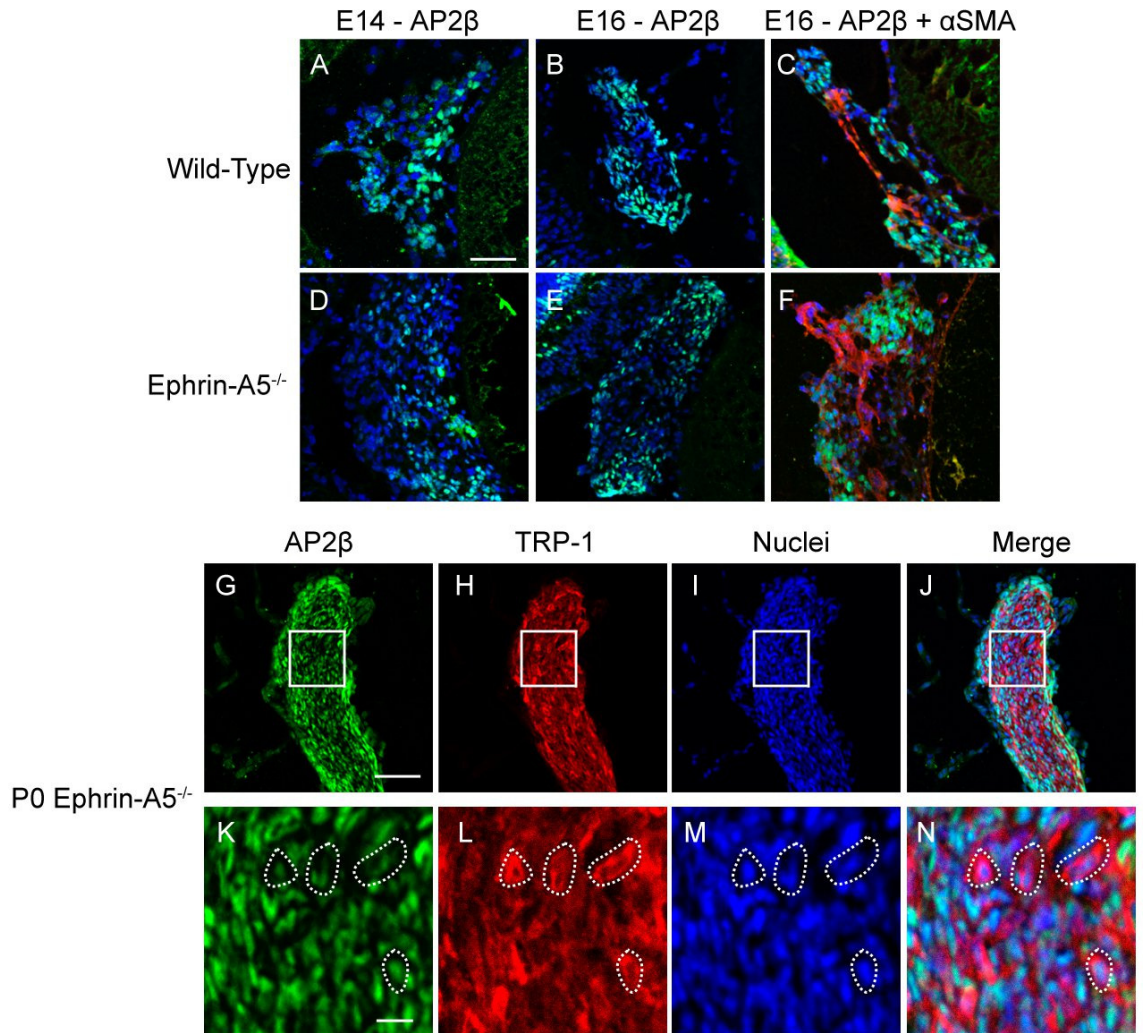
Figure 4-8: The primary vitreous contains neural crest-derived cells
(A and B, D and E) Cells of the primary vitreous stained for neural crest marker AP2β (green). Primary vitreous cells at E14 (A and D) and E16 (B and E) of both wild-type and ephrin-A5$^{-/-}$ tissue are positive for AP2β. Scale bar = 20 μm.
(C and F) Cells of the primary vitreous in both wild-type and ephrin-A5$^{-/-}$ embryos show that AP2B+ cells are in a separate population from the vasculature (aSMA+ cells). Scale bar = 20 μm.
(G-J) The persistent primary vitreous in the P0 ephrin-A5$^{-/-}$ eye is both positive for AP2β and TRP-1. Pigmented cells, defined by the TRP-1 staining (cytoplasmic), co-label with the AP2β marker (nuclear) indicating cells of neural crest lineage. Scale bar = 50 μm.
(K-N) Higher magnification of the boxed region outlined in (G-J), respectively. Dotted white lines indicate select cells co-labeled for both AP2β and TRP-1. Scale bar = 10 μm.

Figure 4-9: Eph receptor expression is observed within the retrolental mass in ephrin-A5$^{-/-}$ eyes

(A-C) Total Eph receptor localization in the primary vitreous mass. The hyperplastic is labeled with ephrin-A5-Fc to identify Eph receptors capable of binding to the ligand. Eph receptor expression is present throughout much of the mass (A) and is not restricted to PDGFR-β+ vasculature (B and C). Nuclei are counterstained in blue. Scale bars = 100 μm.

(D) Relative expression levels of various Eph receptors at postnatal stages in the retrolental mass. Expression of several Eph receptors are observed either moderately (EphA2, EphA5, EphA8, EphB6) or highly (EphA6 and EphB4). n = 4 animals.

(E and F) Localization of receptors EphA2 and EphB4 in the retrolental mass. EphA2 expression is observed in the outer region of the mass (E), while EphB4 labeling is seen throughout the mass and within the blood vessels (F). Scale bars = 100 μm.

Figure 4-10: Ephrin-A5 expression is not detected in the primary vitreous
(A-F) Ephrin-A5 expression in the developing eye. EphA5-AP labeling in the developing eye was used to determine ephrin-A ligand expression. Expression is observed at high levels in the cornea, lens, and peripheral tips of the retina at E12, E14, and E17 in the wild-type (A-C) while absent in the ephrin-A5$^{-/-}$ eye (D-F), indicating ephrin-A5 specificity. However, no labeling is observed in the primary vitreous in either wild-type or ephrin-A5$^{-/-}$ tissues. Scale bars = 200 μm.
(G and H) High magnification images of the primary vitreous at E17 in wild-type (G) and ephrin-A5$^{-/-}$ (H) ocular tissues labeled with EphA5-AP. Staining is not observed in wild-type or ephrin-A5$^{-/-}$ tissues. Primary vitreous is outlined in a black dotted line. Re = Retina, Le = Lens, Co = Cornea. Scale bars = 200 μm.

P7

P21

TRP-1

A

B

C

PHPV Volume By Age

Volume (in mm³)

0.005
0.020
0.005
0.010
0.005
0

*

P7   P21

Age
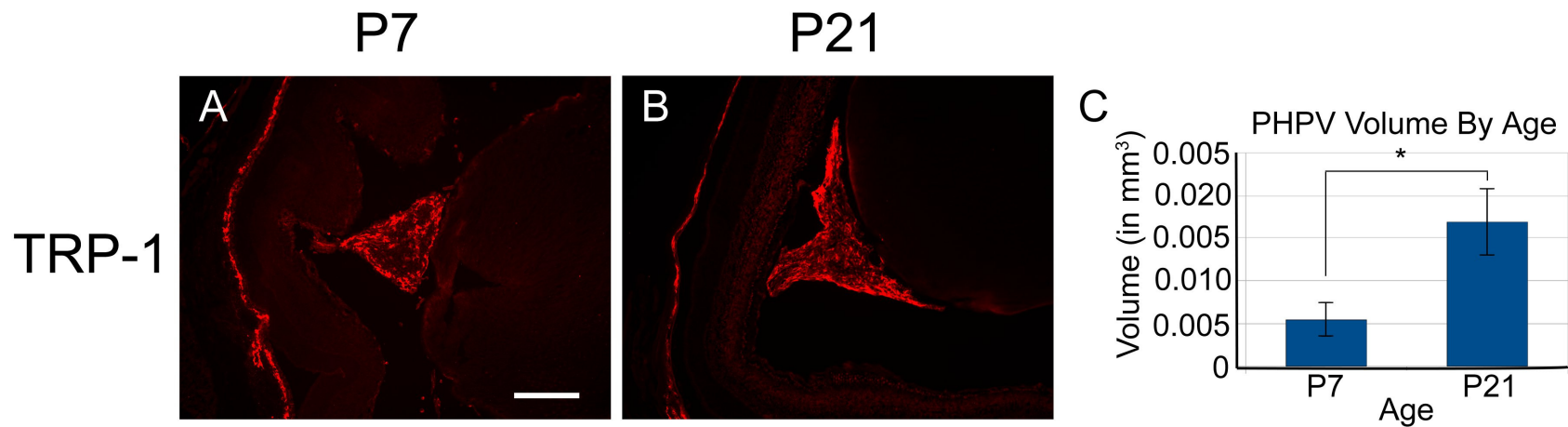
Figure 4-11: The retrolental mass grows continuously in the ephrin-A5^{-/-} eye in postnatal stages

(A and B) Representative pictures of the retrolental mass seen in an ephrin-A5$^{-/-}$ eye at P7 and P21. Sections are labeled with TRP-1 to delineate cells encompassing the mass. Scale bar = 200 μm.

(C) Quantification of the relative volume of the retrolental mass at P7 and P21. The size of the fibroblastic mass is significantly larger at P21 than at P7 ($p < 0.05$, Student's t-test, n = 4 animals per age).
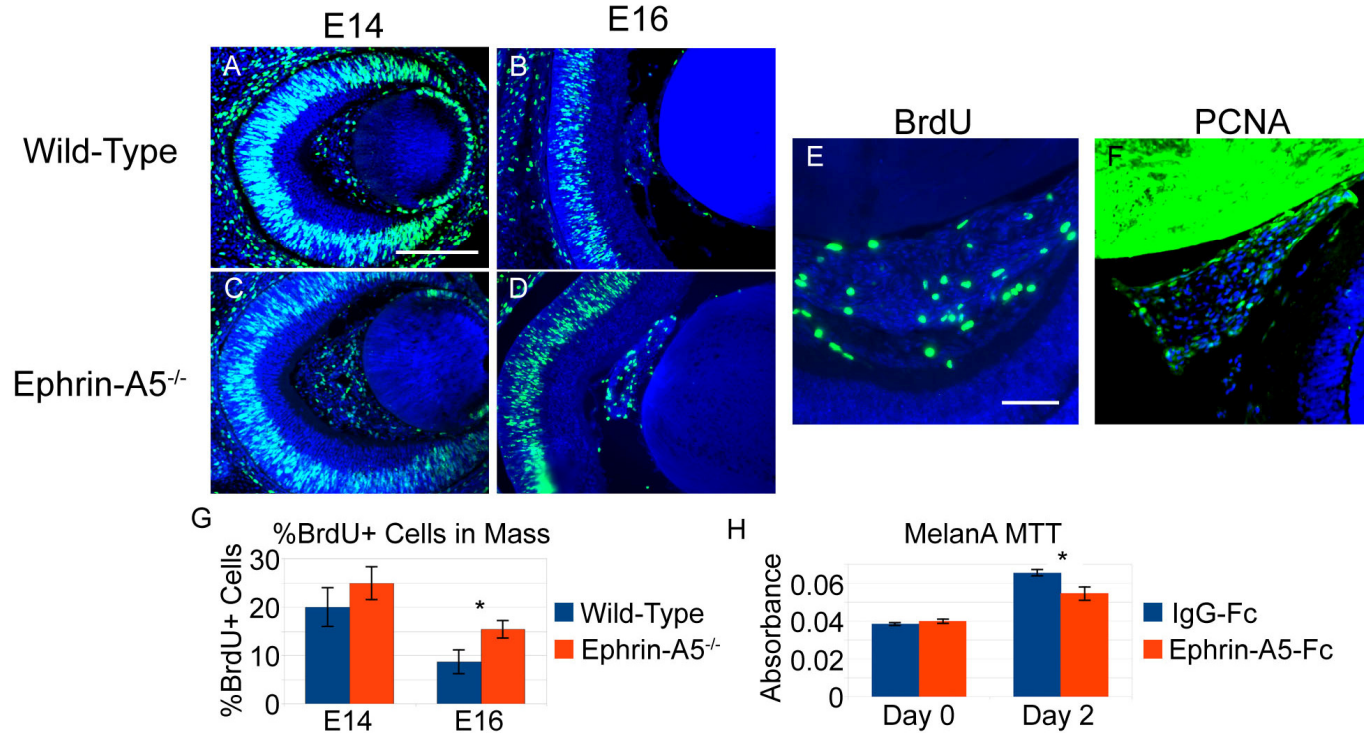
Figure 4-12: Ephrin-A5 regulates cell proliferation in the primary vitreous
(A-D) BrdU incorporation and labeling at various developmental periods in the WT and ephrin-A5^{-/-} eye. Pregnant mice were injected with BrdU 2 hours prior to sacrifice, and embryos were subsequently fixed. Scale bar = 200 μm.
(E and F) BrdU incorporation and PCNA staining of the retrolental tissue in the ephrin-A5^{-/-} eye at P7. Scale bar = 200 μm.
(G) Quantification of the percentage BrdU positive cells in the retrolental mass during development. A greater percentage of BrdU positive cells is observed in the ephrin-A5 null eye at both E14 and E16, though this effect is significant only at E16 (* = $p < 0.05$, Student's t-test, n = 4 animals per group). Scale bar = 200 μm.
(H) MTT assay of MelanA cells with control IgG or ephrin-A5-Fc treatment. Treatment with ephrin-A5-Fc results in a significant decrease in cell growth after 2 days (* = $p < 0.05$, Student's t-test, n = 4 per group).
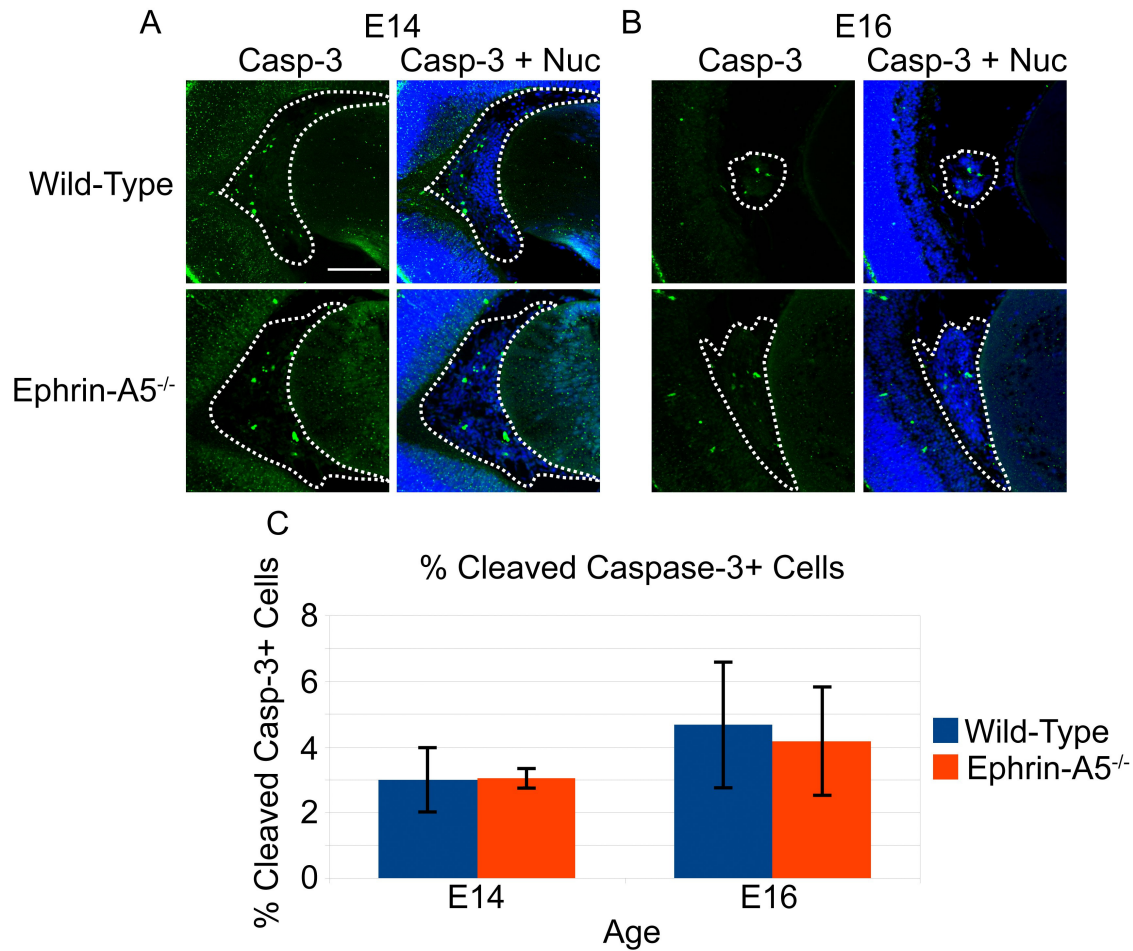
Figure 4-13: Apoptotic cells present during development of primary vitreous in wild-type and ephrin-A5$^{-/-}$ animals

(A and B) Cells labeled for cleaved caspase-3 present in in wild-type and ephrin-A5$^{-/-}$ primary vitreous cells at E14 (A) and E16 (B). Cleaved caspase-3 is observed in both wild-type and ephrin-A5$^{-/-}$ tissues. Scale bar = 100 μm.

(C) Quantification of the percentage of cleaved caspase-3 positive cells in the wild-type and ephrin-A5$^{-/-}$ primary vitreous. The percentage of cells positive for cleaved caspase-3 were not found to be significantly different between wild-type and ephrin-A5$^{-/-}$ animals at either E14 or E16 ($p > 0.05$, Student's t-test, n = 6 animals per group).

CHAPTER 5: CONCLUSIONS AND PERSPECTIVES

A. Summary

This work has focused on the role of ephrin-A5, a molecule traditionally associated with axonal guidance, in the development and maintenance of tissues in the eye. Ephrin-A5 has been found to play a significant role in the maintenance of the lens, as mice lacking the A-class ephrin ligand develop deficits in organization and shape in the mature fiber cell layers. These deformities lead to the formation of large vacuoles in the lens bow region, ultimately resulting in cataract formation. Ephrin-A5 function is mediated, at least in part, by the EphA2 receptor and is critical in preserving the integrity and order of lens fiber cells. Together, these molecules play an integral role in the regulation of the adherens junction, as ephrin-A5$^{-/-}$ mice have completely disruption of N-cadherin localization in the lens. Additionally, both ephrin-A5 and EphA2 enhance the interaction between N-cadherin and β-catenin. Subsequent studies from our group and others have further found other members of the Eph family to play important roles in lens development (Cooper, Son et al. 2008; Jun, Guo et al. 2009; Zhang, Hua et al. 2009; Kaul, Riazuddin et al. 2010; Cheng and Gong 2011; Tan, Hou et al. 2011; Park, Son et al. 2012; Shi, De Maria et al. 2012; Son, Park et al. 2012). This includes the receptor EphA2, as mutations in *EPHA2* have been linked to cataract formation in human populations and EphA2$^{-/-}$ mice have been reported to develop cataracts (Jun, Guo et al. 2009; Zhang, Hua et al. 2009; Kaul, Riazuddin et al. 2010; Tan, Hou et al. 2011; Shi, De Maria et al. 2012).

Additionally, this work has also shown ephrin-A5 to play a significant role in the development of the vitreous humor, namely in the regression of the primary vitreous.

Ephrin-A5$^{-/-}$ animals develop symptoms akin to the human disease PHPV, the most notable of which is the presence of a mass posterior to the lens. The hyperplastic and aberrant tissue consists of both pigmented cells of neural crest lineage innervated by vascular structures. Finally, ephrin-A5 was found to play a significant role in cell cycle dynamics in these cells, as ephrin-A5$^{-/-}$ show enhanced proliferation of the primary vitreous compared to wild-type controls.

B. Mechanism for Ephrin-A5 Regulation of Lens Organization in the Lens

This current work has found that ephrin-A5 plays an integral role in the regulation of the adherens junction within the mature lens fiber cell layers. Given the data, our current model posits that the Eph family is critical in N-cadherin localization, and that this activity is critical for the organization the lens fiber cells and maintenance of the lens (Fig. 5-1). In the wild-type lens, ephrin-A5 interaction with EphA2 would induce EphA2 kinase activation, which in turn would inhibit β-catenin phosphorylation by proteins such as EGF-activated EGFR (Fig. 5-1A). This would result in an enhanced interaction between N-cadherin and β-catenin, and localize N-cadherin on the fiber cell membrane, maintaining the classical hexagonal lens fiber cell shape (Fig. 5-1B) and ultimately preserving the lens to remain crystalline (Fig. 5-1C). In the absence of ephrin-A5, EphA2 would not inhibit β-catenin phosphorylation, causing reduced interactions between β-catenin and N-cadherin (Fig. 5-1D), and this loose binding between both molecules would lead to internalization of N-cadherin (Fig. 5-1E). As a consequence, lens fiber cells lack their distinct fiber cell shape, instead becoming more rounded, and leading to the formation of intercellular vacuoles (Fig. 5-1F). This would ultimately lead to the degeneration of the lens, resulting in cataract formation (Fig. 5-1G).

C. Contributions of PHPV Phenotype to Cataract Formation in Ephrin-A5^{-/-} Mice

PHPV is associated with other ocular deficits in addition to the presence of an aberrant retrolental mass, including the formation of cataracts. Similarly, our ephrin-A5^{-/-} animals develop both phenotypes, raising the question of whether the hyperplastic tissue is the direct cause of the lens degeneration phenotype. Several observations suggest that the PHPV in the ephrin-A5 mutants may play a role in cataract formation, but is not the sole cause. The retrolental mass likely plays a role in the rupturing of the ephrin-A5^{-/-} lens, as the hyperplastic tissue is present at the site of posterior degeneration and has been observed to encompass the lens (Fig. 4-2). However, while about half of all ephrin-A5^{+/-} animals have been found to develop PHPV by 6 months of age (Table 4-1), none of these mice has been found to develop cataracts or lens fiber cell deficits (Cooper, Son et al. 2008), indicating that the changes in lens fiber cell structure are independent of the PHPV phenotype. In addition, ephrin-A5 appears to be directly affecting the molecular dynamics within the lens, as the ephrin-A5^{-/-} lens shows alterations in N-cadherin localization (Fig. 3-3) while other membrane proteins, including β-catenin, are unaffected (Fig. 3-6). Further studies using tissue-specific knock-out mouse models, in which ephrin-A5 is deleted specifically in the lens, may further define the contribution of ephrin-A5 to lens fiber cell maintenance and the role PHPV has on cataracts formation.

D. Future Directions in Elucidating the Function of the Eph Family in the Lens

The importance of the Eph family in lens biology is a new area of study that is growing quickly and providing a greater understanding of lens development and maintenance. This current study and those that have been previously published have established a relationship between the Eph family and the adherens junction, as well as

have uncovered previously unknown roles of the SAM and kinase domains in the EphA2 receptor. However, the precise functional roles this category of receptor tyrosine kinases plays in the lens remains to be fully elucidated.

Thus far, of the members of the Eph family, only the EphA2 receptor and ephrin-A5 ligand have been identified as critical players in lens development. The appearance of such a drastic phenotype is surprising given the large level of redundancy within the system. In addition, several other Eph family molecules are also expressed within the murine lens, and this expression appears early in embryonic development (data not published). However, the cataracts in both the human patients and mouse models indicate that the major deformities occur in the postnatal lens. This early expression indicates that the Ephs may have developmental functions within the lens that are compensated for in early lens development but not in later stages. Understanding the role of the Eph family in early lens development may elucidate other novel functions.

Analysis of EphA2 activity within the lens has indicated that the SAM and kinase domains play significant roles (Jun, Guo et al. 2009; Zhang, Hua et al. 2009; Kaul, Riazuddin et al. 2010; Tan, Hou et al. 2011). The SAM domain mutations are of particular interest given the limited knowledge regarding the function of this domain in Eph receptors. However, given the unique nature of the lens fiber cells and EphA2 expression being observed predominantly within this cellular population, functional studies on the role of EphA2 in the lens may be potentially difficult. Transgenic knock-in mouse studies in which EphA2 is replaced with the various human EPHA2 mutations may prove particularly valuable in elucidating whether protein localization, activation, and/or levels are affected.

Downstream targets of EphA2 and ephrin-A5 also remain to be elucidated. The effects of these molecules on the adherens junction indicate the critical role the Ephs play in regulating intercellular interactions within the lens. These interactions in the mature lens are particular important in maintaining proper lens function. Understanding how the Ephs regulate these adhesion molecules to maintain the unique structure of the lens will provide further insights into lens biology.

E. Future Directions in Ephrin-A5 and Primary Vitreous Regression

Though PHPV has been recognized and studied for nearly a century, the precise mechanisms regulating primary vitreous development and regression remains limited. This study has identified ephrin-A5 as a significant player in the degeneration of the primary vitreous. Other factors, such as the Arf tumor suppressor (McKeller, Fowler et al. 2002; Martin, Thornton et al. 2004; Silva, Thornton et al. 2005; Thornton, Swanson et al. 2007; Freeman-Anderson, Zheng et al. 2009), p53 (Reichel, Ali et al. 1998), Fzd-5 (Zhang, Fuhrmann et al. 2008), and VEGF (Mitchell, Rutland et al. 2006; Rutland, Mitchell et al. 2007) have also been previously identified to also be important factors regulating the regression of this tissue. How ephrin-A5 is involved with these other pathways remains to be studied and understood.

Understanding the mechanisms of primary vitreous regression can have potential impacts on treatment options for patients with PHPV. To date, therapy for the disorder remains limited, with surgical removal of the retrolental mass being the primary choice, though often resulting with poor outcomes (Pollard 1997; Shastry 2009). The targeting of specific factors influencing the primary vitreous, whether through the inhibition of factors promoting the growth of the tissue or the enhancement of targets that influence its

degradation, may provide for non-invasive treatments that maintain the integrity of the visual system.

F. The Impact of Ephrin-A5 on the Visual System

Ephrin-A5 has been traditionally known to play important roles in the visual system, most notably for the formation of the retinotopic map through the inhibition of neuronal migration (Frisen, Yates et al. 1998). The work presented here has identified two additional aspects, namely the organization and maturation of the lens through the regulation of adherens junction interactions in the lens and the development of the vitreous humor through the degeneration of the primary vitreous. Together, this demonstrates the range, diversity in activity, and importance that ephrin-A5 has on the visual system.
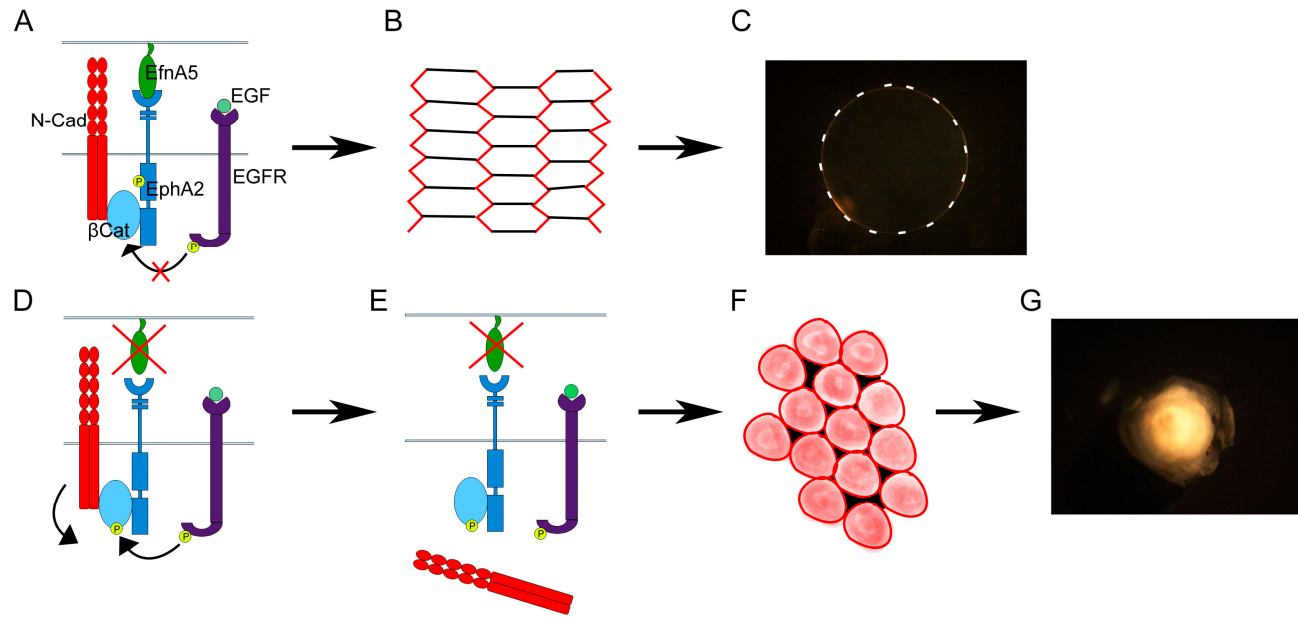
Figure 5-1: Model of Cataract Formation in the Ephrin-A5⁻/⁻ Lens
(A-C) Wild-type lens fiber cell organization with ephrin-A5. Ephrin-A5 interaction with EphA2 induces EphA2 kinase activation, inhibiting β-catenin phosphorylation by other proteins such as EGFR (A). This results in stable N-cadherin localization along the membranes of the shorter edges of lens fiber cells (B, N-cadherin denoted in red), resulting in a crystalline lens (C). N-Cad = N-cadherin, βCat = β-catenin, EfnA5 = Ephrin-A5, EGFR = EGF Receptor.
(D-G) Ephrin-A5⁻/⁻ lens fiber cell disorganization. EphA2 remaining inactive by the absence of ephrin-A5, which results in the phosphorylation of β-catenin by proteins such as EGFR (D). β-catenin phosphorylation results in loose interactions with N-cadherin, leading to its internalization in lens fiber cells (D and E). This results in the disorganization and rounding of lens fiber cells, with some N-cadherin still on the membrane but a significant fraction in the cytoplasm (F, N-cadherin is denoted by the red). This disorganization also leads to the inappropriate packing of fiber cells, leading to the formation of vacuoles which are exacerbated over time (F, black spacing between fiber cells), and ultimately resulting in lens degeneration and cataract formation (G).

CHAPTER 6: MATERIALS AND METHODS

A. Animal Care

Mice were bred and maintained under standard conditions and treat in accordance to the Guidelines for the Care and Use of Laboratory Animals of Rutgers University. Ephrin-A5$^{-/-}$ mice (Frisen, Yates et al. 1998) and EphA2$^{LacZ/LacZ}$ mice (Jun, Guo et al. 2009) have been previously described.

CP49 status was determined using previously established methods (Alizadeh, Clark et al. 2004). Briefly, isolated genomic DNA from tail tissue was prepared for PCR at a volume of 50 μL under the following conditions: 1x PCR buffer, 25 mM MgCl2, 0.1 mM dNTP mix, 0.5 μM of each primer, 0.625 U Taq DNA polymerase (New England Biolabs), and 2 μL (100 to 200 ng) of total DNA. Wild-type CP49 was determined using primers e (5'- TTGGAAACAACCTCCAGACCAGAG - 3') and c' (5'- ACATTCTATTTCGAGGCAGGGTCC - 3') producing a 403 bp product, while mutant CP49 with the 6 kb deletion was determined using primers c (5'- TGGGGTTGGGCTAGAAATCTCAGA - 3') and e' (5' - AGCCCCTACGACCTGATTTTTGAG - 3') producing a 386 bp product (Alizadeh, Clark et al. 2004).

B. Mouse Lens Imaging

For imaging of whole mount lenses, mouse eyes were enucleated and lenses dissected in pre-warmed DMEM (Sigma-Aldrich) over a mesh grid. Imaging was performed using a Nikon SMZ 1500 microscope.

Slit-lamp imaging was performed using a Nikon FS3 Zoom Photo Slit Lamp without the use of anesthesia, with digital images captured using a Pixelink PL-A662 megapixel camera. Mouse eyes were dilated with one drop of 2% phenylephrine and 1% cyclopentolate.

C. Hemotoxylin and Eosin Staining (H&E) Staining

Embryos and postnatal eyes were prepared using lens fixation buffer (65% ethanol, 4% formaldehyde, 5% acetic acid, 3% sucrose) at 4 °C, dehydrated, and embedded in Paraplast (McCormick Scientific). Longitudinal sections were prepared at 5 μm and stained with hemotoxylin and eosin (H&E) (Sigma-Aldrich).

D. Immunohistochemistry

Postnatal wild-type and ephrin-A5$^{-/-}$ eyes were enucleated and fixed in 4% formaldehyde in 1x PBS (pH 7.4) for 10 minutes at room temperature, followed by a rinse in PBS for 5 minutes, and stored in 10% sucrose overnight at 4 °C. Embryonic tissue was fixed in 4% paraformaldehyde in 1x PBS (pH 7.4) for 60 minutes at room temperature, followed by rinses in PBS 3 times 10 minutes each, and stored in 30% sucrose overnight at 4 °C. All tissue was subsequently frozen and cryosectioned at 10 μm. Primary antibodies were incubated overnight at 4 °C, followed by detection using goat or donkey secondary antibodies conjugated with Alexa Fluor 488 (1:200; Invitrogen) or CY3 (1:200; Jackson ImmunoResearch) at room temperature for 2 hours. Nuclear localization was determined using DAPI (1:10,000; Invitrogen) or TO-PRO-3 iodide far red fluorescence dye (1:1000; Invitrogen).

Lens tissue was stained using antibodies against EphA2 (1:200; R&D Systems), β-catenin (1:3000; BD Biosciences), N-cadherin (1:200; Developmental Studies Hybridoma Bank), E-cadherin (1:1000; BD Biosciences), ZO-1 (1:200; Invitrogen), and Cx-46 (1:200; Zymed). To analyze the actin cytoskeleton, sections were stained with Alexa Fluor 546-conjugated phalloidin (1:25, Invitrogen) for 1 hour at room temperature.

Vascular structures were observed using various antibodies. Endothelial cells were determined using antibodies against CD-31 (1:200; BD Biosciences) and the vascular basal membrane marker collagen-IV (1:200; AbD Serotec). Perivascular smooth muscle cells were identified using an antibody against α-smooth muscle actin (1:200; Sigma-Aldrich). Pericytes were identified using an antibody against platelet-derived growth factor-β (PDGFRβ; 1:200; eBioscience). Macrophages were identified using an antibody against F4/80 (1:200; Invitrogen). Pigmented cells were stained using an antibody against Tyrosinase Related Protein (TRP)-1 (1:200; Santa Cruz). Eph receptor localization was determined using antibodies against EphB4 (1:200; R&D Systems) and EphA2 (1:200; R&D Systems). Primary antibodies were incubated overnight at 4 °C and washed in PBS, followed by detection using goat or donkey secondary antibodies conjugated with Alexa Fluor 488 (Invitrogen) or CY3 (Jackson ImmunoResearch) at room temperature for 2 hours.

Ephrin-A5 ligand expression was determined using an EphA3-Fc fusion protein (10 μg/mL; R&D Systems) while Eph receptor localization using ephrin-A5-Fc (10 μg/mL; R&D Systems). Adult eyes were enucleated, fixed, and sectioned as described earlier. Tissue was treated with the appropriate fusion protein overnight at 4 °C and

detected using a biotin-conjugated goat anti-human (1:200; Jackson ImmunoResearch) followed by CY3-conjugated streptavidin (1:1000; Jackson ImmunoResearch).

To determine Eph receptor localization using ephrin-A5-Fc, adult eyes were enucleated, fixed, and sectioned as described earlier. Tissue was treated with ephrin-A5-Fc fusion protein (R&D Systems) at 10 µg/mL overnight at 4 °C and washed in PBS, and labeling detected using a biotin-conjugated goat anti-human antibody (1:200; Jackson ImmunoResearch) followed by CY3-conjugated streptavidin (1:1000; Jackson ImmunoResearch).

Cell division was determined through BrdU treatment and detection and PCNA labeling. BrdU (Sigma-Aldrich) was dissolved in a 0.007 N NaOH solution made in 0.9% NaCl at 5 mg/mL and injected intraperitoneally at a concentration of 50 µg/g body weight. Eye tissue was fixed and sectioned as previously mentioned. Sections were treated in 2 N HCl at 37 °C for 30 minutes, followed by a rinse in 0.1 M sodium borate, pH 8.5, at room temperature for 10 minutes. BrdU incorporation was detected using an antibody against BrdU (1:100; Accurate Chemical & Scientific Corporation). Cell division was also determined using an antibody against PCNA (1:100; Santa Cruz Biotechnology). Prior to staining, slides were boiled in 0.1 M citrate buffer for 10 minutes and cooled at room temperature in the same buffer for 20 minutes. Slides were then immersed in 3% hydrogen peroxide solution in PBS for 10 minutes.

E. Western Blot Analysis

293T cells and A431 cells were maintained in DMEM with 10% FBS and 1% penicillin/streptomycin. Cells were lysed using cell lysis buffer [50 mM Tris-Cl (pH 8.0), 150 mM NaCl, 1% Nonidet P-40 (NP-40), 1x protein inhibitor mixture (Roche

Diagnostics), and 1 mM Na$_3$VO$_4$]. Cell lysates were fractionated using SDS/PAGE (8% Tris-HCl gel, Bio-Rad) and separated proteins were then transferred onto a nitrocellulose membrane. Membranes were blocked in 5% BSA in 1x TBS-T for 1 hour at room temperature, followed by incubation with primary antibody a 4 C overnight. Antibodies binding onto the respective proteins were labeled using peroxidase-conjugated IgG antibodies (1:10,000; Sigma-Aldrich). Detection was done using a chemiluminescence kit (GE Healthcare) under the instructions of the manufacturer. Primary antibodies against EphA2 (1:1000; R&D Systems and 1:500; Abcam), β-catenin (1:1000; BD Biosciences), N-cadherin (1:1000; Developmental Studies Hybridoma Bank), EGFR (1:1000; BD Biosciences), phosphotyrosine (4G10 clone, 1:1000; Millipore); phospho-ERK1/2 (1:1000; Cell Signaling), and total ERK1/2 (1:1000; Cell Signaling) were used.

F. EphA2 Clones

Human EphA2 in the pRcCMV expression vector was a generous gift from Dr. Bingcheng Wang (Case Western University, Cleveland, OH). Human EphA2 2819 C>T mutant clones in the pcDNA3.1 vector were a generous gift from Dr. Xue Zhang (Chinese Academy of Medical Sciences & Peking Union Medical College, Beijing, China). The EphA2 dKin, dSAM, 2842 G>T, 2826/9, and 2915/6 clones were developed under the pcDNA3.1 vector. Fragments containing the indicated mutations were synthesized (Genscript), digested with the appropriate restriction enzymes, and ligated with DNA Ligase (New England Biolabs) by the instructions provided by the manufacturer. The resulting clones were sequenced to verify correct insertion.

G. N-cadherin-β-catenin Interactions

To examine the role of Eph receptor activation on N-cadherin-β-catenin interactions, 293T cells were transfected using Lipofectamine 2000 (Invitrogen) as per the instructions of the manufacturer with human EphA2 under the pRcCMV expression vector. Cells were maintained in growth medium for 24 hours after transfection and then starved in serum-free DMEM medium overnight. Transfected and untransfected groups were treated with ephrin-A5-Fc [2 μg/mL, crosslinked with anti-Human-Fc antibody (Jackson Immunoresearch) in a 5:1 ratio in μgs for 2 hours at 37 ℃; R&D Systems] for 45 minutes. Samples were washed with ice cold 1x PBS 3 times and lysed with cell lysis buffer. N-cadherin was immunoprecipitated with an anti-N-cadherin antibody (Developmental Studies Hybridoma Bank), which was subsequently pulled down using Protein G Agarose beads (Roche Diagnostics). The beads were then washed in cell lysis buffer and boiled in sample running buffer. Co-immunoprecipitated β-catenin protein was analyzed using Western blot analysis using an anti-β-catenin antibody (1:1000; BD Biosciences). Membranes were reprobed for N-cadherin (1:1000; Developmental Studies Hybridoma Bank) to ensure equal loading of protein.

To determine EphA2 interactions with β-catenin, 293T cells were transfected with human EphA2. 48 hours after transfection, samples were lysed in lysis buffer, and EphA2 was immunoprecipitated using an anti-EphA2 antibody (Santa Cruz Biotechnology) and Protein G Agarose beads. Samples were subsequently analyzed through Western blot analysis. Membranes were probed for β-catenin using an antibody against β-catenin (1:1000; BD Biosciences) to determine interactions with EphA2. Blots were reprobed for EphA2 (1:1000; Santa Cruz Biotechnology) to verify equal loading. In

the reciprocal experiment, 293T cells transfected with and without EphA2 were immunoprecipitated with β-catenin and analyzed via Western blot for EphA2. Blots were reprobed with β-catenin to ensure equal loading of samples.

To detect β-catenin phosphorylation activity by ephrin-A5 treatment, A431 cells were starved overnight and treated with IgG-Fc control, cross-linked ephrin-A5-Fc, EGF (20 ng/mL; R&D Systems), or cross-linked ephrin-A5-Fc and EGF for 30 minutes. Cells were washed with ice cold 1x PBS and lysed with cell lysis buffer. β-catenin was immunoprecipitated as described and samples were examined by Western blot. Tyrosine phosphorylation was determined using an anti-phosphotyrosine antibody (4G10 clone, 1:1000; Millipore). Blots were reprobed for β-catenin levels to verify equal loading of pulled-down protein

To reveal the effects of β-catenin phosphorylation activity by various EphA2 mutations, 293T cells were transfected with the constructs for EGFR and the respective human EphA2 clones. Cells were allowed to grow for 24 hours, and serum starved overnight. The samples were treated with ephrin-A5-Fc and EGF for 30 minutes as previously indicated, after which cells were washed with ice cold 1x PBS, lysed in cell lysis buffer, and immunoprecipitated for β-catenin. β-catenin phosphorylation was determined through Western blot as described.

H. Lens Epithelial Whole Mounts

Postnatal wild-type and ephrin-A5-/- eyes were enucleated, and lenses were dissected. The posterior lens capsule was cut and carefully removed in a single sheet with the lens epithelium attached. The dissected tissue was subsequently fixed with 4% formaldehyde in 1x PBS (pH 7.4) for 10 minutes at room temperature, followed by a

rinse in PBS 3 times for 5 minutes each. The lens epithelial sheets were stained with antibodies as described.

I. Alkaline Phosphatase (AP) Staining

EphA5-Alkaline Phosphatase (AP) staining for ephrin ligand expression has been described previously (Zhang, Cerretti et al. 1996; Washburn, Cooper et al. 2007). EphA5-AP contains the extracellular domain of EphA5 fused in-frame to alkaline phosphatase, and thus can bind to A-class ephrins. Ephrin ligand binding was determined on frozen tissue sectioned at 14 μm mounted onto slides. Sections were fixed in 4% paraformaldehyde in PBS for 8 minutes at room temperature, followed 2 washes in PBS 5 minutes each. Media containing EphA5-AP was then applied to the sections for 2 hours, followed by washes in Hank's balanced salt solution with 0.5 mg/mL BSA and 20 mM HEPES (pH 7.0). Sections were fixed again in 3% formaldehyde and 20 mM HEPES (pH 7.5) for 30 seconds, followed by 2 washes in Wash Buffer (150 mM NaCl and 20 mM HEPES [pH 7.5]) for 5 minutes each. Sections were then heated to 65 °C for 15 minutes and washed again in Wash Buffer, followed by a rinse in AP Color Development Buffer (100 mM Tris-HCl [pH. 9.5], 100 mM NaCl, 5 mM $MgCl_2$). Color development was done by adding AP Color Development Buffer with NBT/BCIP solution and incubated at room temperature until sections were sufficiently stained.

J. β-Galactosidase Staining

β-galactosidase staining has been described previously (Cooper, Kobayashi et al. 2009). Embryos and eyes were fresh frozen and cryosectioned at 12 μm. Sections were post-fixed in a 2% paraformaldehyde/0.5% glutaraldehyde solution in 1x PBS for 1

minute, followed by a rinse in 1x PBS for 5 minutes. Samples were then incubated in

reaction buffer (1 mg/mL 5-bromo-4-chloro-3-inodolyl-β-galactopyranoside [X-Gal], 5

mM potassium ferricyanide, 5 mM potassium ferrocyanide, 2 mM magnesium chloride,

0.01% sodium deoxycholate, and 0.02% NP-40) for 18 hours at 37 ºC.

K. Lens Suture Analysis

Analysis of the posterior suture was done using a modified protocol as reported

by Shi et al. (Shi, Barton et al. 2009). Enucleated eyes were dissected and lenses were

removed in pre-warmed DMEM at 37 ºC. The lens capsule was then carefully removed,

and the tissue was incubated in FM4-64 styryl dye (1 µM; Invitrogen) in pre-warmed

DMEM. Decapsulated lenses were incubated in the dye for 15 minutes prior to imaging.

Subsequent confocal images were taken in the presence of the FM4-64 dye.

L. Wholemount Hyaloid Prep

Wild-type and ephrin-A5$^{-/-}$ eyes at P2, P8, and P14 were enucleated and their

corneas removed. The dissected eyes were fixed overnight in 4% paraformaldehyde,

after which the eyes were rinsed in PBS. The retinal cup along with the lens was then

carefully removed from the sclera, after which the retina was dissected apart from the

posterior pole with the hyaloid vessels still intact and attached to the lens. Lenses with

the hyaloid network were stained in FITC-conjugated isolectin-B4 overnight (1:500;

Vector Laboratories), rinsed in PBS, and mounted in Clear Mount Medium (Electron

Microscopy Sciences). Z-stack images were taken using a Nikon Eclipse C1 confocal

microscope system. Quantification of vessels from the tunica vasculosa lentis have been

previously described (Ito and Yoshioka 1999). Briefly, a circle with a radius 70.7% of

the lens was drawn on the posterior lens (equivalent to the 45º latitudinal line), and vessels crossing this line were counted.

M. RT-PCR

Ephrin-A5$^{-/-}$ eyes were enucleated and the retrolental mass was carefully removed under a dissecting microscope. RNA was extracted from the tissue using the RNeasy Mini Kit (Qiagen) as per the manufacturer's instructions. The resulting RNA was amplified using the MessageAmp II aRNA Amplification Kit (Ambion). Reverse transcription of the resulting RNA into cDNA was performed using SuperScript II Reverse Transcriptase (Invitrogen) as per the manufacturer's instructions. Primers of the various Eph receptors that were used have been previously published (van Eyll, Passante et al. 2006). RNA levels were analyzed using the ABI PRISM 7000 system.

N. 3-(4,5-Dimethylthiazol-2-yl)-2,5-diphenyltetrazolium bromide (MTT) Assay

MTT assays were performed in accordance to the instructions of the manufacturer (Roche, Cat. #11465007001). Melan-A cells were plated into 96-well plates at a density of 1×10^3 cells per well. Cells were treated with 2 μg/mL ephrin-A5-Fc (R&D Systems, Cat. #374-EA-200) pre-clustered with rabbit-anti-human-IgG Fcγ fragment (Jackson Immunoresearch, Cat. #309-005-008) at 37 ºC for 2 hours. Controls were treated with pre-clustered IgG alone. Absorbance was read on days 0 and 2 using an Infinite 200 Tecan Plate Reader.

O. Statistical Analysis

For statistical analysis, at least 4 or more samples per group were examined as noted. All data were presented in standard error bars, and statistical significance was

assessed using Student's *t*-test analysis. Statistics were analyzed using Microsoft Office

Excel 2003 and Graphpad Prism 5 software.

Literature

Akaneya, Y., K. Sohya, et al. (2010). "Ephrin-A5 and EphA5 interaction induces synaptogenesis during early hippocampal development." PLoS One **5**(8): e12486.

Alford, S., A. Watson-Hurthig, et al. (2010). "Soluble ephrin a1 is necessary for the growth of HeLa and SK-BR3 cells." Cancer Cell Int **10**: 41.

Alizadeh, A., J. Clark, et al. (2004). "Characterization of a mutation in the lens-specific CP49 in the 129 strain of mouse." Invest Ophthalmol Vis Sci **45**(3): 884-891.

Baldo, G. J., X. Gong, et al. (2001). "Gap junctional coupling in lenses from alpha(8) connexin knockout mice." J Gen Physiol **118**(5): 447-456.

Beebe, D. C. (2008). "Maintaining transparency: a review of the developmental physiology and pathophysiology of two avascular tissues." Semin Cell Dev Biol **19**(2): 125-133.

Bertazolli Filho, R., E. M. Laicine, et al. (1996). "Biochemical studies on the secretion of glycoproteins by isolated ciliary body of rabbits." Acta Ophthalmol Scand **74**(4): 343-347.

Beyer, E. C., J. Kistler, et al. (1989). "Antisera directed against connexin43 peptides react with a 43-kD protein localized to gap junctions in myocardium and other tissues." J Cell Biol **108**(2): 595-605.

Bischoff, P. M., S. D. Wajer, et al. (1983). "Scanning electron microscopic studies of the hyaloid vascular system in newborn mice exposed to O2 and CO2." Graefes Arch Clin Exp Ophthalmol **220**(6): 257-263.

Bishop, P. N., M. Takanosu, et al. (2002). "The role of the posterior ciliary body in the biosynthesis of vitreous humour." Eye (Lond) **16**(4): 454-460.

Brownlee, H., P. P. Gao, et al. (2000). "Multiple ephrins regulate hippocampal neurite outgrowth." J Comp Neurol **425**(2): 315-322.

Burdon, K. P., K. Hattersley, et al. (2008). "Investigation of eight candidate genes on chromosome 1p36 for autosomal dominant total congenital cataract." Mol Vis **14**: 1799-1804.

Chai, Z., D. A. Goodenough, et al. (2011). "Cx50 requires an intact PDZ binding motif and ZO-1 for the formation of functional intercellular channels." Mol Biol Cell.

Chen, J., D. Hicks, et al. (2006). "Inhibition of retinal neovascularization by soluble EphA2 receptor." Exp Eye Res **82**(4): 664-673.

Cheng, C. and X. Gong (2011). "Diverse roles of Eph/ephrin signaling in the mouse lens." PLoS One **6**(11): e28147.

Cheng, H. J., M. Nakamoto, et al. (1995). "Complementary gradients in expression and binding of ELF-1 and Mek4 in development of the topographic retinotectal projection map." Cell **82**(3): 371-381.

Congdon, N. G., D. S. Friedman, et al. (2003). "Important causes of visual impairment in the world today." JAMA **290**(15): 2057-2060.

Cooper, M. A., K. Kobayashi, et al. (2009). "Ephrin-A5 regulates the formation of the ascending midbrain dopaminergic pathways." Dev Neurobiol **69**(1): 36-46.

Cooper, M. A., A. I. Son, et al. (2008). "Loss of ephrin-A5 function disrupts lens fiber cell packing and leads to cataract." Proc Natl Acad Sci U S A **105**(43): 16620-16625.

Danysh, B. P. and M. K. Duncan (2009). "The lens capsule." Exp Eye Res **88**(2): 151-164.

Daugherty, R. L. and C. J. Gottardi (2007). "Phospho-regulation of Beta-catenin adhesion and signaling functions." Physiology (Bethesda) **22**: 303-309.

Drescher, U., C. Kremoser, et al. (1995). "In vitro guidance of retinal ganglion cell axons by RAGS, a 25 kDa tectal protein related to ligands for Eph receptor tyrosine kinases." Cell **82**(3): 359-370.

Dufour, A., J. Egea, et al. (2006). "Genetic analysis of EphA-dependent signaling mechanisms controlling topographic mapping in vivo." Development **133**(22): 4415-4420.

Eiberg, H., A. M. Lund, et al. (1995). "Assignment of congenital cataract Volkmann type (CCV) to chromosome 1p36." Hum Genet **96**(1): 33-38.

Ellsworth, C. A., A. W. Lyckman, et al. (2005). "Ephrin-A2 and -A5 influence patterning of normal and novel retinal projections to the thalamus: conserved mapping mechanisms in visual and auditory thalamic targets." J Comp Neurol **488**(2): 140-151.

Fang, W. B., R. C. Ireton, et al. (2008). "Overexpression of EPHA2 receptor destabilizes adherens junctions via a RhoA-dependent mechanism." J Cell Sci **121**(Pt 3): 358-368.

Feldheim, D. A., Y. I. Kim, et al. (2000). "Genetic analysis of ephrin-A2 and ephrin-A5 shows their requirement in multiple aspects of retinocollicular mapping." Neuron **25**(3): 563-574.

Ferreira-Cornwell, M. C., R. W. Veneziale, et al. (2000). "N-cadherin function is required for differentiation-dependent cytoskeletal reorganization in lens cells in vitro." Exp Cell Res **256**(1): 237-247.

Fitzgerald, P. G., D. Bok, et al. (1983). "Immunocytochemical localization of the main intrinsic polypeptide (MIP) in ultrathin frozen sections of rat lens." J Cell Biol **97**(5 Pt 1): 1491-1499.

Foo, S. S., C. J. Turner, et al. (2006). "Ephrin-B2 controls cell motility and adhesion during blood-vessel-wall assembly." Cell **124**(1): 161-173.

Freeman-Anderson, N. E., Y. Zheng, et al. (2009). "Expression of the Arf tumor suppressor gene is controlled by Tgfbeta2 during development." Development **136**(12): 2081-2089.

Frisen, J., P. A. Yates, et al. (1998). "Ephrin-A5 (AL-1/RAGS) is essential for proper retinal axon guidance and topographic mapping in the mammalian visual system." Neuron **20**(2): 235-243.

Gage, P. J., W. Rhoades, et al. (2005). "Fate maps of neural crest and mesoderm in the mammalian eye." Invest Ophthalmol Vis Sci **46**(11): 4200-4208.

Gao, P. P., C. H. Sun, et al. (2000). "Ephrins stimulate or inhibit neurite outgrowth and survival as a function of neuronal cell type." J Neurosci Res **60**(4): 427-436.

Gao, P. P., Y. Yue, et al. (1998). "Regulation of thalamic neurite outgrowth by the Eph ligand ephrin-A5: implications in the development of thalamocortical projections." Proc Natl Acad Sci U S A **95**(9): 5329-5334.

Garcia, C. M., Y. B. Shui, et al. (2009). "The function of VEGF-A in lens development: formation of the hyaloid capillary network and protection against transient nuclear cataracts." Exp Eye Res **88**(2): 270-276.

Gerety, S. S., H. U. Wang, et al. (1999). "Symmetrical mutant phenotypes of the receptor EphB4 and its specific transmembrane ligand ephrin-B2 in cardiovascular development." Mol Cell **4**(3): 403-414.

Goding, C. R. (2007). "Melanocytes: the new Black." Int J Biochem Cell Biol **39**(2): 275-279.

Gogat, K., L. Le Gat, et al. (2004). "VEGF and KDR gene expression during human embryonic and fetal eye development." Invest Ophthalmol Vis Sci **45**(1): 7-14.

Goldberg, M. F. (1997). "Persistent fetal vasculature (PFV): an integrated interpretation of signs and symptoms associated with persistent hyperplastic primary vitreous (PHPV). LIV Edward Jackson Memorial Lecture." Am J Ophthalmol **124**(5): 587-626.

Gong, X., G. J. Baldo, et al. (1998). "Gap junctional coupling in lenses lacking alpha3 connexin." Proc Natl Acad Sci U S A **95**(26): 15303-15308.

Gong, X., E. Li, et al. (1997). "Disruption of alpha3 connexin gene leads to proteolysis and cataractogenesis in mice." Cell **91**(6): 833-843.

Grunwald, I. C., M. Korte, et al. (2004). "Hippocampal plasticity requires postsynaptic ephrinBs." Nat Neurosci **7**(1): 33-40.

Gumbiner, B. M. (2005). "Regulation of cadherin-mediated adhesion in morphogenesis." Nat Rev Mol Cell Biol **6**(8): 622-634.

Gyllensten, L. J. and B. E. Hellstrom (1954). "Experimental approach to the pathogenesis of retrolental fibroplasia. I. Changes of the eye induced by exposure of newborn mice to concentrated oxygen." Acta Paediatr Suppl **43**(100): 131-148.

Haddad, R., R. L. Font, et al. (1978). "Persistent hyperplastic primary vitreous. A clinicopathologic study of 62 cases and review of the literature." Surv Ophthalmol **23**(2): 123-134.

Hafner, C., G. Schmitz, et al. (2004). "Differential gene expression of Eph receptors and ephrins in benign human tissues and cancers." Clin Chem **50**(3): 490-499.

Hamann, S., T. Zeuthen, et al. (1998). "Aquaporins in complex tissues: distribution of aquaporins 1-5 in human and rat eye." Am J Physiol **274**(5 Pt 1): C1332-1345.

Hammond, C. J., D. D. Duncan, et al. (2001). "The heritability of age-related cortical cataract: the twin eye study." Invest Ophthalmol Vis Sci **42**(3): 601-605.

Hara, Y., T. Nomura, et al. (2010). "Impaired hippocampal neurogenesis and vascular formation in ephrin-A5-deficient mice." Stem Cells **28**(5): 974-983.

Hattersley, K., K. J. Laurie, et al. (2010). "A novel syndrome of paediatric cataract, dysmorphism, ectodermal features, and developmental delay in Australian Aboriginal family maps to 1p35.3-p36.32." BMC Med Genet **11**: 165.

Hattori, M., M. Osterfield, et al. (2000). "Regulated cleavage of a contact-mediated axon repellent." Science **289**(5483): 1360-1365.

Hayashi, T. and R. W. Carthew (2004). "Surface mechanics mediate pattern formation in the developing retina." Nature **431**(7009): 647-652.

Hejtmancik, J. F. (2008). "Congenital cataracts and their molecular genetics." Semin Cell Dev Biol **19**(2): 134-149.

Herath, N. I., M. D. Spanevello, et al. (2006). "Over-expression of Eph and ephrin genes in advanced ovarian cancer: ephrin gene expression correlates with shortened survival." BMC Cancer **6**: 144.

Himanen, J. P., M. J. Chumley, et al. (2004). "Repelling class discrimination: ephrin-A5 binds to and activates EphB2 receptor signaling." Nat Neurosci **7**(5): 501-509.

Himanen, J. P., K. R. Rajashankar, et al. (2001). "Crystal structure of an Eph receptor-ephrin complex." Nature **414**(6866): 933-938.

Himanen, J. P., N. Saha, et al. (2007). "Cell-cell signaling via Eph receptors and ephrins." Curr Opin Cell Biol **19**(5): 534-542.

Hirai, H., Y. Maru, et al. (1987). "A novel putative tyrosine kinase receptor encoded by the eph gene." Science **238**(4834): 1717-1720.

Hodge, W. G., J. P. Whitcher, et al. (1995). "Risk factors for age-related cataracts." Epidemiol Rev **17**(2): 336-346.

Holmberg, J., D. L. Clarke, et al. (2000). "Regulation of repulsion versus adhesion by different splice forms of an Eph receptor." Nature **408**(6809): 203-206.

Hoschuetzky, H., H. Aberle, et al. (1994). "Beta-catenin mediates the interaction of the cadherin-catenin complex with epidermal growth factor receptor." J Cell Biol **127**(5): 1375-1380.

Hu, D. N., J. D. Simon, et al. (2008). "Role of ocular melanin in ophthalmic physiology and pathology." Photochem Photobiol **84**(3): 639-644.

Huse, M. and J. Kuriyan (2002). "The conformational plasticity of protein kinases." Cell **109**(3): 275-282.

Ionides, A. C., V. Berry, et al. (1997). "A locus for autosomal dominant posterior polar cataract on chromosome 1p." Hum Mol Genet **6**(1): 47-51.

Ito, M., M. Nakashima, et al. (2007). "Histogenesis of the intravitreal membrane and secondary vitreous in the mouse." Invest Ophthalmol Vis Sci **48**(5): 1923-1930.

Ito, M. and M. Yoshioka (1999). "Regression of the hyaloid vessels and pupillary membrane of the mouse." Anat Embryol (Berl) **200**(4): 403-411.

Iwao, K., M. Inatani, et al. (2008). "Fate mapping of neural crest cells during eye development using a protein 0 promoter-driven transgenic technique." Graefes Arch Clin Exp Ophthalmol **246**(8): 1117-1122.

Jun, G., H. Guo, et al. (2009). "EPHA2 is associated with age-related cortical cataract in mice and humans." PLoS Genet **5**(7): e1000584.

Kalinski, T., A. Ropke, et al. (2009). "Down-regulation of ephrin-A5, a gene product of normal cartilage, in chondrosarcoma." Hum Pathol **40**(12): 1679-1685.

Kasemeier-Kulesa, J. C., R. Bradley, et al. (2006). "Eph/ephrins and N-cadherin coordinate to control the pattern of sympathetic ganglia." Development **133**(24): 4839-4847.

Kato, M., M. S. Patel, et al. (2002). "Cbfa1-independent decrease in osteoblast proliferation, osteopenia, and persistent embryonic eye vascularization in mice deficient in Lrp5, a Wnt coreceptor." J Cell Biol **157**(2): 303-314.

Kaul, H., S. A. Riazuddin, et al. (2010). "Autosomal recessive congenital cataract linked to EPHA2 in a consanguineous Pakistani family." Mol Vis **16**: 511-517.

Khaliq, S., A. Hameed, et al. (2001). "Locus for autosomal recessive nonsyndromic persistent hyperplastic primary vitreous." <u>Invest Ophthalmol Vis Sci</u> **42**(10): 2225-2228.

Kikawa, K. D., D. R. Vidale, et al. (2002). "Regulation of the EphA2 kinase by the low molecular weight tyrosine phosphatase induces transformation." <u>J Biol Chem</u> **277**(42): 39274-39279.

Kim, J. H., Y. S. Yu, et al. (2010). "Autophagy-induced regression of hyaloid vessels in early ocular development." <u>Autophagy</u> **6**(7): 922-928.

Kinch, M. S., G. J. Clark, et al. (1995). "Tyrosine phosphorylation regulates the adhesions of ras-transformed breast epithelia." <u>J Cell Biol</u> **130**(2): 461-471.

Klein, R. (2009). "Bidirectional modulation of synaptic functions by Eph/ephrin signaling." <u>Nat Neurosci</u> **12**(1): 15-20.

Kozlosky, C. J., T. VandenBos, et al. (1997). "LERK-7: a ligand of the Eph-related kinases is developmentally regulated in the brain." <u>Cytokine</u> **9**(8): 540-549.

Krull, C. E., R. Lansford, et al. (1997). "Interactions of Eph-related receptors and ligands confer rostrocaudal pattern to trunk neural crest migration." <u>Curr Biol</u> **7**(8): 571-580.

Kullander, K. and R. Klein (2002). "Mechanisms and functions of Eph and ephrin signalling." <u>Nat Rev Mol Cell Biol</u> **3**(7): 475-486.

Kullander, K., N. K. Mather, et al. (2001). "Kinase-dependent and kinase-independent functions of EphA4 receptors in major axon tract formation in vivo." <u>Neuron</u> **29**(1): 73-84.

Kuszak, J. R., R. K. Zoltoski, et al. (2004). "Development of lens sutures." <u>Int J Dev Biol</u> **48**(8-9): 889-902.

Lang, R. A. and J. M. Bishop (1993). "Macrophages are required for cell death and tissue remodeling in the developing mouse eye." <u>Cell</u> **74**(3): 453-462.

Leonard, M., Y. Chan, et al. (2008). "Identification of a novel intermediate filament-linked N-cadherin/gamma-catenin complex involved in the establishment of the cytoarchitecture of differentiated lens fiber cells." <u>Dev Biol</u> **319**(2): 298-308.

Leonard, M., L. Zhang, et al. (2011). "Modulation of N-cadherin junctions and their role as epicenters of differentiation-specific actin regulation in the developing lens." <u>Dev Biol</u> **349**(2): 363-377.

Li, J. J., D. P. Liu, et al. (2009). "EphrinA5 acts as a tumor suppressor in glioma by negative regulation of epidermal growth factor receptor." <u>Oncogene</u> **28**(15): 1759-1768.

Li, Y. Y., Z. Mi, et al. (2001). "Differential effects of overexpression of two forms of ephrin-A5 on neonatal rat cardiomyocytes." Am J Physiol Heart Circ Physiol **281**(6): H2738-2746.

Lobov, I. B., S. Rao, et al. (2005). "WNT7b mediates macrophage-induced programmed cell death in patterning of the vasculature." Nature **437**(7057): 417-421.

Lovicu, F. J. and J. W. McAvoy (2005). "Growth factor regulation of lens development." Dev Biol **280**(1): 1-14.

Lovicu, F. J., J. W. McAvoy, et al. (2011). "Understanding the role of growth factors in embryonic development: insights from the lens." Philos Trans R Soc Lond B Biol Sci **366**(1568): 1204-1218.

Marcus, R. C., G. A. Matthews, et al. (2000). "Axon guidance in the mouse optic chiasm: retinal neurite inhibition by ephrin "A"-expressing hypothalamic cells in vitro." Dev Biol **221**(1): 132-147.

Martin, A. C., J. D. Thornton, et al. (2004). "Pathogenesis of persistent hyperplastic primary vitreous in mice lacking the arf tumor suppressor gene." Invest Ophthalmol Vis Sci **45**(10): 3387-3396.

Mathias, R. T., T. W. White, et al. (2010). "Lens gap junctions in growth, differentiation, and homeostasis." Physiol Rev **90**(1): 179-206.

McCarty, C. A. and H. R. Taylor (1996). "Recent developments in vision research: light damage in cataract." Invest Ophthalmol Vis Sci **37**(9): 1720-1723.

McCarty, C. A. and H. R. Taylor (2001). "The genetics of cataract." Invest Ophthalmol Vis Sci **42**(8): 1677-1678.

McKeller, R. N., J. L. Fowler, et al. (2002). "The Arf tumor suppressor gene promotes hyaloid vascular regression during mouse eye development." Proc Natl Acad Sci U S A **99**(6): 3848-3853.

Mellitzer, G., Q. Xu, et al. (1999). "Eph receptors and ephrins restrict cell intermingling and communication." Nature **400**(6739): 77-81.

Miravet, S., J. Piedra, et al. (2003). "Tyrosine phosphorylation of plakoglobin causes contrary effects on its association with desmosomes and adherens junction components and modulates beta-catenin-mediated transcription." Mol Cell Biol **23**(20): 7391-7402.

Mitchell, C. A., W. Risau, et al. (1998). "Regression of vessels in the tunica vasculosa lentis is initiated by coordinated endothelial apoptosis: a role for vascular endothelial growth factor as a survival factor for endothelium." Dev Dyn **213**(3): 322-333.

Mitchell, C. A., C. S. Rutland, et al. (2006). "Unique vascular phenotypes following over-expression of individual VEGFA isoforms from the developing lens." Angiogenesis 9(4): 209-224.

Mitchell, P. J., P. M. Timmons, et al. (1991). "Transcription factor AP-2 is expressed in neural crest cell lineages during mouse embryogenesis." Genes Dev 5(1): 105-119.

Miura, K., J. M. Nam, et al. (2009). "EphA2 engages Git1 to suppress Arf6 activity modulating epithelial cell-cell contacts." Mol Biol Cell 20(7): 1949-1959.

Nagafuchi, A. and M. Takeichi (1988). "Cell binding function of E-cadherin is regulated by the cytoplasmic domain." EMBO J 7(12): 3679-3684.

Nagafuchi, A. and M. Takeichi (1989). "Transmembrane control of cadherin-mediated cell adhesion: a 94 kDa protein functionally associated with a specific region of the cytoplasmic domain of E-cadherin." Cell Regul 1(1): 37-44.

Nielsen, P. A., A. Baruch, et al. (2001). "Characterization of the association of connexins and ZO-1 in the lens." Cell Commun Adhes 8(4-6): 213-217.

Nielsen, P. A., A. Baruch, et al. (2003). "Lens connexins alpha3Cx46 and alpha8Cx50 interact with zonula occludens protein-1 (ZO-1)." Mol Biol Cell 14(6): 2470-2481.

Nowakowski, J., C. N. Cronin, et al. (2002). "Structures of the cancer-related Aurora-A, FAK, and EphA2 protein kinases from nanovolume crystallography." Structure 10(12): 1659-1667.

Ojima, T., H. Takagi, et al. (2006). "EphrinA1 inhibits vascular endothelial growth factor-induced intracellular signaling and suppresses retinal neovascularization and blood-retinal barrier breakdown." Am J Pathol 168(1): 331-339.

Orsulic, S. and R. Kemler (2000). "Expression of Eph receptors and ephrins is differentially regulated by E-cadherin." J Cell Sci 113 (Pt 10): 1793-1802.

Park, E. K., N. Warner, et al. (2004). "Ectopic EphA4 receptor induces posterior protrusions via FGF signaling in Xenopus embryos." Mol Biol Cell 15(4): 1647-1655.

Park, J. E., A. I. Son, et al. (2012). "Human cataract mutations in EPHA2 SAM domain alter receptor stability and function." PLoS One 7(5): e36564.

Parri, M., F. Buricchi, et al. (2005). "EphrinA1 repulsive response is regulated by an EphA2 tyrosine phosphatase." J Biol Chem 280(40): 34008-34018.

Pasquale, E. B. (2005). "Eph receptor signalling casts a wide net on cell behaviour." Nat Rev Mol Cell Biol 6(6): 462-475.

Pasquale, E. B. (2008). "Eph-ephrin bidirectional signaling in physiology and disease." Cell 133(1): 38-52.

Pasquale, E. B. (2010). "Eph receptors and ephrins in cancer: bidirectional signalling and beyond." Nat Rev Cancer **10**(3): 165-180.

Patil, R. V., I. Saito, et al. (1997). "Expression of aquaporins in the rat ocular tissue." Exp Eye Res **64**(2): 203-209.

Patz, A., A. Eastham, et al. (1953). "Oxygen studies in retrolental fibroplasia. II. The production of the microscopic changes of retrolental fibroplasia in experimental animals." Am J Ophthalmol **36**(11): 1511-1522.

Paul, D. L., L. Ebihara, et al. (1991). "Connexin46, a novel lens gap junction protein, induces voltage-gated currents in nonjunctional plasma membrane of Xenopus oocytes." J Cell Biol **115**(4): 1077-1089.

Piedra, J., D. Martinez, et al. (2001). "Regulation of beta-catenin structure and activity by tyrosine phosphorylation." J Biol Chem **276**(23): 20436-20443.

Pollard, Z. F. (1997). "Persistent hyperplastic primary vitreous: diagnosis, treatment and results." Trans Am Ophthalmol Soc **95**: 487-549.

Pontoriero, G. F., A. N. Smith, et al. (2009). "Co-operative roles for E-cadherin and N-cadherin during lens vesicle separation and lens epithelial cell survival." Dev Biol **326**(2): 403-417.

Qiao, F. and J. U. Bowie (2005). "The many faces of SAM." Sci STKE **2005**(286): re7.

Reichel, M. B., R. R. Ali, et al. (1998). "High frequency of persistent hyperplastic primary vitreous and cataracts in p53-deficient mice." Cell Death Differ **5**(2): 156-162.

Resnikoff, S., D. Pascolini, et al. (2004). "Global data on visual impairment in the year 2002." Bull World Health Organ **82**(11): 844-851.

Resnikoff, S., D. Pascolini, et al. (2008). "Global magnitude of visual impairment caused by uncorrected refractive errors in 2004." Bull World Health Organ **86**(1): 63-70.

Rhett, J. M., J. Jourdan, et al. (2011). "Connexin 43 connexon to gap junction transition is regulated by zonula occludens-1." Mol Biol Cell **22**(9): 1516-1528.

Robinson, D. R., Y. M. Wu, et al. (2000). "The protein tyrosine kinase family of the human genome." Oncogene **19**(49): 5548-5557.

Robman, L. and H. Taylor (2005). "External factors in the development of cataract." Eye (Lond) **19**(10): 1074-1082.

Rong, P., X. Wang, et al. (2002). "Disruption of Gja8 (alpha8 connexin) in mice leads to microphthalmia associated with retardation of lens growth and lens fiber maturation." Development **129**(1): 167-174.

Roura, S., S. Miravet, et al. (1999). "Regulation of E-cadherin/Catenin association by tyrosine phosphorylation." <u>J Biol Chem</u> **274**(51): 36734-36740.

Rutland, C. S., C. A. Mitchell, et al. (2007). "Microphthalmia, persistent hyperplastic hyaloid vasculature and lens anomalies following overexpression of VEGF-A188 from the alphaA-crystallin promoter." <u>Mol Vis</u> **13**: 47-56.

Saint-Geniez, M. and P. A. D'Amore (2004). "Development and pathology of the hyaloid, choroidal and retinal vasculature." <u>Int J Dev Biol</u> **48**(8-9): 1045-1058.

Sandilands, A., X. Wang, et al. (2004). "Bfsp2 mutation found in mouse 129 strains causes the loss of CP49' and induces vimentin-dependent changes in the lens fibre cell cytoskeleton." <u>Exp Eye Res</u> **78**(4): 875-889.

Santana, A., M. Waiswol, et al. (2009). "Mutation analysis of CRYAA, CRYGC, and CRYGD associated with autosomal dominant congenital cataract in Brazilian families." <u>Mol Vis</u> **15**: 793-800.

Santiago, A. and C. A. Erickson (2002). "Ephrin-B ligands play a dual role in the control of neural crest cell migration." <u>Development</u> **129**(15): 3621-3632.

Schlessinger, J. (2000). "Cell signaling by receptor tyrosine kinases." <u>Cell</u> **103**(2): 211-225.

Semela, D., A. Das, et al. (2008). "Platelet-derived growth factor signaling through ephrin-b2 regulates hepatic vascular structure and function." <u>Gastroenterology</u> **135**(2): 671-679.

Shastry, B. S. (2009). "Persistent hyperplastic primary vitreous: congenital malformation of the eye." <u>Clin Experiment Ophthalmol</u> **37**(9): 884-890.

Shestopalov, V. I. and S. Bassnett (2000). "Three-dimensional organization of primary lens fiber cells." <u>Invest Ophthalmol Vis Sci</u> **41**(3): 859-863.

Shi, Y., K. Barton, et al. (2009). "The stratified syncytium of the vertebrate lens." <u>J Cell Sci</u> **122**(Pt 10): 1607-1615.

Shi, Y., A. De Maria, et al. (2012). "A role for epha2 in cell migration and refractive organization of the ocular lens." <u>Invest Ophthalmol Vis Sci</u> **53**(2): 551-559.

Shiels, A., T. M. Bennett, et al. (2008). "The EPHA2 gene is associated with cataracts linked to chromosome 1p." <u>Mol Vis</u> **14**: 2042-2055.

Shin, S. S., B. A. Wall, et al. (2010). "AKT2 is a downstream target of metabotropic glutamate receptor 1 (Grm1)." <u>Pigment Cell Melanoma Res</u> **23**(1): 103-111.

Shui, Y. B., X. Wang, et al. (2003). "Vascular endothelial growth factor expression and signaling in the lens." <u>Invest Ophthalmol Vis Sci</u> **44**(9): 3911-3919.

Silva, R. L., J. D. Thornton, et al. (2005). "Arf-dependent regulation of Pdgf signaling in perivascular cells in the developing mouse eye." EMBO J **24**(15): 2803-2814.

Smith, F. M., C. Vearing, et al. (2004). "Dissecting the EphA3/Ephrin-A5 interactions using a novel functional mutagenesis screen." J Biol Chem **279**(10): 9522-9531.

Solanas, G., C. Cortina, et al. (2011). "Cleavage of E-cadherin by ADAM10 mediates epithelial cell sorting downstream of EphB signalling." Nat Cell Biol **13**(9): 1100-1107.

Son, A. I., J. E. Park, et al. (2012). "The role of Eph receptors in lens function and disease." Sci China Life Sci **55**(5): 434-443.

Stapleton, D., I. Balan, et al. (1999). "The crystal structure of an Eph receptor SAM domain reveals a mechanism for modular dimerization." Nat Struct Biol **6**(1): 44-49.

Straub, B. K., J. Boda, et al. (2003). "A novel cell-cell junction system: the cortex adhaerens mosaic of lens fiber cells." J Cell Sci **116**(Pt 24): 4985-4995.

Sundaresan, P., R. D. Ravindran, et al. (2012). "EPHA2 Polymorphisms and Age-Related Cataract in India." PLoS One **7**(3): e33001.

Takeichi, M. (1995). "Morphogenetic roles of classic cadherins." Curr Opin Cell Biol **7**(5): 619-627.

Tan, W., S. Hou, et al. (2011). "Association of EPHA2 polymorphisms and age-related cortical cataract in a Han Chinese population." Mol Vis **17**: 1553-1558.

Taylor, V. L., K. J. al-Ghoul, et al. (1996). "Morphology of the normal human lens." Invest Ophthalmol Vis Sci **37**(7): 1396-1410.

Thanos, C. D., S. Faham, et al. (1999). "Monomeric structure of the human EphB2 sterile alpha motif domain." J Biol Chem **274**(52): 37301-37306.

Thanos, C. D., K. E. Goodwill, et al. (1999). "Oligomeric structure of the human EphB2 receptor SAM domain." Science **283**(5403): 833-836.

Thoreson, M. A., P. Z. Anastasiadis, et al. (2000). "Selective uncoupling of p120(ctn) from E-cadherin disrupts strong adhesion." J Cell Biol **148**(1): 189-202.

Thornton, J. D., D. J. Swanson, et al. (2007). "Persistent hyperplastic primary vitreous due to somatic mosaic deletion of the arf tumor suppressor." Invest Ophthalmol Vis Sci **48**(2): 491-499.

Toth, J., T. Cutforth, et al. (2001). "Crystal structure of an ephrin ectodomain." Dev Cell **1**(1): 83-92.

van Eyll, J. M., L. Passante, et al. (2006). "Eph receptors and their ephrin ligands are expressed in developing mouse pancreas." Gene Expr Patterns **6**(4): 353-359.

Wang, H., S. R. Chadaram, et al. (2001). "Development of inhibition by ephrin-A5 on outgrowth of embryonic spinal motor neurites." J Neurobiol **47**(3): 233-243.

Wang, H. U. and D. J. Anderson (1997). "Eph family transmembrane ligands can mediate repulsive guidance of trunk neural crest migration and motor axon outgrowth." Neuron **18**(3): 383-396.

Wang, H. U., Z. F. Chen, et al. (1998). "Molecular distinction and angiogenic interaction between embryonic arteries and veins revealed by ephrin-B2 and its receptor Eph-B4." Cell **93**(5): 741-753.

Wang, Q., J. W. McAvoy, et al. (2010). "Growth factor signaling in vitreous humor-induced lens fiber differentiation." Invest Ophthalmol Vis Sci **51**(7): 3599-3610.

Wang, Q., R. Stump, et al. (2009). "MAPK/ERK1/2 and PI3-kinase signalling pathways are required for vitreous-induced lens fibre cell differentiation." Exp Eye Res **88**(2): 293-306.

Wang, T. H., J. L. Chang, et al. (2012). "EphrinA5 suppresses colon cancer development by negatively regulating epidermal growth factor receptor stability." FEBS J **279**(2): 251-263.

Washburn, C. P., M. A. Cooper, et al. (2007). "Expression of the tyrosine kinase receptor EphA5 and its ligand ephrin-A5 during mouse spinal cord development." Neurosci Bull **23**(5): 249-255.

Weis, W. I. and W. J. Nelson (2006). "Re-solving the cadherin-catenin-actin conundrum." J Biol Chem **281**(47): 35593-35597.

West, S. K. and C. T. Valmadrid (1995). "Epidemiology of risk factors for age-related cataract." Surv Ophthalmol **39**(4): 323-334.

White, T. W., D. A. Goodenough, et al. (1998). "Targeted ablation of connexin50 in mice results in microphthalmia and zonular pulverulent cataracts." J Cell Biol **143**(3): 815-825.

Wilks, T. A., J. Rodger, et al. (2010). "A role for ephrin-As in maintaining topographic organization in register across interconnected central visual pathways." Eur J Neurosci **31**(4): 613-622.

Winslow, J. W., P. Moran, et al. (1995). "Cloning of AL-1, a ligand for an Eph-related tyrosine kinase receptor involved in axon bundle formation." Neuron **14**(5): 973-981.

Wybenga-Groot, L. E., B. Baskin, et al. (2001). "Structural basis for autoinhibition of the Ephb2 receptor tyrosine kinase by the unphosphorylated juxtamembrane region." Cell **106**(6): 745-757.

Wykosky, J., E. Palma, et al. (2008). "Soluble monomeric EphrinA1 is released from tumor cells and is a functional ligand for the EphA2 receptor." Oncogene **27**(58): 7260-7273.

Xu, L., P. A. Overbeek, et al. (2002). "Systematic analysis of E-, N- and P-cadherin expression in mouse eye development." Exp Eye Res **74**(6): 753-760.

Yap, A. S., C. M. Niessen, et al. (1998). "The juxtamembrane region of the cadherin cytoplasmic tail supports lateral clustering, adhesive strengthening, and interaction with p120ctn." J Cell Biol **141**(3): 779-789.

Yokoyama, N., M. I. Romero, et al. (2001). "Forward signaling mediated by ephrin-B3 prevents contralateral corticospinal axons from recrossing the spinal cord midline." Neuron **29**(1): 85-97.

Yue, X., C. Dreyfus, et al. (2008). "A subset of signal transduction pathways is required for hippocampal growth cone collapse induced by ephrin-A5." Dev Neurobiol **68**(10): 1269-1286.

Zampighi, G. A., J. E. Hall, et al. (1989). "The structural organization and protein composition of lens fiber junctions." J Cell Biol **108**(6): 2255-2275.

Zantek, N. D., M. Azimi, et al. (1999). "E-cadherin regulates the function of the EphA2 receptor tyrosine kinase." Cell Growth Differ **10**(9): 629-638.

Zhang, J., S. Fuhrmann, et al. (2008). "A nonautonomous role for retinal frizzled-5 in regulating hyaloid vitreous vasculature development." Invest Ophthalmol Vis Sci **49**(12): 5561-5567.

Zhang, J. H., D. P. Cerretti, et al. (1996). "Detection of ligands in regions anatomically connected to neurons expressing the Eph receptor Bsk: potential roles in neuron-target interaction." J Neurosci **16**(22): 7182-7192.

Zhang, Q., X. Guo, et al. (2004). "Clinical description and genome wide linkage study of Y-sutural cataract and myopia in a Chinese family." Mol Vis **10**: 890-900.

Zhang, T., R. Hua, et al. (2009). "Mutations of the EPHA2 receptor tyrosine kinase gene cause autosomal dominant congenital cataract." Hum Mutat **30**(5): E603-611.

Zhu, M., M. C. Madigan, et al. (2000). "The human hyaloid system: cell death and vascular regression." Exp Eye Res **70**(6): 767-776.